

Power System Controller Design by Optimal Eigenstructure Assignment

by

Niraj Kshatriya

A Thesis submitted to the Faculty of Graduate Studies of
The University of Manitoba
in partial fulfilment of the requirements of the degree of

DOCTOR OF PHILOSOPHY

Department of Electrical and Computer Engineering
University of Manitoba
Winnipeg

Copyright © 2010 by Niraj Kshatriya

Abstract

In this thesis the eigenstructure (eigenvalues and eigenvectors) assignment technique based algorithm has been developed for the design of controllers for power system applications. The application of the algorithm is demonstrated by designing power system stabilizers (PSSs) that are extensively used to address the small-signal rotor angle stability problems in power systems. In the eigenstructure assignment technique, the critical eigenvalues can be relocated as well as their associated eigenvectors can be modified. This method is superior and yield better dynamical performance compared to the widely used frequency domain design method, in which only the critical eigenvalues are relocated and no attempt is made to modify the eigenvectors.

The reviewed published research has demonstrated successful application of the eigenstructure assignment technique in the design of controllers for small control systems. However, the application of this technique in the design of controllers for power systems has not been investigated rigorously.

In contrast to a small system, a power system has a very large number state variables compared to the combined number of system inputs and outputs. Therefore, the eigenstructure assignment technique that has been successfully applied in the design of controllers for small systems could not be applied as is in the design of power system controllers. This thesis proposes a novel approach to the application of the eigenstructure assignment technique in the design of power system controllers. In this new approach, a multi-objective nonlinear optimization problem (MONLOP) is formulated by quantifying different design objectives as a function of free parametric vectors. Then the MONLOP is solved for the free parametric vectors using a nonlinear optimization technique. Finally, the solution of the controller parameters is obtained using the solved free parametric vectors.

The superiority of the proposed method over the conventional frequency domain method is demonstrated by designing controllers for three different systems and validating the controllers through nonlinear transient simulations. One of the cases includes design of a PSS for the Manitoba Hydro system having about 29,000 states variables, which demonstrates the applicability of the proposed algorithm for a practical real-world system.

Acknowledgements

The author expresses gratitude to his advisor Dr. Udaya Annakkage for valuable support, encouragement, and advice throughout this project.

The author would like to extend his warmest thanks to Dr. Aniruddha (Ani) Gole, his co-advisor, for his inspiring discussion, valuable suggestions, and encouragement. The author highly appreciates the time and effort he has devoted, as well as the sympathy and interest he has shown.

My thanks goes to the other members of the examining committee for carefully reading the dissertation and making helpful suggestions.

The author wishes to thank Dr. Ioni Fernando (Manitoba Hydro) for her advise and support during the time author spent at Manitoba Hydro for research; Dr. Brian Archer (Manitoba Hydro) for providing Manitoba Hydro system data and for providing insight into the small-signal stability problem in general and as it pertains specifically to the system; Dr. F. Michael Hughes for providing the case of the DFIG system and its MATLAB code, and valuable discussions and advise on controller tuning; and Donald Nordman for meticulously proofreading this thesis.

The financial support from Manitoba Hydro and the National Science and Engineering Research Council (NSERC) is greatly appreciated. I would like to thank my current employer, Teshmont Consultants LP, for encouragement and for permitting the flexible work hours that I requested for thesis writing.

Last, but not least, I would like to acknowledge the support from my family. I am grateful to my parents for their moral support and encouragement during the difficult times. I would especially like to thank to my wife Sonal for her great love, patience, understanding, support, and for the many personal sacrifices she made throughout my work. I would also like to thank my daughter Shveta and my son Dev for their love and for showing understanding at such young ages.

Niraj Kshatriya

September 2010

Contents

Title	i
Abstract	ii
Acknowledgment	iv
Contents	v
List of Tables	x
List of Figures	xiii
1 Introduction	1
1.1 Power System Stability	2
1.2 Eigenstructure and its Significance in Small-Signal Stability Analysis	4
1.3 Motivation for the Research	6
1.3.1 Conventional Frequency Domain PSS Design	6
1.3.2 Eigenstructure Assignment Technique for Controller Design . .	9
1.3.3 Applications of Eigenstructure Assignment	12
1.4 Goals and Objectives of the Research	14
2 Linear Analysis	17
2.1 Linearized Power System	17
2.2 Eigenvalues and Eigenvectors	18

2.3	Residues, Participation Factors and Sensitivities	20
3	Conventional PSS Design Method	24
3.1	The Concept of PSS	25
3.2	PSS Siting	27
3.3	PSS Parameter Selection	28
3.3.1	Washout Filter	29
3.3.2	Lead-Lag Compensator and Gain	29
3.3.2.1	Residue Based Design [1]	30
3.3.2.2	Frequency Response Based Design [2], [3]	32
3.4	PSS Design for an Example System	34
3.4.1	PSS Location Selection	37
3.4.2	PSS Parameters Selection	37
3.4.2.1	Parameters Selection Using the Residue Method	38
3.4.2.2	Parameters Selection Using Frequency Response (Without Any Assumption)	40
3.4.2.3	Parameters Selection Using the Conventional Method (Approximated Frequency Response)	41
3.5	Conclusions	45
4	Eigenstructure Assignment Technique	47
4.1	Power System Controller and Identification of Suitable ESA Technique	47
4.2	The Control System	50
4.3	The Partial Eigenstructure Assignment Technique	53
4.3.1	Partial Left Eigenstructure Assignment	53
4.3.2	Partial Right Eigenstructure Assignment	55
4.3.3	Discussion	57
4.4	Conventional Eigenstructure Assignment Procedure	58

5	PSS Design Algorithm Based on the Partial Left Eigenstructure Assignment Technique	61
5.1	Suitable PSS Model	62
5.2	Suitability of Right and Left Eigenstructure Assignment for PSS Design	64
5.2.1	Possible Inputs and Outputs of the System	65
5.2.2	Assessment of Right and Left Eigenstructure Assignment . . .	66
5.3	Inadequacy of Conventional Left Eigenstructure Assignment Technique for Power System Controller Design[4]	69
5.3.1	The Objectives of Left Eigenstructure Assignment Technique Based Controller Design	70
5.3.2	Critical Eigenvalues May Not Move to Desired Locations . . .	71
5.3.3	The Set of Unassigned Eigenvalues May be Unacceptable . . .	72
5.4	Multi-Objective Nonlinear Optimization Problem (MONLOP)[4] . . .	73
5.4.1	Decision Variables	73
5.4.2	Ensuring the Critical Eigenvalues move to the Desired New Locations	74
5.4.3	Selection of the Optimal Left Eigenvector to Minimize Excitation of Problem Modes	76
5.4.4	Controlling Unassigned Eigenvalues	76
5.4.5	Minimizing Controller Effort	77
5.5	MONLOP and the Solution[4]	78
5.6	Power System Controller Design Procedure	79
5.7	Proposed Algorithm and Practical Controller Design	86
6	Application of Proposed PSS Design Algorithm	88
6.1	Two-Area, Four-Generator System	89
6.1.1	Open Loop System Analysis	90
6.1.2	Selection of PSS Location	92
6.1.3	Conventional PSS Designed in the Frequency Domain	93

6.1.3.1	PSS Parameters	94
6.1.3.2	Results	95
6.1.4	SS type PSS Design using the Eigenstructure Assignment Technique	99
6.1.4.1	Filters	99
6.1.4.2	Critical Eigenvalues and Their New Locations	100
6.1.4.3	Selection of the Dimension of the Dynamic Compensator	101
6.1.4.4	SS type PSS Parameters	101
6.1.4.5	Results	103
6.2	System with a Wind Turbine Generator[4]	111
6.2.1	System Description	111
6.2.2	Controller Design Specifications	115
6.2.3	Controller Design Results	117
6.3	Large Power System	123
6.3.1	System Description	123
6.3.2	System Open Loop Analysis	125
6.3.3	Conventional PSS Designed in Frequency Domain	128
6.3.3.1	PSS Parameters	129
6.3.3.2	Results	129
6.3.4	SS PSS Design Using the Proposed Technique	132
6.3.4.1	Inputs to the SS type PSS	132
6.3.4.2	Desired New Location of Electromechanical Modes	133
6.3.4.3	Dynamic Compensator States	133
6.3.4.4	SS type PSS Parameters	134
6.3.5	Results	134
6.3.6	Conclusions	138
7	Conclusions and Future Work	140
7.1	Summary and Conclusions	140

7.2 Recommendations	142
Bibliography	149
Appendices	150
A Linearized State Equations	150
B Change in eigenvalue due to dynamic output feedback controller	154
C Computational Methods for a Very Large Power System	159
C.1 Calculation of Eigenvalue and Eigenvector of Very Large Power System	160
C.1.1 The Arnoldi Factorization Method	160
C.1.2 The ARPACK Software	161
C.1.3 The Shift and Invert Transformation	162
C.1.4 Computing $u = (A - \sigma I_n)^{-1}v$	163
C.2 Multiplication of Large Sparse Matrices	164
C.3 Solution to a Sparse System of Linear Equations	165
D Dynamic Device Data	166
D.1 2-Area 4-Generator Sample System of Chapter 3	166
D.2 2-Area 4-Generator Sample System of Chapter 6	166
D.3 Kelsey Generating System Data	167
E Nelder-Mead Simplex Algorithm	168

List of Tables

3.1	Electromechanical modes and their properties without PSS.	36
3.2	Generator rank for PSS siting based on the magnitude of residues and participation factors.	37
3.3	The PSS parameters designed using the residue method when a PSS is to be installed on different generators.	38
3.4	PSS design using residue method: The final PSS gain that is required to achieve damping ratio of 5.0% for the inter-area mode when the PSS is installed on different generators and the inter-area mode with the PSS.	39
3.5	Sensitivity of inter-area mode to overall gain of a PSS.	39
3.6	Frequency response between V_{ref} as input and T_e as output for different generators for inter-area mode frequency.	41
3.7	Necessary phase compensation and the approximate gain calculated using the frequency response method and that calculated using the residue method.	41
3.8	Analysis of the necessary phase compensation using the residue method and using the conventional method (approximated phase compensation).	43
3.9	The PSS parameters designed using the conventional method when a PSS is to be installed on different generators.	43

3.10	PSS design using conventional method: The final PSS gain that is required to achieve damping ratio of 5.0% for the inter-area mode when the PSS is installed on different generators and the inter-area mode with the PSS.	44
3.11	Sensitivity analysis of inter-area mode of the system with a PSS (designed using conventional method) on different generators.	44
6.1	Electromechanical modes of the system without a PSS.	91
6.2	Magnitude of the residues between the generator speed and power output and the exciter V_{ref} input of different generators for the critical inter-area mode.	92
6.3	Argument of the residue between the generator speed and power output and the exciter V_{ref} input of different generators for the critical inter-area mode.	93
6.4	The lead-lag type PSS parameters designed using the residue method.	95
6.5	Electromechanical modes of the system with the speed input lead-lag type PSS.	95
6.6	Electromechanical modes of the system with the power input lead-lag type PSS.	97
6.7	Filter and transducer parameters [5] for the dual-input SS type PSS.	100
6.8	Parameters of the speed input, power input and speed-power (dual) input SS type PSSs.	102
6.9	Electromechanical modes of the system with the speed input SS type PSS.	104
6.10	Electromechanical modes of the system with the power input SS type PSS.	106
6.11	Electromechanical modes of the system with the dual-input SS type PSS.	108

6.12	Modal Properties of the inter-area mode and the Area-2 plant mode of the system without any PSS and of the system with different types of PSS.	110
6.13	DFIG three mass model data.	113
6.14	Various operating conditions of the DFIG system.	115
6.15	Critical Modes of the system without controller.	116
6.16	Residues between various DFIG outputs and P_{s-ref} as input for the critical modes.	116
6.17	New locations of the critical modes.	117
6.18	MAPP power system summary.	124
6.19	Summary of powerflow of the MAPP power system.	124
6.20	Summary of EHV and HV bus and branch in the MAPP power system.	125
6.21	Modal analysis of critical plant and local plant modes.	126
6.22	Residues of critical plant mode, $\bar{\lambda}_1, \bar{\lambda}_1^* = 0.0951 \pm j3.7464$ between various outputs and exciter V_{ref} input of Kelsey and Kettle generators.	128
6.23	Residues of interplant mode, $\bar{\lambda}_2, \bar{\lambda}_2^* = -0.25 \pm j8.18$ between various outputs and exciter V_{ref} input of Kelsey and Kettle generators.	128
6.24	Lead-lag type PSS parameters.	129
6.25	Comparisons of electromechanical modes with the lead-lag PSS and without a PSS.	130
6.26	Magnitudes of electromechanical modes in different generator variables due to disturbance.	135

List of Figures

1.1	Block diagram of a lead-lag type PSS.	7
1.2	Block diagram of a generator plant connected to a power system. . .	7
3.1	Block diagram of a generator plant connected to a power system. . .	26
3.2	Single input lead-lag type PSS.	29
3.3	New preferred location of a poorly damped eigenvalue.	31
3.4	One line diagram of 2-Area 4-generator system.	35
3.5	Block diagram of the IEEE type AC4A excitation system.	35
5.1	Block diagram of single input lead-lag type PSS.	63
5.2	Block diagram of the state-space (SS) type PSS that is designed using the proposed eigenstructure assignment technique.	65
5.3	Potential problems with conventional left eigenstructure assignment technique (a) Critical eigenvalue $\bar{\lambda}_j$ gets worse while non-critical eigen- value $\bar{\lambda}_k$ moves to assigned location λ_j ; (b) Non-critical eigenvalue $\bar{\lambda}_u$ becomes unstable.	72
5.4	Acceptable and unacceptable region of the closed-loop eigenvalues. . .	77
5.5	(a) Schematic of the control system comprising a linearized power sys- tem, a filter and a dynamic compensator. (b) Equivalent linear pro- portional output feedback control system.	85
6.1	One line diagram of 2-Area, 4-generator system.	89
6.2	Transient response of the speed of generators without a PSS.	91

6.3	Single input PSS1A (lead-lag) type PSS.	93
6.4	Transient response of the speed of generators for the case without a PSS and that for the case with the speed input PSS1A (lead-lag) PSS.	96
6.5	Transient response of the speed of generators for the case without a PSS and that for the case with the power input PSS1A (lead-lag) PSS.	98
6.6	Transient response of the speed of generators for the case with the power input PSS1A (lead-lag) PSS and that for the case with the speed input PSS1A (lead-lag) PSS.	98
6.7	Block diagram of the single input state-space (SS) type PSS.	99
6.8	Block diagram of the dual input state-space (SS) type PSS.	100
6.9	Mode traces of the system with the speed input SS type PSS for increasing gain from zero to the designed value.	104
6.10	Transient response of the speed of generators for the case with the speed input SS PSS and that for the case with the speed input PSS1A (lead-lag) PSS.	105
6.11	Mode traces of the system with the power input SS type PSS for increasing gain from zero to the final design value.	107
6.12	Transient response of the speed of generators with the power input SS PSS and that for the case with the power input PSS1A (lead-lag).	107
6.13	Mode traces of the system with the dual input SS type PSS for increasing gain from zero to the final design value.	109
6.14	Transient response of speed of generators for the case with the speed-power (dual) input SS PSS and that for the case with the speed input PSS1A (lead-lag) PSS.	109
6.15	One line diagram of the system comprising DFIG wind generation.	111
6.16	Schematic of the wind turbine and the doubly fed induction generator system.	112
6.17	Three mass model of DFIG wind turbine.	113

6.18	Block diagram of flux magnitude-angle controller (FMAC).	114
6.19	State-space (SS) type controller for the DFIG system.	117
6.20	Transient response of speeds for the case with <i>Controller</i> ₁ and that for the case with <i>Controller</i> ₂ when operating at <i>slip</i> = -0.1 pu. . . .	121
6.21	Transient response of speeds for the case with <i>Controller</i> ₁ and that for the case with <i>Controller</i> ₂ when operating at <i>slip</i> = +0.2 pu. . . .	121
6.22	Transient response of speeds for the case with <i>Controller</i> ₁ and that for the cases with <i>Controller</i> ₃ when operating at <i>slip</i> = -0.1 pu. . .	122
6.23	Transient responses of speeds for the case with <i>Controller</i> ₃ when op- erating at different slips.	122
6.24	Transient response of variables of generators without a PSS.	126
6.25	Manitoba Hydro northern area power system.	127
6.26	Transient response of Kelsey generator variables for the case with the speed input STAB1 (lead-lag) PSS and that for the case without a PSS.	130
6.27	Transient response of Kettle generator variables for the case with the speed input STAB1 (lead-lag) PSS and that for the case without a PSS.	131
6.28	Block diagram of the three input SS type PSS.	132
6.29	Mode trace of the system with the three input SS type PSS for varying gain from zero to the final value.	136
6.30	Transient response of Kelsey generator variables for the case with the three input SS type PSS and that for the case with the speed input STAB1 (lead-lag) PSS.	136
6.31	Transient response of Kettle generator variables for the case with the three input SS type PSS and that for the case with the speed input STAB1 (lead-lag) PSS.	137

E.1 New simplex after (a) *reflection* step (b) *expansion* step (c) *contraction* step; and (d) *shrinking*. The simplex at the beginning of iteration is shown with a solid line and the new simplex at the end of one iteration is shown with a dashed line. 169

Chapter 1

Introduction

Power systems are the largest dynamic systems ever constructed by humankind. A modern power system comprises extensive interconnections of generating systems and loads that are often thousands of miles apart. Large amounts of power transfer over long transmission lines, high gain automatic voltage regulators (AVRs), and fast acting exciters give rise to low frequency (0.2 Hz to 2 Hz) generator rotor oscillations under small disturbances that manifest as power and voltage oscillations in the system, and if such oscillations persist for a long time or grow in magnitude, they threaten system security and restrict the allowable power flow in the network. Power system stabilizers (PSSs), controllers that provide auxiliary control signals to the excitation system of generators, have been successfully used to damp such oscillations for several decades. Recently, controllers have been implemented for power electronics based devices, such as high voltage dc (HVDC) systems, static VAR compensators (SVCs), thyristor controlled series capacitors. In this thesis, a new algorithm based on the eigenstructure assignment technique is presented, which can be applied in the design of such controllers. A superior dynamic performance can be achieved by employment of a controller designed using the proposed algorithm compared to that can be achieved using a controller designed using the conventional frequency domain design method. Because, using the proposed algorithm it is possible to design a controller

that can alter the eigenvectors of the closed-loop system, the possibility of which is ignored in the conventional method.

The eigenstructure assignment technique has been successfully used in the design of controllers for small systems, such as in aerospace applications; however, it is relatively new to power system controller design. In this thesis, the inadequacies of the conventional application of the technique in the design of controllers for power systems are identified, and a novel optimization-based algorithm is presented to address these inadequacies.

In this chapter, the motivation for the research, the goals of the research, the definition of the problem, and the methodology adopted in the research are presented. Prior to that, an overview of stability problems in power systems is presented, followed by an introduction to the concepts of eigenvalues and eigenvectors, which are the basic concepts of small-signal (linear) analysis and controller design. Then, the conventional frequency domain method for power system controller design is reviewed followed by a brief description of the eigenstructure assignment technique.

1.1 Power System Stability

A power system comprises geographically separated generators and loads interconnected through a network of transmission lines, complex control systems, power electronics based devices, and other equipment and machines. The generators must constantly meet the demands of continuously changing loads through an ever-changing transmission network by continuously adjusting their operating parameters. Additionally, a power system intermittently experiences many severe disturbances, for example, fault due to an insulation failure or a lightning strike on a transmission line, a loss of a transmission line, or loss of a generator. Maintaining overall power system stability when the power system is constantly being disturbed from its operating equilibrium is an important problem for secure power system operation. The

overall stability of a power system can be defined more formally as “that property of a power system that enables it to remain in a state of operating equilibrium under normal operating conditions and to regain an acceptable state of equilibrium after being subjected to a disturbance” [6].

Due to its nature, a power system exhibits different types of instability depending on the system configuration. Though the different types of instability are interrelated, they cannot be treated as a single problem; therefore, they are classified into various stability problems such as voltage stability, frequency stability, small-signal stability, and transient stability [7]. This thesis is concerned with the small-signal stability of the power system.

A small-signal stability analysis involves the stability study of a power system under small disturbances. If the disturbances permit linearization of the dynamic equations of the power system for the purpose of analysis, then they are classified as small disturbances. Small changes in load or generation, change in the voltage reference of the excitation system, and tripping of transmission lines carrying a small load are examples of small disturbances.

A small-signal study can be undertaken to identify and solve many types of problems in power systems, such as rotor angle stability, subsynchronous resonance, controller interaction, and stability of the power system due to power electronics based devices. Small-signal rotor angle stability is concerned with the stability of synchronous generator speed oscillations. Such oscillations are called electro-mechanical oscillations because they arise as a result of unbalance in electrical and mechanical torques under small disturbances. Rotor angle stability is a frequently encountered problem in power systems because generating systems are in the majority among the various dynamic devices in power systems. It is also one of the important problems because the generating systems are the almost exclusive sources to meet the power demand. In this thesis, the superiority of the proposed control design technique over the conventional frequency domain design method is demonstrated by designing

controllers that successfully address small-signal rotor angle stability problems.

1.2 Eigenstructure and its Significance in Small-Signal Stability Analysis

Eigenstructure (eigenvalues and eigenvectors) of the plant matrix of a linearized system can be used to describe the small-signal behavior of a power system. Power systems are inherently nonlinear in nature; that is, the dynamics of the system are governed by a set of first order nonlinear ordinary differential equations. For the purpose of small-signal stability analysis, the system can be linearized around an operating point in order to yield a set of linear differential equations

$$\dot{x}(t) = Ax(t) \tag{1.1}$$

where $x(t) \in \mathbb{R}^n$ is state vector and $A \in \mathbb{R}^{n \times n}$ is called the plant matrix. The procedure for linearization of a power system is described in detail in Appendix A. The plant matrix of a linearized power system is a real square matrix.

The eigenanalysis of A produces n real and/or self conjugate eigenvalues $\{\lambda_1, \dots, \lambda_n\}$ and associated right eigenvectors $\{v_1, \dots, v_n\}$ and left eigenvectors $\{w_1, \dots, w_n\}$. The eigenvectors are column vectors. The eigenvalues are assumed to be distinct for the sake of simplicity. The mathematical definitions of eigenvalues and eigenvectors are presented in § 2.2.

In order to understand the usefulness of the eigenvalues and eigenvectors in small-signal analysis, consider a case in which a power system is not at steady state equilibrium following a disturbance, and the system is let go free. The well-known time domain solution of state variable $x(t)$ is given by [6]

$$x_i(t) = \sum_{j=1}^n v_{ji} c_j e^{\lambda_j t} \tag{1.2}$$

where

$$c_j = \sum_{k=1}^n w_{jk} x_k(0). \quad (1.3)$$

In (1.2) and (1.3) v_{pq} (w_{pq}) is q^{th} element of the right (left) eigenvector associated with the p^{th} eigenvalue; and $x(0)$ is the initial condition of the state vector evaluated numerically by taking the difference of the state value at the time when the system is let go free and at the stable operating point, at which the system will eventually settle and around which the system is linearized.

It is clear from (1.2) and (1.3) that both eigenvalues and eigenvectors together determine the dynamic response of the system.

By investigating the exponential part in (1.2), it is evident that eigenvalues determine the rate of decay (or rise) and frequency of oscillations. A complex conjugate pair of eigenvalues $\lambda_i, \lambda_i^* = \alpha \pm j\omega$ constitute a mode; and the mode will decay at the rate of $e^{\alpha t}$ and the frequency of oscillation of the mode will be ω rad/s. If the system has one or more eigenvalues with a positive real part, those modes will be unstable, which will cause the system to become unstable. Such modes are called unstable modes. If the system has one or more eigenvalues with their real part negative but close to zero, then the system will exhibit oscillation of variables lasting for a long period of time before attaining the equilibrium. Such modes are called poorly damped modes.

When small-signal analysis reveals the presence of unstable or poorly damped modes controllers are implemented in order to improve the small-signal behavior of the system.

In addition to eigenvalues, the eigenvectors are also key parameters that determine the shape of the transient responses. From (1.2) it is evident that the right eigenvector v_j determines the presence of the j^{th} mode in various state variable time responses, and from (1.3) it is apparent that the left eigenvector w_j determines the excitation of the j^{th} mode for a given initial condition.

1.3 Motivation for the Research

Controllers known as power system stabilizers (PSSs) have been extensively used to address the most frequently encountered small-signal rotor angle stability problems of power systems. In this section, the conventional frequency domain PSS design method is reviewed and a description of the eigenstructure assignment controller design technique is presented. This is followed by a review of successful applications of the eigenstructure assignment technique in the design of controllers for small systems. Then, the motivation for the research work regarding the application of the technique in the design of the controllers for power systems is presented.

1.3.1 Conventional Frequency Domain PSS Design

Poorly damped or unstable low frequency (0.2 Hz to 2 Hz) electromechanical modes are mainly due to power transmission over a long distance with weak ac ties and the application of fast acting exciters in conjunction with high gain AVRs. Since the 1960s, controllers known as power system stabilizers (PSSs) have been successfully used in power systems to damp these low frequency oscillations. The concept of PSS was first introduced in [2]. PSSs aid in improving the stability and dynamic performance of the system by introducing a component of electrical torque in phase with the generator rotor speed (damping torque) by modulating the voltage reference signal of the excitation system.

Four distinct widely used PSS models are described in IEEE Std 421.5 [8]. For three of the PSSs described in the standard, the underlying structure can be summarized as shown in Fig. 1.1. The other PSS can be thought of as three such PSSs in parallel, each targeting a specific frequency range, with the final output obtained by summing the outputs of the individual PSSs. Generator speed, bus frequency, and generator power are some of the common stabilizer input signals.

The function of the filter is to remove unwanted frequency components from the

input signal, and the high pass filter is the most commonly employed filter type for that purpose. In the case of a two-input PSS, an additional role of the filter is to synthesize inputs and generate a signal that is representative of the rotor speed. The phase compensator blocks provide the necessary phase compensation to the signal, which is amplified by a proportional gain to yield the final PSS output.

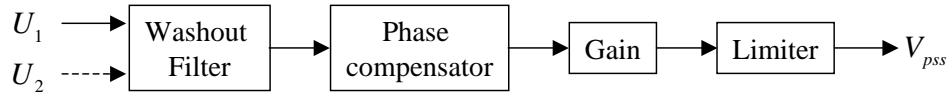


Figure 1.1: Block diagram of a lead-lag type PSS.

The design of a single PSS in frequency domain is relatively straight-forward; and many excellent references are available that provide guidance regarding the selection of the PSS parameters, such as [6], [9], [10], [11], [3], [12], [13] and [14]. The coordinated design of multiple controllers in a multi-machine power systems requires a different approach [14]. In this thesis, the design problem of a single controller in a multi-machine power system is investigated in order to demonstrate the application of the proposed algorithm. Therefore, the theoretical concept of the design of a single PSS in frequency domain is explained below.

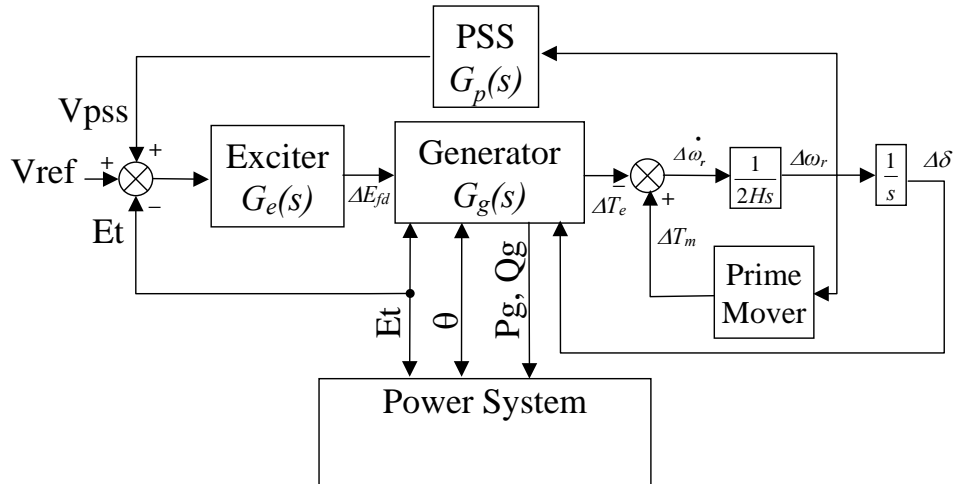


Figure 1.2: Block diagram of a generator plant connected to a power system.

Fig. 1.2 shows the block diagram of a single generating station connected to a power system. As shown in the figure, the generating system comprises an exciter, a generator, a prime mover, and a speed input PSS. The speed of the local generator is conditioned by the PSS shown in Fig. 1.1, and is fed back at the V_{ref} summing junction of the exciter. Often a signal other than the speed are used as input to the PSS; nevertheless, the concept of phase compensator and gain parameter selection will be the same. The objective of a PSS is to introduce a component of electrical torque (ΔT_e) in phase with the rotor speed to improve the damping of electromechanical oscillations. As can be seen from Fig. 1.2, the signal V_{pss} passes through the exciter and the generator before introducing any electrical torque, which introduces phase lag to the signal. Hence, the phase compensator is designed to introduce the necessary phase lead over a range of frequencies to compensate the phase lag introduced by the exciter and the generator. The necessary phase response can be evaluated using the frequency response of the system [3], and then phase compensator parameters are selected to achieve the desired phase response. After selecting the phase compensator parameters, the gain of the PSS is gradually increased and damping is evaluated by eigenvalue analysis. Usually, the increase in gain results in increased damping to a certain point, beyond which further increase in gain decreases damping. Ideally, the gain that results in maximum damping is selected.

Thus, the objective of the conventional frequency domain design of a PSS is limited to pushing the critical eigenvalues further left in the complex $X - Y$ plane, and no attempt is made to explore the advantages of assigning eigenvectors. As mentioned in the previous section, the real parts of the eigenvalues determine the rates of decay of the system variables. However, the eigenvectors also play a role in shaping the response. Therefore, if the eigenvectors of the critical modes are exploited in addition to moving them to a better damped location, then a better performing controller in terms of the dynamic response of the system during small disturbances can be achieved. The technique that assigns the eigenvalues and the associated eigen-

vectors is termed the eigenstructure assignment technique. The technique has been successfully used in the design of controllers for aerospace applications.

The following subsection describes the eigenstructure assignment technique, the degrees of freedom available in controller design, and the possible distribution of these degrees of freedom among eigenvalues and eigenvectors.

1.3.2 Eigenstructure Assignment Technique for Controller Design

As described previously, the conventional PSS design solution to addressing small-signal stability is based on the concept of introducing electrical torque in phase with the speed deviation. As an alternate approach, the design techniques available in classical control theory can be used to address the small-signal stability problem of power systems. Some fundamental results from the control theory regarding controller design for linear systems are presented in the following.

Consider a linear time invariant control system

$$\begin{aligned}\dot{x}(t) &= Ax(t) + Bu(t) \\ y(t) &= Cx(t)\end{aligned}\tag{1.4}$$

where $x(t)$, $u(t)$, and $y(t)$ are n , r , and m -dimensional state, input, and output vectors respectively; and A , B , and C are the plant, input, and output matrices of the appropriate dimensions. In order to demonstrate the classical eigenstructure assignment method, it is assumed that $m + r > n$. This criterion inevitably fails in the case of a power system and is one of the important conditions considered in the research work that will be discussed later along with related problems and solutions. Without loss of generality, it is assumed that B and C are of full rank. Let the proportional output feedback law be applied to the above control system as

$$u(t) = Ky(t)\tag{1.5}$$

where K is an $m \times r$ real matrix; then, the resulting closed-loop system is given by

$$x(t) = (A + BKC)x(t) \tag{1.6}$$

$$= A_c x(t). \tag{1.7}$$

The above represents a very general form of an LTI output feedback control system. Complete state feedback, partial state feedback, single-input, and single-output type LTI feedback systems encountered in practical situations are specific cases of the above system, differentiated by the appropriate and specific choices of the number of inputs and outputs and by the output matrix.

In the field of control theory, the controller design problem evolved as eigenvalue assignment followed by eigenstructure assignment. In the 1960s, the research was focused on identifying the number of eigenvalues that can be assigned arbitrarily to the closed-loop system A_c in (1.7) through the gain feedback matrix K . It was well known that for a controllable single-input complete-state output system ($m = 1$, $r = n$, $C = I_n$) the complete spectrum (n eigenvalues) can be assigned arbitrarily. In [15] it was proved that this property of a complete-state output feedback system also applies to a controllable multi-input system ($m > 1$, $r = n$, $C = I_n$) as well. Then, in [16] and [17] it was shown that for a controllable multi-input, multi-output system ($m, r > 1$) at least the $\max(m, r)$ eigenvalues can be assigned to the closed-loop system. Later in [18] and [19] it was proved that it is possible to arbitrarily assign up to $\min(n, m + r - 1)$ eigenvalues for the observable and controllable MIMO system.

In the meantime, in [20] and [21] it was identified that there are extra degrees of freedom in the design of feedback gain K for a multi-input, complete-state output feedback system ($m > 1$, $r = n$, $C = I_n$), and algorithms were presented to assign n -eigenvalues and associated right eigenvectors. Later, in [22] it was shown that (under the assumption that $m + r - 1 \leq n$) in addition to assigning $(m + r - 1)$ eigenvalues, m entries in $(r - 1)$ right eigenvectors can be arbitrarily prescribed.

Since the above results regarding utilization of degrees of freedom in state and output feedback were published, many methods and algorithms for the design of a

proportional gain feedback matrix have emerged to assign an eigenstructure to the closed-loop control system. The different methods and algorithms consider different constraints on the system.

The principle of eigenstructure assignment in very general form is described in [23]. It is suitable for an uncontrollable or an unobservable system having multiple open-loop eigenvalues, and the eigenvalues to be assigned can be multiple and can be identical to those of the open-loop system.

In this thesis, a controller design algorithm suitable for a large power system is presented based on one of the eigenstructure assignment techniques described in [24], in which a complete parametric multi-stage solution to compute an output feedback matrix is presented. According to the technique, p -eigenvalues with $1 \leq p \leq \min(m + r - 1, n)$ can be assigned arbitrarily to the closed-loop system. Additionally, if $p \leq m$, then a maximum $(r - 1)$ -entries can be prescribed arbitrarily to the associated left eigenvector; and if $p \leq r$, then maximum $(m - 1)$ -entries can be selected arbitrarily for the associated right eigenvector.

If the desired degrees of freedom in the assignment of eigenvalues and associated eigenvectors are not provided by the given number of inputs and outputs of the system, then the available degrees of freedom can be increased to the desired level by employing a dynamic compensator, instead of proportional output feedback controller, between the inputs and the outputs of the system. The dynamic compensator with a -dimensional state vector $z(t)$ is given by

$$\begin{aligned}\dot{z}(t) &= D z(t) + E \bar{y}(t) \\ \bar{u}(t) &= F z(t) + G \bar{y}(t).\end{aligned}\tag{1.8}$$

An LTI system with the above dynamic compensator can be transformed into its equivalent LTI proportional output feedback system having a -additional inputs and outputs of the system [25], which increases the total available degrees of freedom to $(m + a)(r + a)$.

1.3.3 Applications of Eigenstructure Assignment

The eigenstructure assignment technique has been applied in the design of controllers for various kinds of systems, and the results demonstrate the superiority of eigenstructure assignment over eigenvalue assignment in terms of transient performance. However, the majority of the applications are related to the field of aerospace, for example helicopters, aircraft, and missiles [23]. Partial decoupling of the lateral dynamics modes is achieved through appropriate eigenstructure assignment when designing the controllers for an L-1011 aircraft in [26] and for an advanced fighter aircraft in [27]. In [28], a controller is designed for an electronics navigation box to minimize the vibration of the box, and the authors note that the results would have been difficult to achieve using any other technique. The partial eigenstructure assignment technique is developed in [29] and applied for modal control of large flexible space structure systems.

The application of the eigenstructure assignment technique for power system controller design is reported in [30] and [31]. In these references, it is claimed that the magnitude of the critical modes in the transients of generator speeds can be reduced through appropriate right eigenstructure assignment. However, in the research work there are some shortcomings as described below.

In [30], the right eigenstructure of the inter-area mode of the 14-generators system was modified by designing power system stabilizers for each of the generators. The local generator speed and rotor angle were used as input to each of these PSSs. This is the first limitation of the paper; the rotor angle is not an easily measurable variable. The results presented show that the response of the closed-loop system (the system with all the PSSs implemented) is better than the response of the open-loop system (the system without any PSSs). However, the results do not prove that the improvement is due to right eigenstructure assignment and is not due to improved damping. If the improvement is solely due to eigenvalue relocation, then a similar closed-loop system response can be achieved by designing PSSs using the conventional

frequency domain method.

In [31], the controller design problem of assigning partial right eigenstructure is formulated as a constrained optimization problem, and its application is illustrated by designing decentralized controllers for a sample three-generator system. It is demonstrated that assigning right eigenvectors in addition to assigning eigenvalues yields better dynamic performance. Again, this application does not prove that PSSs designed using the eigenstructure assignment technique would perform better than those designed using the conventional frequency domain method.

Apart from the above shortcomings, the applications considered in [30] and [31] may not represent practical situations. For example, if a new generating station is to be connected to an existing system, the design problem would be to appropriately design PSSs for the incoming generators, and the utility would likely prefer to keep the existing settings of the installed PSSs that have been proven to work well so far.

In spite of aforementioned shortcomings, the work presented in [30] and [31] show the potential of the eigenstructure assignment technique in the design of controllers for power system applications.

In summary, the eigenstructure assignment technique has been applied successfully in small systems, such as in the field of aerospace, and research has demonstrated its limited applications for power systems; but the full potential of the technique in the design of power system controllers has not been explored, and it is not known whether the technique is superior to the conventional frequency domain design method.

This has motivated the author to explore possible avenues for the eigenstructure assignment technique in the design of power system controllers, to investigate the possible advantages of the eigenstructure assignment technique over the conventional frequency domain method, and to devise a controller design method that is suitable for a large-scale power system.

1.4 Goals and Objectives of the Research

The research presented in this thesis has following goals.

1. Use the eigenstructure assignment technique in the design of power system controllers so that the following objectives are achieved.
 - Critical eigenvalues are moved to, preselected, well damped locations
 - Optimal eigenvectors are assigned to the closed-loop eigenvalues
 - The non-critical eigenvalues that are not prescribed new values are acceptable subsequent to the application of the controller
 - The new modes introduced by the controller are well damped
2. Evaluate the advantages of using the eigenstructure assignment technique over using conventional frequency domain design methods in the design of controllers for power systems.

Following is the methodology adopted in the research to achieve the above goals.

1. Define the objectives of the power system controller design.

The rotor angle stability problem due to poorly damped or unstable electromechanical oscillations is a well known small-signal stability problem in power systems. Hence, as a first step the conventional solution to the stability problem will be reviewed, and using the basic results of eigenstructure assignment technique, additional objectives that can be achieved using the technique will be determined.

2. Identify a suitable eigenstructure assignment technique.

As mentioned, many eigenstructure assignment techniques have recently been developed to design controllers. Each of these techniques is based on specific assumptions about the system. Hence, the next step will be to review the available techniques and identify the one with the following characteristics:

- Its underlying assumptions are applicable for the power system controller design case. If an assumption cannot be applied, then the technique should be flexible enough so that it can be modified before applying it in the design of power system controllers.
- It can achieve all the objectives of power system controller design identified in the previous step.
- It is implementable with relative ease for the design of controller for a large power system in which the number of states of the control system can easily be in the tens of thousands.

3. Identify limitations of the available technique.

The eigenstructure assignment technique has been applied successfully in the design of controllers for small systems, but power systems are different than small systems in many ways, and not all the assumptions underlying the technique are applicable to power system, and so all the objectives of power system controller design may not be achievable readily. Hence, the next step is to identify the problems that may arise when the technique is applied in the design of controllers for a power system.

4. Devise an algorithm for power system controller design.

After identifying the inadequacy of the selected eigenstructure assignment technique, the next step is to devise a new algorithm based on the technique in order to be able to design power system controllers that achieve the design objectives.

5. Evaluate the advantages of the eigenstructure assignment technique over the conventional frequency domain method by design controllers for sample power systems.

First, the algorithm will be tested by designing controllers for small sample systems. If necessary, the algorithm will be further modified by implementing

additional measures after small-signal analysis and nonlinear analysis of the systems. In this manner, the benefits of using the eigenstructure assignment technique over the conventional frequency domain method will be established.

6. Design a PSS for a large power system.

In order to prove the usefulness of the newly developed algorithm for real-world applications, the algorithm will be used in the design of a controller for a large power system, and the performance of the controller will be compared to that of the controller designed using the conventional frequency domain method.

Chapter 2

Linear Analysis

Small-signal rotor angle stability is classified as one of the stability problems that threatens the secure operation of power systems, and is defined as “the ability of the power system to maintain synchronism under small disturbances” [7]. In this chapter, the small-signal (linear) analysis of a power system is reviewed, and the concepts of eigenstructure, sensitivity, residues, and participation factors, which are fundamental concepts of linear analysis, are presented.

2.1 Linearized Power System

Generators, exciters, prime movers, and the governing system are the most common dynamic devices in the power system. Some of the other dynamic devices frequently encountered in power systems are motors, High Voltage DC (HVDC) systems, Flexible AC Transmission System (FACTS) devices, static var compensators, and synchronous condensers. The modeling of the dynamic devices for stability studies has been investigated extensively. The references [6] and [32] provide comprehensive analytical details of these dynamic devices and their industry-wide accepted models for use in stability studies. The formulation of a linear time invariant (LTI) control system for a power system is described in Appendix A. The dynamics of each of the dynamic

devices in a power system may be described in a very general form. Then, in conjunction with transmission network node equations, the linearized model of a power system can be obtained as

$$\dot{x} = Ax + Bu \quad (2.1a)$$

$$y = Cx \quad (2.1b)$$

where

x is the n -dimensional vector of states of the system,

u is the m -dimensional vector of input to the system,

y is the r -dimensional vector of output of the system,

A is the $n \times n$ real plant (system) matrix,

B is the $n \times m$ real input matrix, and

C is the $r \times n$ real output matrix.

If the outputs of the system are some generator variable (e.g., generator speed or generator power) or some network variable (e.g., line flow or bus voltages), then they are independent of the inputs to the system. This is usually the case, and therefore, y in (2.1b) is shown to be a function of the states and not of the inputs.

2.2 Eigenvalues and Eigenvectors

The eigenvalues of the plant matrix A in (2.1a) are n solutions, $\lambda_1, \dots, \lambda_n$, of the characteristic equation obtained by expanding

$$|\lambda I_n - A| = 0. \quad (2.2)$$

For a real plant matrix, the eigenvalues are either real or complex conjugate pairs. The eigenvalues are assumed to be distinct throughout this document for the sake of simplicity.

The right and left eigenvectors, v_i and w_i , respectively, associated with the eigenvalue λ_i of the plant matrix A are non-trivial n -dimensional column vectors (i.e.,

$v_i \neq 0$ and $w_i \neq 0$) those satisfy

$$(\lambda_i I_n - A) v_i = 0; \quad i = 1, \dots, n \quad (2.3)$$

and

$$w_i^T (\lambda_i I_n - A) = 0; \quad i = 1, \dots, n. \quad (2.4)$$

If the eigenvalues are real, then their associated eigenvectors are also real; and if the eigenvalues are complex conjugate pairs, then their associated eigenvectors form complex conjugate pairs. The right and left eigenvectors associated with different eigenvalues are orthogonal, that is

$$w_i^T v_j = 0 \quad (2.5)$$

where $i, j = 1, \dots, n$ and $i \neq j$.

It is common practice to normalize eigenvectors of an eigenvalue such that

$$w_i^T v_i = 1, \quad i = 1, \dots, n. \quad (2.6)$$

Let the modal matrices of the right and left eigenvectors, V and W , respectively, and diagonal matrix Λ of the eigenvalues be defined as

$$V = (v_1 \dots v_n), \quad W = (w_1 \dots w_n), \quad \Lambda = \text{diag}(\lambda_i), \quad i = 1, \dots, n.$$

The following results can be obtained using (2.3)-(2.6)

$$A V = V \Lambda, \quad (2.7)$$

$$W^T A = \Lambda W^T, \quad (2.8)$$

$$W^T V = I_n. \quad (2.9)$$

Simple manipulations of the modal matrices yields

$$W^T A V = \Lambda, \quad (2.10)$$

$$A = V \Lambda W. \quad (2.11)$$

One of the very important and useful properties of a matrix is

$$f(A) = V f(\Lambda) W^T \quad (2.12)$$

where $f()$ is some function of matrix.

2.3 Residues, Participation Factors and Sensitivities

The concept of residues and participation factors for a linear system are reviewed in this section. Then, the sensitivity of an eigenvalue to a parameter of the dynamic output feedback controller is presented. Following that, the specific conditions in which the sensitivity will coincide either with the participation factor or with the residue are described.

1. Residues

The transfer function of the system in (2.1) is given by

$$G(s) = \frac{y(s)}{u(s)} \quad (2.13)$$

$$= C(sI_n - A)^{-1}B. \quad (2.14)$$

Using (2.12), the above equation becomes

$$G(s) = C V (sI_n - \Lambda)^{-1} W^T. \quad (2.15)$$

Since $(sI_n - \Lambda)$ is a diagonal matrix, its inverse is also a diagonal matrix, and therefore, the above can be rewritten as

$$G(s) = \sum_{h=1}^n \frac{C v_h w_h^T B}{s - \lambda_h} \quad (2.16)$$

$$= \sum_{h=1}^n \frac{R_h}{s - \lambda_h} \quad (2.17)$$

where

$$R_h = C v_h w_h^T B \quad (2.18)$$

is the residue matrix of the transfer function at eigenvalue λ_h .

2. Participation factors

The concept of participation factors was first introduced in [33]. The generalized participation factors can be computed using the i^{th} and the j^{th} component of the h^{th} right and left eigenvectors, respectively, as

$$p_{ij}^h = v_{ih} w_{jh}. \quad (2.19)$$

The p_{ij}^h describes the relative presence of the h^{th} mode in the i^{th} state due to excitation of the j^{th} state variable. Participation factor is a widely used parameter to study the power system. For a particularly case of $i = j$, the participation factor describes the participation of the i^{th} state in the h^{th} mode and vice versa [33].

3. Sensitivities[34]

Let the dynamic output feedback control law

$$\begin{aligned} \dot{z} &= D z + E y \\ u &= F z + G y \end{aligned} \quad (2.20)$$

be applied to the system (2.1), where the vector z is the a -dimensional vector of the dynamic compensator states. Then, the closed-loop system can be described as

$$\dot{\bar{x}} = A_c \bar{x}$$

where

$$\bar{x} = \begin{pmatrix} x \\ z \end{pmatrix}, \quad \text{and} \quad A_c = \begin{pmatrix} A + B G C B F \\ E C \quad D \end{pmatrix}.$$

The transfer function of the feedback system is given by

$$H(s) = F (s I_a - D)^{-1} E + G. \quad (2.21)$$

Let λ be an eigenvalue of the closed-loop plant matrix A_c , and v and w be the associated right and left eigenvectors, respectively. The eigenvectors can be partitioned in accordance with the dimension of the system and the compensator state variables as

$$v = \begin{pmatrix} v_1 \\ v_2 \end{pmatrix} \quad w = \begin{pmatrix} w_1 \\ w_2 \end{pmatrix}$$

where subscripts 1 and 2 denote the association of part of the eigenvector with system states x and controller states z , respectively.

As shown in Appendix B, the sensitivity of closed-loop eigenvalue λ to a parameter q of feedback system transfer function, $H(s)$, is given by

$$\lambda' = w_1^T B H'(\lambda, q) C_1 v_1 \quad (2.22)$$

where the prime over a variable denotes partial derivative of the variable with respect to parameter q . Using (2.18), the above can be written as [34]

$$\lambda' = \text{trace}(R H'(\lambda, q)). \quad (2.23)$$

In [34], very important properties regarding the sensitivity of eigenvalues are identified. Consider a case in which static gain is employed between a single output and a single input of the system. In such a case, the residue becomes a scalar (complex scalar if the eigenvalue is complex, real otherwise) and sensitivity will coincide with residue, i.e.,

$$\lambda' = R \quad \text{if} \quad H(s, q) = q. \quad (2.24)$$

Consider a case in which the state x_i is an output of the system. If this output is multiplied by a proportional gain q and added to \dot{x}_j , it will alter the a_{ij} element of the plant matrix. For such case, the following results can be obtained :

1. The residue R_h of the eigenvalue λ_h coincides with the participation factor p_{ij}^h
2. The sensitivity of the eigenvalue λ_h to the parameter q coincides with the participation factor p_{ij}^h . In other words the participation factor p_{ij}^h is the sensitivity of the eigenvalue λ_h to the a_{ij} element of the plant matrix.

Chapter 3

Conventional PSS Design Method

The objective of this thesis is to implement the eigenstructure assignment technique in the design of the controllers for the power systems. In order to demonstrate the applications of this technique, controllers are designed using it to improve the eigenstructure of the system and address the most commonly encountered small-signal problem in the power systems, which is poorly damped or unstable electromechanical oscillations. The advantage of this technique is demonstrated by comparing the dynamic performance of the controller designed using it with that of the controller designed using the conventional frequency domain method.

Before proceeding to the application of the eigenstructure assignment technique in the design of controllers for power systems, the concept of PSS and the conventional frequency domain design method of a single PSS in a multi-machine system are reviewed. The local generator speed input is the most widely used PSSs in power systems. Therefore, in this chapter and later in this thesis, speed input PSS is considered to be the conventional PSS.

In this chapter, the concept of PSS is presented first. The design of a PSS involves two distinct steps. The first step in the design is identification of the most suitable generator to equip with PSS, and the second step is selection of PSS parameters. The PSS siting selection based on residue and participation factor is reviewed, fol-

lowed by the PSS parameter selection procedure. Evaluation of the necessary phase compensation is one of the key steps in PSS parameter selection. Three methods to calculate necessary phase compensation are described in this chapter: (1) the residue method; (2) the method based on the frequency response of the generator and the exciter; and (3) the conventional method, which uses the frequency response method with the assumption that the participation factors are real. Through analysis and with the aid of an example, it is demonstrated that the residue method is the most accurate for identifying the best location for PSS. Additionally, it is shown that the residue and frequency response methods are identical methods for the selection of PSS parameters, and that the eigenvalues can be relocated more accurately using these methods than using the conventional method.

Later, the controllers designed using the residue method will be used to evaluate the performance of the controllers designed using the proposed eigenstructure assignment based method.

3.1 The Concept of PSS

The basic concept of a PSS was presented in §1.3.1, is summarized here using Fig. 3.1, which is reproduced from that section.

System perturbations disturb the equilibrium of the electrical torque T_e and the mechanical torque T_m . This causes a generator or a group of generators to accelerate or decelerate resulting in deviation of their rotor speed and angle from their constant values. Such oscillations are termed electromechanical oscillations; and it is well-recognized that the frequency of such oscillations is in the range of 0.1 Hz to 2.0 Hz.

Power system stabilizers (PSSs) are installed if the system would exhibit poorly damped or unstable electromechanical oscillations. Usually, a single PSS is sufficient to improve damping of a single mode that is deemed critical from the system perfor-

mance point of view. A generator is equipped with a PSS with a complex structure or a number of generators are equipped with PSSs if damping of more than one critical mode must be improved. Here, a problem of a single PSS design to improve damping of a electromechanical mode is analyzed.

PSS introduces signal V_{pss} to modulate voltage reference signal of an exciter V_{ref} , as shown in Fig. 3.1. The additional signal introduced by the PSS would generate additional electrical torque.

When the signal V_{pss} is introduced to modulate V_{ref} , the exciter and generator introduce phase lag into the signal before it can introduce any electrical torque. The PSSs are designed to compensate phase lag so that when the signal arrives at ΔT_e it is in phase with the speed deviation $\Delta\omega_r$.

Introduction of electrical torque in such a manner will provide additional braking torque whenever the rotor speed advances from the steady state value, and it will provide additional accelerating torque whenever the rotor speed recedes from the steady state value thereby improving the damping of the electromechanical oscillations.

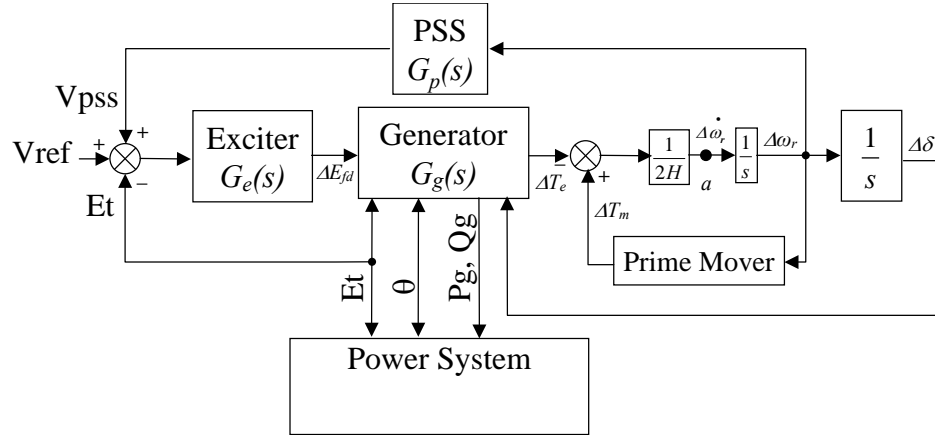


Figure 3.1: Block diagram of a generator plant connected to a power system.

Finding the most suitable PSS location for improving the damping of the critical mode(s) and shaping the frequency response of the PSS are two distinct steps involved

in PSS design and are discussed in following sections.

3.2 PSS Siting

A power system comprises many generators, and not all of them are equally suitable for equipping with PSS to improve damping of an electromechanical mode. The procedure for selecting the generator to equip with a PSS is reviewed in this section.

The PSS modulates the V_{ref} of an exciter; therefore, smaller gain in the feedback path is desirable in order to minimize its interference with the voltage control action of the exciter. Hence, the best generator to equip with PSS is the one that requires minimum gain to move the critical mode a given distance.

In the previous chapter it was shown that the sensitivity of an eigenvalue to a static output feedback gain between a given input-output pair is given by the residue between the input-output pair for the eigenvalue. Therefore, the best location to install PSS is the generator having the highest residue among all the generators, which will, in turn, require minimum gain to move the eigenvalue to a given distance. It should be noted that the residue depends on the units of the variables, and that care must be exercised in comparing the residues. However, if consistent units of measurement are used throughout the system for all the variables, then residues can be compared directly without any further processing. Determining the most suitable location based on the residue was first suggested in [1]. However, the algorithm involved the calculation of a complete set of right and left eigenvectors of the plant matrix, which is impossible for a large system. In [34] and [35] this obstacle was removed by showing that the residues can be calculated using the right and left eigenvectors of only the critical eigenvalue(s).

In [34] it was suggested that the generator that has the largest participation factor between its rotor speed and the critical mode be selected for PSS siting. This suggestion was based on the conclusion that for a large system the residues coincide

with the participation factors. Also, similar participation factor based method was proposed in [36]. This is a simpler approach and a great deal of computational effort can be saved because the input/output pair for each of the generators in the system need not be defined to calculate the participation factor.

However, the use of the participation factor is not accurate and may lead to selection of a generator that is not optimal for improving the damping of the critical mode. The participation factor between speed and an eigenvalue is the sensitivity of the eigenvalue to the proportional feedback gain employed between the speed output and input to its time derivative, which is point a in Fig. 3.1. Clearly, selecting a generator based on the participation factor does not take into consideration the gain or attenuation that a signal experiences while going through the exciter and the generator. Hence, this approach may fail to find the optimal location.

Later, in [13], an approach that combines the use of the participation factor and the residue, was suggested. Accordingly, the most suitable generator to equip with PSS can be selected using the participation factor to screen the potential locations, and then evaluating them using residues.

In this thesis, the PSS siting or the controller siting is determined according to the residue method if the dimension of the system under study permits evaluation of the residue of all the generators; if that is not feasible, the approach based on the combined use of the participation factor and the residue described above will be used. After the most suitable location is determined, the controller (PSS) is designed using the proposed algorithm or the conventional frequency domain method. The conventional method of PSS design is described in the following section.

3.3 PSS Parameter Selection

The most widely used single input lead-lag type PSS is shown in Fig. 3.2. PSS parameters selection consists of selection of the washout filter time constant T_w , the

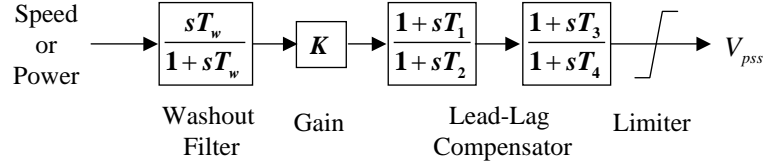


Figure 3.2: Single input lead-lag type PSS.

stabilizer gain K_s , and the lead-lag compensator constants $T_1 - T_4$. The parameters selection procedure is presented in the following subsections.

3.3.1 Washout Filter

A washout filter is a high pass filter employed to remove the unwanted dc components present in the signal and to allow only the rotor speed oscillations signal. The parameter T_w must be selected so that the rotor oscillation signals at the frequencies of interest are passed relatively unchanged. Also, T_w must be large enough so the washout filter does not introduce excessive phase lead at the frequency of interest.

If the modes of interest are local mode (frequencies in the range of 0.8 Hz to 2.0 Hz), then a filter time constant of 2.0 s is satisfactory. This will introduce a phase lead of 5.6 degrees and provide a gain of 0.995 at the frequency of 0.8 Hz. For inter-area modes having frequencies in the range of 0.1 Hz to 0.8 Hz, the time constant of 10.0 s can be selected. This value of washout filter will introduce a phase lead of 9.0 degrees and a gain of 0.988 at 0.1 Hz. In general, the washout filter time constant T_w can range from 1.0 s to 20.0 s [3], and it does not play a very critical role in PSS performance.

In this thesis, washout filters are designed using the above guidelines.

3.3.2 Lead-Lag Compensator and Gain

The purpose of the lead-lag compensator is to introduce phase lead or lag to the signal; and the compensator along with the gain play a critical role in the PSS design.

Two methods of calculating the necessary phase compensation to be provided by the lead-lag compensator, residue analysis and frequency response analysis, are analyzed in this section, followed by a description of the procedure to determine the necessary PSS gain.

3.3.2.1 Residue Based Design [1]

The transfer function of the PSS shown in Fig. 3.2 is

$$G_p(s) = K_s \left(\frac{s T_w}{1 + s T_w} \right) \left(\frac{1 + s T_1}{1 + s T_2} \right) \left(\frac{1 + s T_3}{1 + s T_4} \right) \quad (3.1a)$$

$$= K_s H_w(s) H_p(s) \quad (3.1b)$$

where $H_w(s)$ and $H_p(s)$ are the washout filter and phase compensator transfer functions, respectively. Let λ_i be the critical eigenvalue whose damping is to be improved, and let R_i be its residue for a given input-output pair.

Using the results presented in § 2.3, the sensitivity of an eigenvalue λ_i to gain K_s is given by

$$\lambda'_i = R_i G_p(\lambda_i)' \quad (3.2a)$$

$$= R_i H_w(\lambda_i) H_p(\lambda_i) \quad (3.2b)$$

where prime denotes partial derivative with respect to gain K_s . Using the above equations, the change in eigenvalue after introducing the PSS is given by

$$\Delta\lambda_i = R_i H_w(\lambda_i) H_p(\lambda_i) K_s. \quad (3.3)$$

For the complex mode all the variables in the above equation are complex values except K_s , which is a real constant. As shown in Fig. 3.3, the objective of the PSS is to improve the damping factor of the critical eigenvalue λ_i to at least $\zeta (= \sin(\phi))$. If λ_i is moved to point y , where $\Delta\lambda_i$ makes a right angle with the $\zeta = \text{constant}$ line, then the objective is achieved by moving λ_i the least distance. In practice, the real part of the critical eigenvalue and the angle ϕ are very small values. Hence, if the

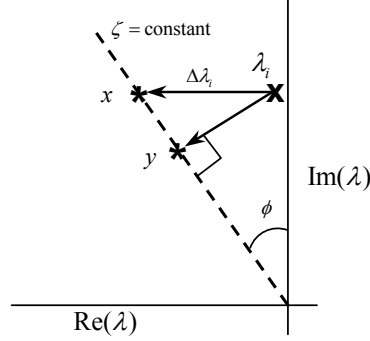


Figure 3.3: New preferred location of a poorly damped eigenvalue.

λ_i is moved parallel to X -axis to point x , then the additional distance to be moved is not significant. Moving the critical eigenvalues parallel to X -axis is the standard practice in PSS design. Therefore,

$$\angle \Delta \lambda_i = \pi. \quad (3.4)$$

Using (3.3), the necessary phase compensation to be provided by PSS is

$$\angle H_p(\lambda_i) = \angle \Delta \lambda_i - \angle R_i - \angle H_w(\lambda_i) \text{ rad} \quad (3.5a)$$

$$= \pi - \angle R_i - \angle H_w(\lambda_i) \text{ rad}. \quad (3.5b)$$

The required phase compensation may be divided among two phase compensator blocks equally, and the time constants T_1 to T_4 may be calculated using standard design technique. Then, again using (3.3), the necessary gain K_s is

$$K_s = \frac{|\Delta \lambda_i|}{|R_i| |H_w(\lambda_i)| |H_p(\lambda_i)|}. \quad (3.6)$$

When a PSS is implemented with the phase compensation and the gain calculated using (3.5b) and (3.6), respectively, the critical eigenvalue may not move precisely to the desired location because the system is nonlinear. Minor adjustment in phase compensation and gain may be necessary in such cases.

3.3.2.2 Frequency Response Based Design [2], [3]

As noted in § 2.3, the sensitivity of λ_i to static output feedback gain between generator speed and input point a in Fig. 3.1 coincides with the participation factor. Therefore, the sensitivity of an eigenvalue λ_i to the static gain K_s employed between generator speed and its time derivative is given by

$$\lambda'_i = p_{jj}^i \quad (3.7)$$

where j is the location of the generator speed in the state vector and $\Delta\lambda'_i$ is the partial derivative with respect to K_s . When the PSS is employed between the generator speed and the V_{ref} summing junction, as shown in Fig. 3.1, the sensitivity of λ_i to gain K_s of the PSS transfer function $G_p(s)$, using (3.7), is given by

$$\lambda'_i = -p_{jj}^i G_p(\lambda_i)' G_e(\lambda_i) G_g(\lambda_i) \frac{1}{2H}. \quad (3.8)$$

Using (3.1b), the change in eigenvalue after implementing PSS is given by

$$\Delta\lambda_i = -p_{jj}^i K_s H_w(\lambda_i) H_p(\lambda_i) G_e(\lambda_i) G_g(\lambda_i) \frac{1}{2H}. \quad (3.9)$$

In the above equations, all the variables are complex except K_s and H , which are real values. The phase relationship using the above equation is given by

$$\angle\Delta\lambda_i = \pi + \angle p_{jj}^i + \angle H_w(\lambda_i) + \angle H_p(\lambda_i) + \angle G_e(\lambda_i) + \angle G_g(\lambda_i) \text{ rad}. \quad (3.10)$$

Substituting π for $\angle\Delta\lambda_i$, according to (3.4), in the above equation will yield

$$\pi + \angle H_w(\lambda_i) + \angle H_p(\lambda_i) + \angle p_{jj}^i + \angle G_e(\lambda_i) + \angle G_g(\lambda_i) = \pi \quad (3.11a)$$

$$\angle H_w(\lambda_i) + \angle H_p(\lambda_i) + \angle p_{jj}^i + \angle G_e(\lambda_i) + \angle G_g(\lambda_i) = 0 \quad (3.11b)$$

and

$$\angle H_p(\lambda_i) = -\angle p_{jj}^i - \angle G_e(\lambda_i) - \angle G_g(\lambda_i) - \angle H_w(\lambda_i) \text{ rad}. \quad (3.12)$$

Theoretically, the calculation of the necessary phase compensation using the above equation is an alternate approach to the residue method, and the value of $\angle H_p(\lambda_i)$,

calculated using (3.12), will be identical to the value calculated using (3.5b). In conventional PSS design, assumptions/approximations are made in the above frequency response method as described in the following.

The participation factor between the rotor speed and the electromechanical modes is considered to have a positive real part and a comparatively very small imaginary part [2], [3], [13], [34], that is $\angle p_{jj}^i \approx 0$. Also, the phase lead introduced by the washout filter is ignored, that is $\angle H_w(\lambda_i) \approx 0$, because the phase lead is very little at the frequency of interest. Therefore, the approximate necessary phase compensation is

$$\angle H_p(\lambda_i) \approx -(\angle G_e(\lambda_i) + \angle G_g(\lambda_i)) \text{ rad.} \quad (3.13)$$

In other words, the lead-lag compensator should be designed to have inverse phase response to that of the combined exciter and generator. The design of the lead-lag block in this manner is an industry-wide practice in lieu of the use of the more accurate residue method and the frequency response method without assumptions, as described earlier.

It must be noted that if the lead-lag blocks are designed to compensate the phase angle given by (3.13), then $\angle \Delta \lambda_i$ using (3.10) is given by

$$\angle \Delta \lambda_i = \pi + \angle(p_{jj}^i) + \angle H_w(\lambda_i) \quad (3.14)$$

$$\approx \angle -p_{jj}^i. \quad (3.15)$$

Hence, the lead-lag block designed to provide phase compensation calculated using (3.13) will improve the damping of the critical mode only if the phase of the participation factor between the speed of the generator to be equipped with the PSS and the critical mode is close to zero. This is what has been observed, however there is no mathematical proof for it. Hence, this method should be used carefully.

The combined lead or lag introduced by the exciter and the generator may be obtained using the frequency response between input V_{ref} and output T_e shown in Fig. 3.1, (provided speed deviation is the input to the PSS). When calculating the

frequency response, the inertia of the generator must be assumed to be very large in order to avoid any feedback due to change in generator angle, and thereby yield the frequency response only between the exciter and the generator where the PSS is to be installed [3].

After designing the lead-lag compensator, as described earlier, the necessary gain using (3.8) may be given by

$$K_s = \frac{2H|\Delta\lambda_i|}{|p_{jj}^i||H_w(\lambda_i)||H_p(\lambda_i)||G_e(\lambda_i)||G_g(\lambda_i)|}. \quad (3.16)$$

Similar to the case in which the residue method is used, the critical eigenvalue may not move precisely to the desired location using gain calculated using (3.16) because the system is nonlinear and adjustment may be necessary.

3.4 PSS Design for an Example System

The frequency domain techniques of PSS design, described in the previous section, were employed for a two-area four-generator system. The results of the application of these techniques are compared in this section. It has been shown that the residue method correctly identifies the best generator to equip with PSS, and that the participation factor based method does not. Additionally, if the argument of the participation factor is not close to zero, the phase compensation determined using the conventional frequency response-based method will not move the critical eigenvalue as intended. However, the phase compensation determined by using the residue method or by using the frequency response based method without any approximation will move the eigenvalue in a direction very close to the desired one.

The example power system in Fig. 3.4 has two areas, each with two generators, interconnected through a high-impedance transmission line. All the generators are equipped with a fast acting IEEE type AC4A excitation system. The block diagram of the excitation system is shown in Fig. 3.5. The line impedances and load flow are marked in the figure and the synchronous generator and exciter data are listed in

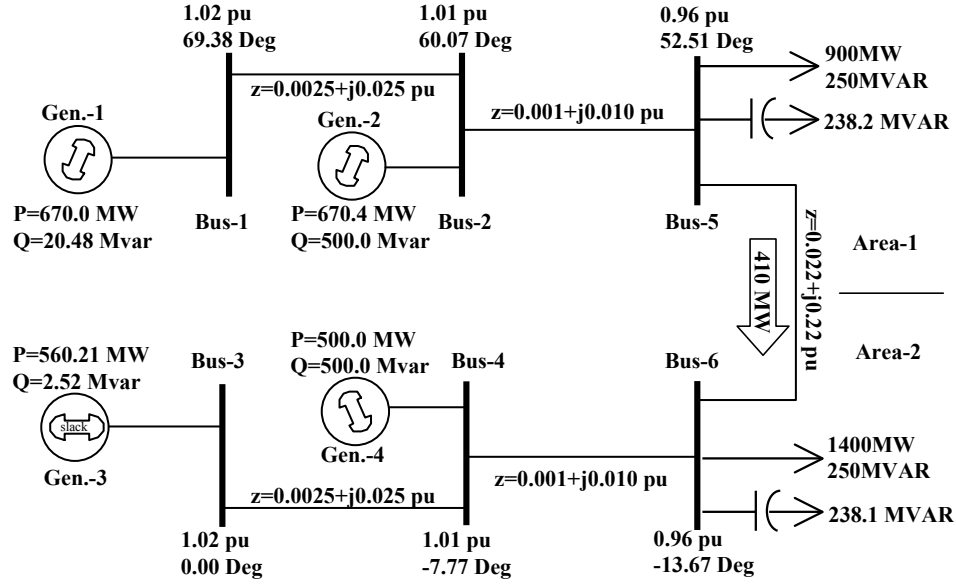


Figure 3.4: One line diagram of 2-Area 4-generator system.

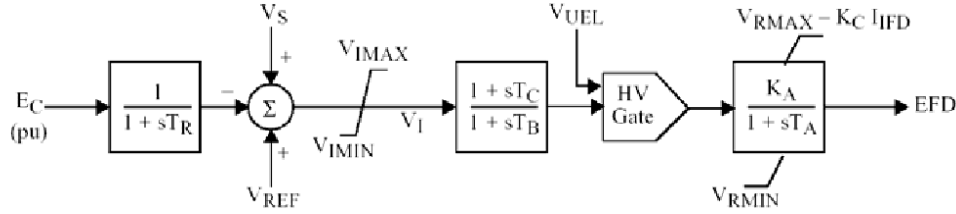


Figure 3.5: Block diagram of the IEEE type AC4A excitation system.

Appendix D. Power transfer of 410 MW from Area-1 to Area-2 is considered. The generators are modeled using a two-axis model with one winding in each axis, and each has four states: rotor angle δ , rotor speed ω , field winding flux linkage ψ_{fd} , and quadrature axis flux linkage ψ_{qd} . One state is associated with each of the T_R , T_B , and T_A blocks in the exciter model (Fig. 3.5). Thus, each exciter has three states. Each plant has seven states; the system has twenty-eight states in the absence of any PSS. The loads are modeled as constant impedance.

The eigenanalysis reveals the presence of three electromechanical modes. Table 3.1 shows these modes along with the magnitude of the participation factors and the argument of the right eigenvectors (mode shape) for the generator speeds. The partic-

Table 3.1: Electromechanical modes and their properties without PSS.

Mode	M1		M2		M3	
	λ_1, λ_1^*		λ_2, λ_2^*		λ_3, λ_3^*	
Eigenvalue	$0.001 \pm j2.1034$		$-1.07 \pm j8.00$		$-1.35 \pm j7.81$	
Freq. (Hz)	0.3348		1.2736		1.2433	
Damp. Ratio	-0.0005		0.1329		0.1703	
Generator	PF	\angle REV	PF	\angle REV	PF	\angle REV
G1	0.5007	124.66	0.9594	177.42	0.0048	123.38
G2	0.3616	135.21	1.00	0.00	0.0054	-24.5620
G3	1.000	0.00	0.0049	140.00	0.8998	176.277
G4	0.9576	-4.6708	0.0057	-68.10	1.00	0.000

icipation factors and the right eigenvectors are normalized so that the maximum value is unity. The 0.3348 Hz mode M1 is the inter-area mode since all the generator speeds have high participation in that mode, and the angle of right eigenvector for Area-1 and Area-2 are out of phase with each other. The modes M2 and M3 are Area-1 and Area-2 local modes, respectively, since only the generators in the respective areas participate the most and the angle of the right eigenvectors of the generators of the respective areas are out of phase with each other. The inter-area mode is unstable due to the positive real part, and the objective is to find the most suitable location for the PSS and select its parameters so the damping factor is improved to 0.05. If the eigenvalues are moved parallel to the X -axis, their new location will be $-0.1053 \pm j2.1034$.

In the following subsection, a PSS is designed for each of the generators, and the results are compared to demonstrate the concepts developed in previous subsections.

Table 3.2: Generator rank for PSS siting based on the magnitude of residues and participation factors.

Gen.	Residue		PF ¹	
	Normalized	Rank	Normalized	Rank
G1	0.221	4	0.50	3
G2	0.48	2	0.36	4
G3	0.34	3	1.00	1
G4	1.00	1	0.96	2

¹ PF=Participation Factor

3.4.1 PSS Location Selection

In § 3.2, two methods for selecting the most suitable location for the PSS are described: the residue based method and the participation factor based method. The magnitude of the residues and the participation factors for all of the generators as well as their rank in terms of suitability for PSS location based on those two values are shown in Table 3.2. The two methods are not in agreement regarding the ranking. The participation factors based method is not a precise method, and in this particular case it fails to correctly rank the generators. Therefore, the participation factor based method cannot be relied upon for the selection of the most suitable generator to locate PSS.

This is verified in the following subsection by comparing the gains required in four different cases when a PSS is installed on one of the four generators to improve the damping of the inter-area mode to a preselected value.

3.4.2 PSS Parameters Selection

The washout filter time constant of 10.0 s is selected according to § 3.3.1. The washout filter transfer function has a gain of 0.96 and introduces a phase lead of 2.7 *deg* at the inter-area mode frequency, that is $H_w(\lambda_1) = 0.96\angle 2.7^\circ$.

3.4.2.1 Parameters Selection Using the Residue Method

Table 3.3 shows the magnitude and the argument of the residues between the input V_{ref} of the exciter and the speed output for each generator in the inter-area mode, as well as the necessary phase compensation to be provided by the lead-lag blocks and the approximate gain if a PSS is installed on individual generators. The necessary phase compensation and the approximate gain are calculated using the procedure described in § 3.3.2.1. The parameters $T1 - T4$ of the lead-lag blocks are calculated using standard techniques so that each of the lead-lag block will provide half of the necessary phase compensation and maximum gain at the frequency of interest. The values of K_s were further adjusted to achieve a damping factor of 0.05 for the inter-area mode and the final values are shown in Table 3.4.

The results of the eigenanalysis and sensitivity analysis of the four cases of a PSS installed on different generators are presented in Table 3.4 and Table 3.5. It can be seen from the tables that the PSSs moved the eigenvalue almost parallel to the X -axis and the actual sensitivities of the eigenvalue are very close to its residues. If the generators are ranked according to the overall gain of the PSS, the ranking is in agreement with what is predicted using the residues.

Table 3.3: The PSS parameters designed using the residue method when a PSS is to be installed on different generators.

PSS Location	Residue		Required phase comp. (deg)	T1=T3	T2=T4	Approximate gain
	Mag.	Phase				
Gen-1	0.00566	154.86	22.42	0.57035	0.38457	13.50
Gen-2	0.01234	136.72	40.56	0.68061	0.33010	4.44
Gen-3	0.00870	-161.17	-21.55	0.39200	0.57237	18.89
Gen-4	0.02552	-179.57	-3.15	0.45710	0.48295	4.66

Table 3.4: PSS design using residue method: The final PSS gain that is required to achieve damping ratio of 5.0% for the inter-area mode when the PSS is installed on different generators and the inter-area mode with the PSS.

PSS Location	Final K_s	Close-loop Inter-Area Mode
Gen-1	17.15	$-0.1062 \pm j2.1190$
Gen-2	4.99	$-0.1046 \pm j2.0889$
Gen-3	21.15	$-0.1051 \pm j2.0981$
Gen-4	4.37	$-0.1050 \pm j2.0971$

Table 3.5: Sensitivity of inter-area mode to overall gain of a PSS.

PSS Location	Effective Gain $ G_p(\lambda) $ ¹	$\Delta\lambda$		Actual sensitivity ²	Residue magnitude
		Mag.	Phase		
Gen-1	25.23	0.10843	171.74	0.004298	0.00566
Gen-2	10.24	0.10669	-172.17	0.010415	0.01234
Gen-3	14.47	0.10633	-177.12	0.007348	0.00870
Gen-4	4.13	0.10629	-176.58	0.025739	0.02552

$$^1 |G_p(\lambda)| = K_s |H_w(\lambda)| |H_p(\lambda)|$$

$$^2 \text{Actual sensitivity} = \frac{|\Delta\lambda|}{|G_p(\lambda)|}$$

3.4.2.2 Parameters Selection Using Frequency Response (Without Any Assumption)

As an alternative to using the residue, the necessary phase compensation can be calculated using the frequency response of the generator and the exciter in conjunction with the participation factors, as described in § 3.3.2.2. In this subsection it is demonstrated, as was anticipated, that if no assumption is employed regarding the value of the participation factors, then the necessary phase compensation and the approximate gain calculated in this manner will be same as if they were calculated using the residue method.

The results of the frequency response between the V_{ref} of the exciter as an input and generator electrical torque as an output of the system are shown in Table 3.6. While evaluating the frequency response, the inertia (H) of the generator of interest was increased to one-hundred times [6].

The necessary phase compensation and the approximate gain calculated using the frequency response method and the residue methods are compared in Table 3.7. The calculated approximate gains using the frequency response method are obtained using (3.16) and using the lead-lag parameters determined based on the residue method that are shown in Table 3.4. The lead-lag parameters determined based on the residue method are used in this case because the necessary phase compensation calculated using the frequency response method is identical to that calculated using the residue method.

The necessary phase compensation and the approximate gain are identical for each method. Hence, a PSS designed using the frequency response method will be identical to a PSS designed using the residue method, provided no assumptions are made regarding the participation factors.

Table 3.6: Frequency response between V_{ref} as input and T_e as output for different generators for inter-area mode frequency.

Location	Mag	Argument (deg)
Gen-1	0.7667	11.70
Gen-2	2.3111	-13.30
Gen-3	0.5878	1.40
Gen-4	1.8056	-10.50

Table 3.7: Necessary phase compensation and the approximate gain calculated using the frequency response method and that calculated using the residue method.

PSS location	Necessary phase compensation (deg)		Approximate gain	
	Frequency response method	Residue method	Frequency response method	Residue method
Gen-1	22.56	22.42	12.76	12.90
Gen-2	40.59	40.56	4.20	4.24
Gen-3	-21.60	-21.55	17.92	18.06
Gen-4	-3.22	-3.15	4.41	4.46

3.4.2.3 Parameters Selection Using the Conventional Method (Approximated Frequency Response)

The conventional PSS design method is a simplified form of the frequency response method using the assumption that the participation factors are positive real values.

It is shown here that a PSS designed using such assumption will not move the critical eigenvalue in the desired direction. As described in § 3.3.2.2, in the conventional method the lead-lag parameters are designed to provide an inverse phase response to that of the combined exciter and generator. The phase response at the inter-area mode frequency between V_{ref} of the exciter as an input and generator electrical torque as an output of the system presented in the previous subsection is reproduced in Table 3.8. The necessary phase compensation calculated using the conventional method is shown in the table and compared to the necessary phase compensation calculated using the residue method. The value of required phase compensation calculated using these two methods differs from the value calculated using the residue method by the angle of participation factor, as expected.

In order to evaluate the conventional method, the lead-lag blocks of the PSS are designed to provide the necessary phase compensation shown in Table 3.8. The PSS parameters and the approximate gain required to improve the damping factor of the inter-area mode to 0.05, calculated using (3.16), are shown in Table 3.9.

The PSSs are installed on different generators as separate cases and the gains, K_s , were further adjusted to achieve the desired damping factor for the inter-area mode. The final values of K_s and the new locations of the inter-area modes are tabulated in Table 3.10. The sensitivity of the eigenvalue to the effective gain shown in Table 3.11 is close to the residues shown in Table 3.3. As predicted in § 3.3.2.2, the eigenvalue moved in the direction opposite to the phase of the participation factors.

Table 3.8: Analysis of the necessary phase compensation using the residue method and using the conventional method (approximated phase compensation).

PSS Location	Frequency response argument (deg)	Phase compensation using		Difference (b-a)	Participation factor argument (deg)
		Conventional method (deg) (a)	Residue method (deg) (b)		
Gen-1	11.70	-14.43	22.42	36.85	-36.99
Gen-2	-13.30	10.57	40.56	29.99	-30.029
Gen-3	1.40	-4.13	-21.55	-17.42	17.46
Gen-4	-10.50	7.77	-3.15	-10.92	10.99

Table 3.9: The PSS parameters designed using the conventional method when a PSS is to be installed on different generators.

Phase Compensation (deg)	T1=T3	T2=T4	Approximate gain
-14.43	0.4181	0.5383	24.21
10.57	0.5203	0.4325	7.19
-4.13	0.4594	0.4938	13.21
7.77	0.5060	0.4418	3.65

Table 3.10: PSS design using conventional method: The final PSS gain that is required to achieve damping ratio of 5.0% for the inter-area mode when the PSS is installed on different generators and the inter-area mode with the PSS.

PSS Location	Adjusted K_s	closed-loop Inter-area Mode
Gen-1	49.20	$-0.1094 \pm j2.1841$
Gen-2	8.55	$-0.1072 \pm j2.1422$
Gen-3	16.50	$-0.1036 \pm j2.069$
Gen-4	3.75	$-0.1038 \pm j2.0752$

Table 3.11: Sensitivity analysis of inter-area mode of the system with a PSS (designed using conventional method) on different generators.

PSS Location	Effective Gain	$\Delta\lambda$		$\angle -p_{jj}^i$	Actual sensitivity
		Mag.	Phase		
Gen-1	38.15	0.13683	143.8649	143.01	0.003587
Gen-2	10.26	0.11504	160.3013	149.98	0.011215
Gen-3	15.31	0.11021	-161.792	-162.54	0.007197
Gen-4	4.28	0.10862	-164.934	-162.54	0.025366

3.5 Conclusions

In this chapter, the conventional PSS and its frequency domain design methods were presented. PSS design is a two-step process. The first step is to identify the most suitable generator to equip with a PSS to ensure that the critical eigenvalues can be moved to a given distance with minimum gain in order to minimize the interference of the PSS with exciter operation. Use of the participation factors, residues, and a combination of these two parameters in the selection of the siting of the PSS were reviewed. It was shown that the use of the residues is the most accurate method and that the use of the participation factors, though they are easy to calculate, is less accurate. The combined use of the participation factor and the residue recommended in [13] is a practical approach for the selection of the optimal location for the PSS in a large power system.

Once the location of the PSS has been determined, the next step is to design the filter, the lead-lag blocks, and the gain components of the PSS. The filters do not play a critical role, and the filter time constant can be selected in a straightforward manner. The design of lead-lag parameters requires knowledge of the necessary phase compensation to be provided at the frequency of interest. The residues and the frequency response based methods, the two most accurate methods for determining the required phase compensation, were described in this chapter. The conventional method, which uses the frequency response based method with the assumption that the participation factor is real, was also analyzed. It was demonstrated that the lead-lag parameters designed based on the results of the residues and the frequency response are identical, and that the new location of the critical eigenvalues can be predicted more accurately. It was also shown that the conventional method is less accurate than the other two methods and should be used with due diligence.

Later in this thesis, the eigenstructure assignment technique is employed in the design of the power system controllers that comprise a filter and a dynamic compensator. The controller siting and filter parameter selection methods used for the

conventional PSS described in this chapter are used in these cases. The dynamic compensator is designed using the new technique and is used in lieu of the lead-lag type compensator of the conventional PSS.

Chapter 4

Eigenstructure Assignment

Technique

The objectives and characteristics of a typical controller in a power system are described in this chapter, followed by description of the eigenstructure assignment technique that is suitable for use in the design of controllers in power systems.

4.1 Power System Controller and Identification of Suitable ESA Technique

The objective of this thesis is to apply the eigenstructure assignment technique in the design of PSS in order to address the small-signal rotor angle stability problem of power systems. In general, the characteristics of the PSS can be summarized as follows:

1. The PSS should relocate the critical modes to relatively more damped locations in the complex plane.
2. The PSS should not introduce unstable or poorly damped modes or degenerate the damping of other modes in the system to an unacceptable level.

3. Since the PSS modulate the voltage reference signal of the exciter, the PSS should not interfere excessively with the normal function of exciter, which is to maintain the voltage to the set value.
4. The combined number of the inputs and outputs of the system is very small compared to the number of states of the system. For example, a typical PSS for a power system would have one system input (the voltage reference signal of the exciter) and a few system outputs (for example, generator rotor speed, terminal voltage, power),but it would have tens of thousands of states.
5. A conventional PSS utilizes a single conveniently available local output of the system as its input, and has a single output that is used as a local input to the system. Usually, it is possible to increase the number of system outputs. However, it is not possible to increase the number of system inputs, which is dictated by the physical arrangement.
6. Generally the structure of the PSSs is such that it can be classified as *output feedback controller*. That is, the input to the PSS is some output of the system, which can be a function of more than one system state variables.
7. A PSS designed for one operating condition should work effectively for a variety of operating conditions and disturbances.

Researchers have proposed several algorithms for controller design that assign suitable eigenstructure [23]. Each of these algorithms has been developed to address a specific control system problem.

The parametric approach to assign eigenstructure developed in [24] was identified as the most suitable among those reviewed in terms of applicability to power system controller design. Its important features are described below.

1. It offers a parametric solution for the controller, allowing implementation of optimization using the parametric vectors as decision variables. This is a very

useful feature because, as identified later, optimization is a necessary part of the controller design for power system applications.

2. It is possible to assign q eigenvalues where $1 < q < \min(n, m + r - 1)$. Hence, assignment of the complete spectrum is not a prerequisite to obtain a solution of the proportional output feedback controller.
3. The conditions and requirements in the solution of the output feedback controller are as follows:
 - Open-loop eigenvalues cannot be assigned to the closed-loop system.
 - Only real or complex conjugate pairs of eigenvalues can be assigned to the closed-loop system.

The above conditions are easy to satisfy during the design of controllers for power systems.

4. Either the right, the left, or both eigenstructures can be assigned. (However, the number of inputs and outputs of the system will determine the available degrees of freedom in the assignment of eigenvectors. Also, the input and output variables will be key variables in determining the assignable eigenvectors. The degrees of freedom and the assignable eigenvectors are general results of the eigenstructure assignment method and are not limited to just this particular technique.)

The technique is inadequate from the power system controller design perspective because of the following:

1. In the case of a power system, the combined number of system inputs and outputs is very few compared to the number of states of the system. Hence, when using the eigenstructure assignment technique it is not possible to assign the complete spectrum; rather, only a subset of eigenvalues can be assigned.

This leaves the possibility that some of the closed-loop eigenvalues from the remaining subset are unacceptable; and such unacceptable eigenvalues could not be anticipated or discovered during the design of the controller.

2. The objective of a PSS is to relocate the critical eigenvalues to new preselected locations in the complex plane. A controller designed using the technique will assign the prescribed set of eigenvalues (and additionally the associated eigenvectors) to the closed-loop system; however, it is not possible to ensure that the eigenvalues deemed critical have moved to the prescribed locations.

These inadequacies will pose some challenges when the technique is applied in the design of controllers for power systems, and it cannot be applied in the manner in which it has been applied in the design of controllers for small systems. A new optimization based algorithm for controller design is presented in this thesis to address the inadequacies of the technique for use in power system controller design. These inadequacies, their implications, and a new algorithm based on the eigenstructure assignment technique are discussed in next chapter. The eigenstructure assignment technique developed in [24] is presented in the following sections.

4.2 The Control System

In this section, the linear control system model of a power system and the dynamic compensator type output feedback controller are described. The linear system is transformed into an equivalent augmented system in which the dynamic compensator is transformed into a proportional output feedback controller. Later, a proportional output feedback controller is designed for this system using the eigenstructure assignment technique.

The linearized uncompensated power network in state variable form can be de-

scribed as

$$\begin{aligned}\dot{\bar{x}}(t) &= \bar{A}\bar{x}(t) + \bar{B}\bar{u}(t) \\ \bar{y}(t) &= \bar{C}\bar{x}(t)\end{aligned}\tag{4.1}$$

where $\bar{x}(t) \in \mathbb{R}^{\bar{n}}$, $\bar{u}(t) \in \mathbb{R}^{\bar{m}}$, and $\bar{y}(t) \in \mathbb{R}^{\bar{r}}$ are the state, control input, and output vector of the system, respectively, and \bar{A} , \bar{B} , and \bar{C} are the constant real plant, input, and output matrix of the system, respectively. In (4.1), it is assumed that the output is only a function of the states and not a function of the input, which is generally true for linearized power systems. The state-space representation of a power system includes any dynamics associated with the filters employed for the system outputs.

Let the dynamic output feedback control law described using

$$\begin{aligned}\dot{z}(t) &= D z(t) + E \bar{y}(t) \\ \bar{u}(t) &= F z(t) + G \bar{y}(t)\end{aligned}\tag{4.2}$$

be applied to the system (4.1), where $z(t) \in \mathbb{R}^a$ is the state vector of the controller and D , E , F , and G are matrices of appropriate dimensions that describe the dynamics of the controller. During the design of a PSS, the dimension of dynamic compensator state vector $z(t)$, a , is selected judiciously as described later in this thesis. In a special case of $a = 0$ the matrices D , E , and F vanish and the dynamic output feedback control system reduces to proportional output feedback control system given by

$$\bar{u}(t) = G \bar{y}(t).\tag{4.3}$$

For the case of $a > 0$, the system in (4.1) can be transformed into an equivalent proportional output feedback control system as described by [25]

$$\begin{aligned}\dot{x}(t) &= A x(t) + B u(t) \\ y(t) &= C x(t) \\ u(t) &= K y(t)\end{aligned}\tag{4.4}$$

where the new plant, input, and the output matrices, and the proportional output feedback matrix are given by

$$A = \begin{pmatrix} \bar{A} & 0 \\ 0 & 0 \end{pmatrix}, B = \begin{pmatrix} \bar{B} & 0 \\ 0 & I_a \end{pmatrix}, C = \begin{pmatrix} \bar{C} & 0 \\ 0 & I_a \end{pmatrix}, K = \begin{pmatrix} G & F \\ E & D \end{pmatrix} \quad (4.5)$$

and the new state, input, and output vectors are given by

$$x(t) = \begin{pmatrix} \bar{x}(t) \\ z(t) \end{pmatrix}, u(t) = \begin{pmatrix} \bar{u}(t) \\ \dot{z}(t) \end{pmatrix}, y(t) = \begin{pmatrix} \bar{y}(t) \\ z(t) \end{pmatrix}. \quad (4.6)$$

The modified system in (4.4) will have n, m , and r states, inputs, and outputs, respectively, where

$$n = \bar{n} + a, \quad (4.7a)$$

$$m = \bar{m} + a, \quad (4.7b)$$

$$r = \bar{r} + a. \quad (4.7c)$$

Without loss of generality, the following assumption is made for the system (4.4)

$$\text{rank}(B) = m; \text{rank}(C) = r. \quad (4.8)$$

The resulting closed-loop system can be described as

$$\dot{x}(t) = (A + B K C)x(t) = A_c x(t). \quad (4.9)$$

In the following subsection, the eigenstructure assignment technique for a linear output feedback control system is presented. This technique is directly applicable to the system given by (4.1) when proportional output feedback is employed (i.e., $a = 0$). When dynamic output feedback control law is employed, i.e., $a > 0$, the analysis can be applied in a straightforward manner to its equivalent system (4.4). The parametric approach to assign left and/or right eigenstructure developed in [24] is presented in the following section.

4.3 The Partial Eigenstructure Assignment Technique

The eigenstructure assignment problem is to determine gain matrix K in (4.4) such that the closed loop system plant matrix A_c in (4.9) is assigned a prescribed self conjugate set of eigenvalues and associated permissible right and/or left eigenvectors. The left and right eigenstructure assignment technique developed in [24] is presented in the following subsection. In this approach, the prescribed set of eigenvalues to be assigned to the closed-loop system is selected first, and then the solution of assignable (left or right) eigenvectors and, subsequently, the solution of the gain matrix K is obtained as a function of the set of free parametric vectors. The distribution of degrees of freedom in assigning eigenvalues and eigenvectors using the eigenstructure assignment technique is discussed in a subsequent subsection to provide insight into the solution to the eigenstructure assignment problem offered by this technique.

4.3.1 Partial Left Eigenstructure Assignment

Let the partial set of distinct self-conjugate eigenvalues $\{\lambda_1, \dots, \lambda_p\}$, $p \leq m \leq n$ be assigned to the closed-loop system matrix A_c in (4.9). The conditions for the eigenvalues to be assigned are explained later in the section. The left eigenvector associated with λ_i ; $i = 1, \dots, p$ is given by [24]

$$w_i^T = g_i^T C (\lambda_i I_n - A)^{-1}; \quad i = 1, \dots, p \quad (4.10)$$

where the r -dimensional parametric vectors g_i ; $i = 1, \dots, p$ can be arbitrarily selected.

For the case of $p < m$, the $m \times r$ matrix K and the $n \times m$ matrix B are partitioned as

$$K = \begin{pmatrix} K_1 \\ K_2 \end{pmatrix}, B = [B_1 \quad B_2] \quad (4.11)$$

where K_1 and K_2 are of dimension $p \times r$ and $(m - p) \times r$, respectively; and B_1 and

B_2 are of dimension $n \times p$ and $n \times (m - p)$, respectively. Then, the output feedback controller gain matrix K_1 that will assign the desired eigenstructure, $\{\lambda_1, \dots, \lambda_p\}$, $\{w_1, \dots, w_p\}$, to the closed-loop system is given by [24]

$$K_1 = (W_p B_1)^{-1} (G_p - W_p B_2 K_2) \quad (4.12)$$

where K_2 is arbitrary and

$$W_p = \begin{pmatrix} w_1 & \dots & w_p \end{pmatrix}^T; \quad G_p = \begin{pmatrix} g_1 & \dots & g_p \end{pmatrix}^T. \quad (4.13)$$

There remain unused degrees of freedom for the case of $p < m$, resulting in non-unique K due to arbitrary K_2 . Whereas all the available degrees of freedom are utilized for the case of $p = m$, in which case the partition of K and B according to (4.11) is not required and from (4.12) the unique solution of K for a given parametric vectors matrix G_m is given by:

$$K = (W_m B)^{-1} G_m. \quad (4.14)$$

Equations (4.10), (4.12), and (4.14) give solutions of (w_1, \dots, w_m) , K_1 and K as a function of free parametric vectors (g_1, \dots, g_m) and assigned eigenvalues $(\lambda_1, \dots, \lambda_m)$. The assigned eigenvalues and the free parameter vectors must satisfy the following conditions [24]:

1. A necessary condition for the assigned (closed-loop) eigenvalues is that they must be different from the n original (open-loop) eigenvalues. This follows from the invertibility requirement of the matrices $(\lambda_i I_n - A)^{-1}$ in (4.10).
2. The necessary and sufficient condition for real eigenvalue λ_i to be assignable to the closed-loop is

$$\text{rank}(C((\lambda_i I_n - A)^{-1})B) \geq 1.$$

By extension of the above, the complex conjugate pair of eigenvalues λ_i, λ_i^* is assignable if

$$\text{rank}[C((\lambda_i I_n - A)^{-1})B C((\lambda_i^* I_n - A)^{-1})B] \geq 2.$$

3. The matrix $W_m B$ must be full rank (i.e., $|W_m B| \neq 0$) so that $(W_m B)^{-1}$ exists and K_1 and K can be calculated using (4.12) and (4.14), respectively.
4. For the design to be physically implementable, the matrix K must be real. For that reason, the parametric vector g_i must be real if the corresponding eigenvalue λ_i is real. Similarly, if the assigned eigenvalues form a complex conjugate pair the corresponding parametric vector, must also form a complex conjugate pair.

4.3.2 Partial Right Eigenstructure Assignment

Let the partial set of distinct self-conjugate eigenvalues $\{\lambda_1, \dots, \lambda_p\}$, $p \leq r \leq n$ be assigned to the closed-loop system matrix A_c in (4.9). Then, using the non-unique m -dimensional free parametric vectors f_i , $i = 1, \dots, p$, the right eigenvector associated with λ_i , $i = 1, \dots, p$ is given by [24]

$$v_i = (\lambda_i I_n - A)^{-1} B f_i; \quad i = 1, \dots, p. \quad (4.15)$$

For the case of $p < r$, the $m \times r$ matrix K and the $r \times n$ matrix C can be partitioned as

$$K = [K_1 \quad K_2], \quad C = \begin{pmatrix} C_1 \\ C_2 \end{pmatrix} \quad (4.16)$$

where K_1 and K_2 are of dimension $m \times p$ and $m \times (r - p)$, respectively, and C_1 and C_2 are of dimension $p \times n$ and $(r - p) \times n$, respectively. Then, the output feedback controller gain matrix K_1 that will assign the desired eigenstructure, $\{\lambda_1, \dots, \lambda_p\}$, $\{v_1, \dots, v_p\}$, to the closed-loop system is given by [24]:

$$K_1 = (F_p - K_2 C_2 V_p) (C_1 V_p)^{-1} \quad (4.17)$$

where K_2 is arbitrary and

$$V_p = \begin{pmatrix} v_1 & \dots & v_p \end{pmatrix}; F_p = \begin{pmatrix} f_1 & \dots & f_p \end{pmatrix}. \quad (4.18)$$

Similar to the case of left eigenstructure assignment, there remain unused degrees of freedom if $p < r$, resulting in non-unique K due to arbitrary K_2 . Whereas all the available degrees of freedom are utilized for the case of $p = r$, in which case the partition of K and C according to (4.16) is not required and from (4.17) the unique solution of K is given by

$$K = F_m (C V_m)^{-1}. \quad (4.19)$$

Equations (4.15), (4.17), and (4.19) give solutions of (v_1, \dots, v_m) , K_1 , and K in terms of free parametric vectors (f_1, \dots, f_m) , and assigned eigenvalues $(\lambda_1, \dots, \lambda_m)$. The assigned eigenvalues and the free parameter vectors must satisfy the following conditions [24]:

1. A necessary condition for the new assigned (closed-loop) eigenvalues is that they must be different from the n original (open-loop) eigenvalues. This follows from the invertibility requirement of the matrix $(\lambda_i I_n - A)^{-1}$ in (4.15).
2. The necessary and sufficient condition for a real closed-loop eigenvalue λ_i to be assignable to the closed-loop system is

$$\text{rank}(C((\lambda_i I_n - A)^{-1})B) \geq 1;$$

and for a complex conjugate pair of eigenvalues λ_i, λ_i^* it is

$$\text{rank}[C((\lambda_i I_n - A)^{-1})BC((\lambda_i^* I_n - A)^{-1})B] \geq 2.$$

3. The matrix $C_1 V_m$ must be full rank (i.e., $|C_1 V_m| \neq 0$) so that $(C_1 V_m)^{-1}$ exists and K_1 and K can be calculated using (4.17) and (4.19), respectively.

4. For the design to be physically implementable, the matrix K must be real. Therefore, the parametric vector f_i must be real if the corresponding eigenvalue λ_i is real. Similarly, if the eigenvalues to be assigned form a complex conjugate pair λ_i, λ_i^* the corresponding parametric vector must also form a complex conjugate pair f_i, f_i^* .

4.3.3 Discussion

In the design procedure, the total degrees of freedom available are mr , which corresponds to the independently selectable number of elements of the proportional gain output feedback matrix K .

The possible distribution of available degrees of freedom in the design of proportional output feedback controller using the partial left eigenstructure assignment technique presented in § 4.3.1 is described in the following. Similar results regarding the possible distribution of the degrees of freedom using the right eigenstructure assignment technique can be obtained by like analysis of the technique that is presented in § 4.3.2.

1. Using the partial left eigenstructure assignment technique, it is possible to assign up to m eigenvalues utilizing equal amounts of degrees of freedom. Each of the associated left eigenvectors can be selected using the r -dimensional parametric vector suggesting the utilization of r degrees of freedom in each eigenvector. However, multiplying a left eigenvector by a constant is essentially the same eigenvector, and therefore, only $(r - 1)$ degrees of freedom are consumed in the selection of each of the eigenvectors. If $p < m$ eigenvalues and associated left eigenvectors are assigned, then p degrees of freedom are utilized in the assignment of the eigenvalues and $p(r - 1)$ are utilized in assignment of the left eigenvectors, resulting in a total utilization of $p + p(r - 1) = pr$ degrees of freedom.

2. For the case of $p = m$, all the degrees of freedom available in the selection of output feedback matrix are utilized.
3. A maximum of $(r - 1)$ entries of the left eigenvector associated with each of eigenvalues can be selected precisely.
4. The left eigenvector associated with each of the eigenvalues that can be assigned to the closed-loop system matrix lie in r -dimensional subspace spanned by rows of $C(\lambda_i I_n - A)^{-1}$.
5. If the number of inputs to the system are same as the number of states (i.e., $m = n$), then it is possible to assign the complete spectrum.
6. For the case of $p < m$, $(m - p)r$ degrees of freedom are unused and can be utilized in further assignment of the right or left eigenstructure.

4.4 Conventional Eigenstructure Assignment Procedure

The right or left eigenstructure assignment techniques presented in the previous section may be employed in the design of a proportional output feedback controller in the following manner.

Select the eigenvalues to assign:

The first step is to select eigenvalues to assign to the closed-loop system that satisfy the conditions described in § 4.3.1 (if left eigenstructure assignment technique is to be employed) or § 4.3.2 (if the left eigenstructure assignment technique is to be employed) so that they are assignable.

Select the eigenvectors to assign:

After selecting the desired closed-loop eigenvalues, the next step is to select

the desired eigenvector associated with each of the eigenvalues based on the system performance criteria. However, a desired eigenvector may not reside in the allowable subspace and therefore cannot be achieved. In that case, an optimal choice for an achievable eigenvector can be made by projecting the desired eigenvector onto allowable subspace.

Determine the free parametric vectors:

Once the desired and allowable choice of eigenvalues and eigenvector has been made, the free parametric vectors can be uniquely determined by back-solving the linear system of equations of the right or left eigenvectors as the case may be.

Calculate the controller gain matrix K :

As a final step, the controller gain matrix can be calculated by appropriately using (4.12), (4.14), (4.17), or (4.19).

Using the above single stage procedure and employing the left eigenstructure assignment technique, a maximum m eigenvalues can be assigned along with precise selection of $(r - 1)$ elements in each of the associated left eigenvectors. If the partial right eigenstructure assignment technique is employed, then a maximum r eigenvalues can be assigned along with the precise selection of $(m - 1)$ elements in each of the associated left eigenvectors.

Thus, in a single-stage process, the maximum eigenvalues that can be assigned to the closed-loop system is $\min\{\max(m, r), n\}$, and if $\max(m, r) < n$, then the complete spectrum cannot be assigned. However, if the number of system inputs and outputs is such that $\max(m, r) < n \leq (m + r - 1)$, then it is possible to assign the complete spectrum because, as noted earlier, by using a proportional output feedback controller the maximum number of eigenvalues that can be assigned is $\min(n, m + r - 1)$. The assignment of the complete spectrum can be accomplished in two or more stages by successive application of the above described procedure. After

each stage is completed, and before proceeding to the next stage, the already assigned eigenstructure can be preserved by appropriately modifying the control system [24]. In general, however, the multistage controller design process results in the reduced degrees of freedom in assignment of right and/or left eigenvectors.

For small system to which the eigenstructure assignment technique has successfully been applied, it is possible to achieve the condition of $\min(n, m + r - 1) = n$ and, thereby, it is possible to assign n eigenvalues. A power network is considerably different than small systems. The assignment of all the eigenvalues is not feasible for a large-scale power network because it is not possible to achieve the above condition. Hence, straightforward application of the eigenstructure assignment technique (single stage or multistage) in the manner described above is not suitable and is at risk for some potential problems. The challenges that arise when applying the conventional procedure in the design of controllers for power systems are discussed and the optimization based design algorithm to address these challenges is presented in the following chapter.

Chapter 5

PSS Design Algorithm Based on the Partial Left Eigenstructure Assignment Technique

In this chapter, first the conventional lead-lag type PSS described in Chapter 3, which is the most suitable for frequency domain design, is assessed as to its suitability for the application of the eigenstructure assignment technique. Based on this assessment, a conventional PSS is shown to be unsuitable due to the insufficient degrees of freedom offered by the structure of the PSS. Then the generic dynamic compensator type PSS is justified.

In the previous chapter, the objectives and requirements of a power system controller were identified. Also, an elegant and simple parametric eigenstructure assignment technique was presented. However, the application of that technique in the design of a power system controller is inadequate when applied in a conventional manner. The shortcomings of the conventional eigenstructure assignment based controller design procedure for meeting the objectives and requirements of a power system controller are identified in this chapter. This is followed by a description of the use of an optimization based algorithm to address the inadequacies of the conventional tech-

nique. Finally, the complete power system controller design procedure that can be used to assign optimal eigenstructure is presented in this chapter.

5.1 Suitable PSS Model

The PSS models widely used in power systems are described in IEEE Std. 421.5-2005 [8]. These PSS models comprise two or three phase-compensation blocks of first or second order transfer functions. This allows the designer to design the controller with a certain frequency response. PSSs with similar structures have been in use since the 1960s. These conventional PSSs were discussed in Chapter 3.

The eigenstructure assignment method is an alternate method of controller design. The parametric solution for the proportional output feedback controller was presented in Chapter 4. The solution assumes that each parameter of the controller is independent and can be assigned an arbitrary real value. This provides the maximum degrees of freedom possible for a given number of system inputs and outputs. The eigenstructure assignment technique based on this assumption forms the basis of the PSS design algorithm presented in this thesis.

It is possible to design the conventional PSS comprising lead-lag type phase compensators, shown in Fig. 5.1, using the proposed algorithm to assign the eigenstructure; however, the structure of the PSS will not offer all the possible degrees of freedom. The design of the gain and lead-lag blocks parameters is usually the main focus of the design; they are marked as “Dynamic Compensator” in Fig. 5.1. For the purpose of the design of the gain and lead-lag blocks parameters using the eigenstructure assignment technique, the dynamic compensator needs to be transformed into state-space form and then into an equivalent proportional output feedback controller.

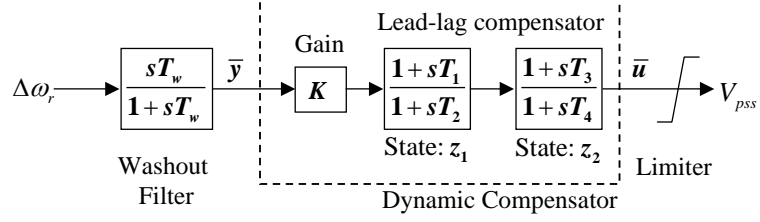


Figure 5.1: Block diagram of single input lead-lag type PSS.

It can be shown that the proportional output feedback controller K given by

$$K = \begin{pmatrix} \frac{K T_1 T_3}{T_2 T_4} \left(\frac{T_3}{T_4} - \frac{T_1 T_3}{T_2 T_4} \right) \left(1 - \frac{T_3}{T_4} \right) & & \\ \frac{K}{T_2} & \frac{-1}{T_2} & 0 \\ \frac{K T_1}{T_2 T_4} \left(\frac{1}{T_4} - \frac{T_1}{T_2 T_4} \right) & \frac{-1}{T_4} & \end{pmatrix} \quad (5.1)$$

is one of the representations of the dynamic compensator output feedback controller. The proportional controller K of dimension 3×3 given by (5.1) has only five independently assignable parameters. This is consistent with the number of independently selectable PSS parameters, $K, T_1 - T_4$. The remaining four elements of K are either dependent parameters or have fixed values. The number of free elements in the set of parametric vectors cannot be greater than the number of independently assignable controller parameters. So, in such a case the number of arbitrarily assignable elements in the set of parametric vectors is reduced to five. Thus, design of a conventional PSS using the proposed technique renders less degrees of freedom. This is not desirable since as many degrees of freedom are needed as possible in order to be able to assign the best eigenvector.

Even if the maximum possible number of free parameters are selected (five in this case), then the calculation of K and the extraction of the PSS parameters requires additional processing. The novel approach to controller design presented later in this chapter requires the minimization of an objective function using the optimization technique. The additional processing required is especially onerous for such an optimization-based approach. Therefore, the design of a conventional PSS using the proposed techniques increases the computational burden in addition to offering

reduced degrees of freedom.

Therefore, in order to utilize every possible degree of freedom and to minimize the computational burden, a state-space type power system controller, shown in Fig. 5.2, is considered in this thesis when designing a controller using the eigenstructure assignment technique. It consists of two functional blocks: (1) a filter, and (2) a dynamic compensator. The filter serves a purpose similar to that of the conventional PSS described earlier in § 3.3.1, and the filter parameter is selected accordingly. Any dynamics associated with filters are included in the state-space representation of a linearized power system described by § 4.2. The dynamic compensator is the main controller in a state-space (SS) type PSS described by

$$\begin{aligned}\dot{z} &= D z + E \bar{y} \\ \bar{u} &= F z + G \bar{y}.\end{aligned}\tag{5.2}$$

where

$$z \in \mathbb{R}^a, \bar{y} \in \mathbb{R}^{\bar{r}}, \bar{u} \in \mathbb{R}^{\bar{m}}.$$

The objective of the proposed eigenstructure assignment based design algorithm is to determine the parameters of the dynamic compensator that will assign optimal eigenstructure. The dimension of the state vector a is a design parameter and a method for its selection is detailed later. As described in § 4.2, a system with such a controller can be transformed into an equivalent system having a proportional output feedback controller whose parameters are independently selectable.

5.2 Suitability of Right and Left Eigenstructure Assignment for PSS Design

In this section, the suitability of the partial right and left eigenstructure assignment techniques are examined from the point of view of their application to power systems.

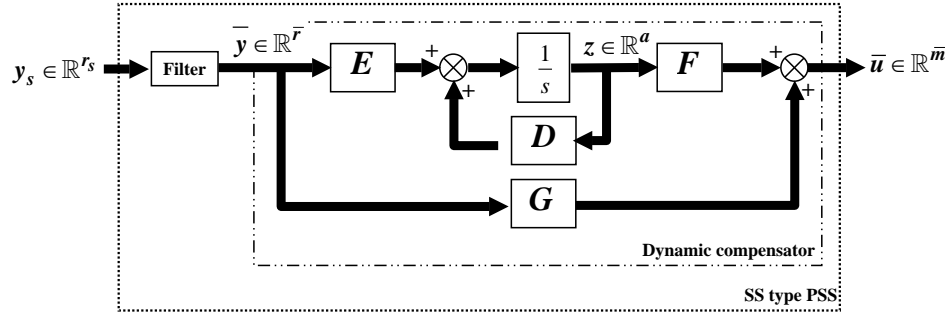


Figure 5.2: Block diagram of the state-space (SS) type PSS that is designed using the proposed eigenstructure assignment technique.

5.2.1 Possible Inputs and Outputs of the System

The operating condition of a generator in a power system is uniquely defined by the generated power and the voltage of a bus (usually its own, but it can be that of some other system bus). Therefore, a generator control system provides two inputs for reference signals, which are set by operator, to achieve the desired power generation and voltage when system is operating in a closed-loop: (a) V_{ref} of an exciter to generate the desired bus voltage; (b) P_{ref} of the prime-mover governor to generate the desired electrical power.

Transient and small-signal stability enhancement are the main objectives of the PSS. To be effective in achieving these objectives “the controller must act within 0.5 to 0.75 s following a disturbance during when the generator rotor angle swing normally peaks” [6]. The turbines are inherently slow in response to change in the P_{ref} of the governor and cannot respond that quickly. Therefore, modulating P_{ref} of the governor is not effective in achieving the objectives. Whereas “use of high-initial-response excitation systems supplemented with PSS is by far the most effective and economical method of enhancing the overall system stability” [6]. Thus, the possible maximum number of system input is one (i.e., $\bar{m} = 1$ in (4.1)) when designing a controller of the generator to address the small-signal stability problem.

The speed of the generator, its terminal voltage, and its electrical power are

the most common outputs of the system employed as input(s) to the PSS for the following reasons: a) the electromechanical modes, which are usually of concern, are most observable in these outputs; b) the outputs are easy to measure. Therefore, there is some freedom in selecting the number of outputs of the system (i.e., $\bar{r} \geq 1$ in (4.1)) when designing the PSS of a generator.

The objective of employing a controller is to push the critical electromechanical oscillatory modes further left in the complex plane. Hence, the controller should be able to assign at least two eigenvalues (i.e., $p \geq 2$) to the system. If more than one critical mode is to be addressed, the controller shall be able to assign even more eigenvalues.

So, considering $\bar{m} = 1$, $\bar{r} \geq 1$, and $p \geq 2$, and assuming that a dynamic compensator of any dimension can be selected, the suitability of partial left and right eigenstructure assignment techniques are analyzed in following subsection.

5.2.2 Assessment of Right and Left Eigenstructure Assignment

The right eigenvector of a mode determines the presence of that mode in different state variables during disturbances; whereas, the left eigenvector of a mode determines the excitation magnitude of that mode during disturbances (§ 1.2). Thus, appropriate assignment of the right and/or left eigenstructure will improve the dynamical performance of the system. However, it is not possible to assign any desired eigenvector. The input and output matrices are the key parameters that determine the subspace where the assignable right and left eigenvector, respectively, lie, as was described in Chapter 4. In what follows, the suitability of the right and left eigenstructure assignments are assessed from the point of view of the available freedom in selection of the number of system inputs and outputs for the case of power systems, which was discussed in the previous section.

Using the partial right eigenstructure assignment technique, the maximum number

of eigenvalues that can be assigned to the closed-loop system is the same as the number of outputs of the system. If the number of eigenvalues to be assigned exceeds the number of outputs of the system, a dynamic compensator with the appropriate number of states can be employed. Hence, as many eigenvalues as desired (up to the combined number of system and dynamic compensator states) can be assigned to the closed-loop system by employing a dynamic compensator with the appropriate number of states. .

In order to assess the assignability of the right eigenvectors, consider, for the sake of simplicity, a real eigenvalue λ_i is to be assigned to the closed-loop system. The assignable right eigenvector associated with the real eigenvalue λ_i is a combination of the columns of the matrix $M_{nm} = (\lambda_i I_n - A)^{-1} B$ of dimension $n \times m$. Substituting for A and B from (4.5) reveals that the right eigenvector is a combination of columns of

$$M_{nm} = \begin{pmatrix} (\lambda_i I_n - \bar{A})^{-1} \bar{B} & 0 \\ 0 & \frac{1}{\lambda_i} I_a \end{pmatrix} = \begin{pmatrix} M_{\bar{n}\bar{m}} & 0 \\ 0 & M_{aa} \end{pmatrix}. \quad (5.3)$$

In (5.3) the partitioned matrix $M_{\bar{n}\bar{m}}$ has \bar{m} columns. It is apparent that the right eigenvector entries corresponding to the system states are linear combinations of the columns of $M_{\bar{n}\bar{m}}$. As identified in the previous section, $\bar{m} = 1$ is the usual case when designing a PSS for a power system. In this case the matrix $M_{\bar{n}\bar{m}}$ degenerates to a column vector and the entries corresponding to the system states are scalar multiple of that column vector. Therefore, using a single input PSS, the magnitude of the entries of the right eigenvector corresponding to the system states can be altered; however, the underlying structure of the right eigenvector that determines the relative presence of the modal variable in the state variables remains unaltered. A similar conclusion can be drawn regarding the right eigenvectors of an assignable complex conjugate pair of eigenvalues.

Using the partial left eigenstructure assignment technique, the maximum number of eigenvalues that can be assigned to the close-loop system is the same as the number of inputs of the system. If the number of eigenvalues to be assigned exceeds the

number of system inputs, then, somewhat like the previous case, the effective number of the system inputs can be increased by employing a dynamic compensator with the appropriate number of states, and as many eigenvalues as desired (up to the combined number of system and dynamic compensator states, maximum) can be assigned to the closed-loop system. The left eigenvector associated with each of the real eigenvalues to be assigned is a combination of the rows of the $m \times n$ matrix $M_{rn} = C(\lambda_i I_n - A)^{-1}$. Substituting C and A by (4.5) yields that the left eigenvector is obtained by a combination of the rows of the matrix M_{rn} given by

$$M_{rn} = \begin{pmatrix} \bar{C}(\lambda_i I_n - A)^{-1} & 0 \\ 0 & \frac{1}{\lambda_i} I_a \end{pmatrix} = \begin{pmatrix} M_{\bar{r}\bar{n}} & 0 \\ 0 & M_{aa} \end{pmatrix}. \quad (5.4)$$

In (5.4) the partitioned matrix $M_{\bar{r}\bar{n}}$ has \bar{r} rows and M_{aa} has a rows. If $\bar{r} = 1$, then the available degrees of freedom are not sufficient to alter the structure of the part of the left eigenvector that is associated with the system states. Thus, for such a control system the relative contribution of system states to the excitation of the mode remains unaltered. However, it is always possible to employ an increased number of outputs of the system (i.e., constructing the system with $\bar{r} > 1$). In that case, the left eigenvector entries corresponding to the system states are linear combinations of rows of the matrix $M_{\bar{r}\bar{n}}$. This allows the selection of an alternate structure for the part of the left eigenvector associated with the system states. Thus, the eigenvectors closer to the desired one can be assigned by employing increased system outputs.

In order to assess the advantage of left eigenstructure assignment, consider a linear time invariant control system $\dot{x} = Ax$. The free response of the state variable $x_i(t)$ is given by [6]

$$x_i(t) = \sum_{j=1}^n v_{ji} c_j e^{\lambda_j t} \quad (5.5)$$

where

$$c_j = \sum_{k=1}^n w_{jk} x_k(0) \quad (5.6)$$

where v_i and w_i are right and left eigenvectors of eigenvalue λ_i , and $x(0)$ is the initial condition of the state vector.

The elements of the left eigenvector w_j can be selected to give a small value for c_j , the magnitude of excitation of the j th mode. However, it is the product $v_{ji}c_j$ which really determines the presence of the j th mode in state variable response $x_i(t)$. Therefore, it is theoretically possible that reducing c_j may still result in a larger $v_{ji}c_j$ and the presence of the j th mode in state variable x_i is increased. This may defeat the prime objective of the controller design, which is improvement in the transient response of the state variables by means of a reduction in the magnitude of the assigned mode. However, this possibility is unlikely for a single input system. Because, as argued in previous subsection, for such a system (a system with a single input) it is not possible to alter the right eigenstructure of the system.

It is clear from above analysis that if a control system permits only a single system input and more than one system output, there would be a greater possibility of assigning the left eigenstructure closer to the one desired than would be the case if the right eigenstructure were assigned. Therefore, in this thesis the design algorithm has been developed to assign the left eigenstructure when designing controllers for power systems. However, the algorithm can be extended without much modification to assign the right eigenstructure if that is the design requirement for a multi-input system.

5.3 Inadequacy of Conventional Left Eigenstructure Assignment Technique for Power System Controller Design[4]

For smaller systems, to which the left eigenstructure assignment technique has successfully been applied in the past [23], the available degrees of freedom permit assign-

ment of all the eigenvalues (and additionally, partial right and/or left eigenvectors) by following the conventional procedure described in § 4.4. Power systems are much different from smaller systems. Assignment of all the eigenvalues is not feasible in a much larger power system because it is not practical to obtain information from remote geographic locations. Also, assigning all the eigenvalues (which could number in the tens of thousands) is computationally impractical. Hence, only a smaller subset of m eigenvalues can be assigned. This can potentially result in the deficiencies described below.

5.3.1 The Objectives of Left Eigenstructure Assignment Technique Based Controller Design

Consider the linearized proportional output feedback power system with n -state, m -input, and r -output, developed in § 4.2

$$\dot{x}(t) = A x(t) + B u(t) \quad (5.7a)$$

$$y(t) = C x(t) \quad (5.7b)$$

$$u(t) = K y(t). \quad (5.7c)$$

By substituting for $u(t)$ and $y(t)$ in (5.7a), the closed-loop system can be described as

$$\dot{x}(t) = (A + B K C)x(t) = A_c x(t). \quad (5.8)$$

Based on the linear analysis of the system, the m -eigenvalues of the open-loop plant matrix must be relocated from $\bar{\Lambda}_m = \{\bar{\lambda}_1, \dots, \bar{\lambda}_m\}$ to a new location $\Lambda_m = \{\lambda_1, \dots, \lambda_m\}$. Then the desired objectives can be stated as follows:

- Move $\bar{\Lambda}_m$ to Λ_m .
- Assign the left eigenvectors W_m , corresponding to the set of eigenvalues Λ_m , to the closed-loop system that will minimize the excitation of the critical modes.

- The modes corresponding to the remaining $(n - m)$ closed-loop eigenvalues must be stable and well-damped.
- The controller should be able to achieve above objectives without excessive control action.

The straightforward application of eigenstructure assignment according to the procedure described in § 4.4 can fail to achieve the controller design objectives, as described below.

5.3.2 Critical Eigenvalues May Not Move to Desired Locations

The design procedure does indeed assign the desired eigenvalue $\{\lambda_1, \dots, \lambda_m\}$ to the closed-loop system. However, there is no guarantee that it is precisely the previously targeted critical eigenvalues $\bar{\Lambda}_m = \{\bar{\lambda}_1, \dots, \bar{\lambda}_m\}$ that have moved to the desired new locations. It is possible that some other open-loop eigenvalues (previously deemed non-critical) may have moved to the assigned locations. Fig. 5.3.a shows that eigenvalue $\bar{\lambda}_j$ was supposed to occupy location λ_j , but instead it is $\bar{\lambda}_k$ that has done so. In such a case, the objective of PSS design is defeated for two reasons: (1) the critical mode may move further to the right in the complex plane making it an even more poorly damped mode or, in the worst case, making the system unstable, as shown in Fig. 5.3a; (2) even if a critical eigenvalue $\bar{\lambda}_j$ move to an acceptable region, but not precisely to the assigned location λ_j , the design may fail to achieve the objective because the eigenvector associated with the new location of the critical eigenvalue will be unknown during design and it would not be possible to determine whether the eigenvector has been altered as desired.

5.3.3 The Set of Unassigned Eigenvalues May be Unacceptable

Even if the design moves all critical $\bar{\Lambda}_m$ precisely to Λ_m , a number of unassigned eigenvalues may move to unacceptable locations in the complex plane, as shown by the movement of eigenvalue $\bar{\lambda}_u$ to λ_u in Fig. 5.3.b. This is again due to the fact that for the power system controller design problem it is practically possible to assign only a subset of the m eigenvalues of the n system eigenvalues and, using the conventional approach, there is no control over the unassigned eigenvalues.

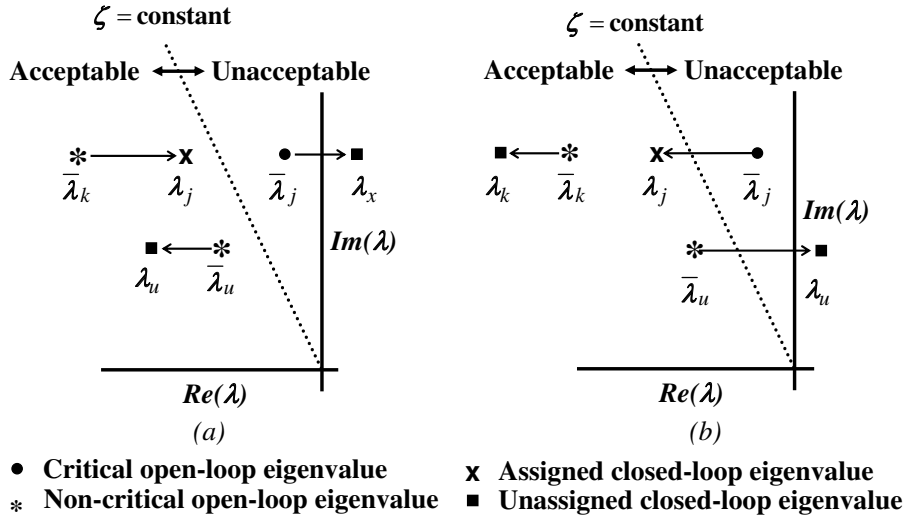


Figure 5.3: Potential problems with conventional left eigenstructure assignment technique (a) Critical eigenvalue $\bar{\lambda}_j$ gets worse while non-critical eigenvalue $\bar{\lambda}_k$ moves to assigned location λ_j ; (b) Non-critical eigenvalue $\bar{\lambda}_u$ becomes unstable.

Thus, controller design objectives cannot be achieved using a straightforward application of the partial left eigenstructure assignment technique. A modified multi-objective nonlinear optimization problem (MONLOP) algorithm that uses the iterative method is introduced in this thesis to address these problems.

5.4 Multi-Objective Nonlinear Optimization Problem (MONLOP)[4]

A major contribution of this thesis is the development of a procedure that overcomes the drawbacks of the straightforward application of the eigenstructure assignment technique described in the previous section. The proposed technique reformulates the left eigenstructure assignment objectives into a multi-objective nonlinear optimization problem (MONLOP) that is solved by an iterative technique. In MONLOP, individual objectives are quantified as a sub-objective function of the free parametric vectors $\{g_1, \dots, g_m\}$ in (4.10) in such a manner that the function has its smallest value (typically zero) when the objective is satisfied. The overall objective function that attempts to fulfill all individual objective requirements is then realized as a suitable weighted sum of the sub-objective functions. The resulting optimization problem having this multi-objective functions is subsequently solved to obtain the values of $\{g_1, \dots, g_m\}$.

5.4.1 Decision Variables

Different choices of the parametric vectors $\{g_1, \dots, g_m\}$ in (4.10) result in different controllers with the same m assigned eigenvalues for the closed-loop system. Comparison amongst all possible choices for the set $\{g_1, \dots, g_m\}$ allows the selection of the optimal set that gives the best system performance. A nonlinear optimization procedure is one way of achieving this. Most optimization programs use scalar real variables as the ‘decision variables’, i.e., those variables for which optimal values are to be found. In order to convert the parametric vectors to this form, the real and imaginary parts of each of the parametric vector elements are treated as one of the elements of the decision variable vector ϕ .

5.4.2 Ensuring the Critical Eigenvalues move to the Desired New Locations

One drawback of a straightforward application of the left eigenstructure assignment technique is that there is no guarantee that the assigned eigenvalues Λ_m of the closed-loop system are precisely the eigenvalues ($\bar{\Lambda}_m$) targeted for relocation (§ 5.3.2). The procedure discussed in this subsection attempts to rectify this problem. By calculating the sensitivity of a typical original targeted eigenvalue ($\bar{\lambda}_i$) to the feedback controller gain K , it is possible to get an indication of where the eigenvalue has moved for a given choice of K . If this estimate is close to (λ_i) , the objective is deemed to have been achieved; if not, then it means a non-critical eigenvalue has surreptitiously occupied the position (λ_i) .

By consideration of (5.8) it is clear that the system with $K = 0$ includes all poles in the open-loop (non augmented) system. Let $\bar{\lambda}$ be the eigenvalue of \bar{A} in (4.1) and \bar{w}_i and \bar{v}_i be the associated left and right eigenvectors, respectively. The corresponding eigenvector of the augmented system, say w_i , includes the elements of \bar{w}_i as its first \bar{n} elements. When the linear output feedback control law described by (5.2) is employed, the approximate change $\Delta\bar{\lambda}_i$ in an eigenvalue $\bar{\lambda}_i$ is given by (Appendix B)

$$\Delta\bar{\lambda}_i = \bar{w}_i^T \bar{B} G \bar{C} \bar{v}_i + \bar{w}_i^T \bar{B} F M(\bar{\lambda}_i) E \bar{C} \bar{v}_i \quad (5.9)$$

where

$$M(\bar{\lambda}_i) = (\bar{\lambda}_i I_n - D)^{-1}. \quad (5.10)$$

Using the above equation, the approximate new location of $\bar{\lambda}$ is given by

$$\tilde{\lambda}_i = \bar{\lambda}_i + \Delta\bar{\lambda}_i. \quad (5.11)$$

Also, each choice of parametric vectors $\{g_1, \dots, g_m\}$ results in a unique K (§ 4.3.1). Note that K is made up of the sub-matrices D, E, F , and G as seen in (4.5). Hence (5.9) and (5.11) may be used to estimate the closed-loop pole locations. Equation

(5.9) is based on linearization; it only gives a first order estimate of the movement of the given pole. If the predicted location of each (say, i th pole) of the m poles ($\bar{\lambda}_i + \Delta\bar{\lambda}_i$) from the above sensitivity analysis closely agrees with its assigned pole location (λ_i), then it can be assumed that the critical poles have moved to the new locations. If this is not the case, it means that some of the non-critical poles have moved to some of the new locations. Therefore, setting up a nonlinear optimization problem that minimizes the distance between the assigned poles and their values predicted via (5.9) and (5.11) provides a means to discriminate between those solutions that actually move only the critical eigenvalues to the new locations and those solutions that undesirably move non-critical eigenvalues to the new locations. To further improve the discrimination, the distance between non-critical eigenvalues and the new locations can be maximized by adding a second sub-objective to the original minimization problem: minimizing the inverse of the distance between the approximate new locations of the non-critical eigenvalues (which can be calculated as before using (5.9) and (5.11)) and the assigned eigenvalues. With $\tilde{\lambda}_i$, $i = 1, \dots, m$, representing the predicted (and hence approximate) values of the critical eigenvalues and $\tilde{\lambda}_j$, $j = m + 1, \dots, n$, representing the non-critical eigenvalues, the objective function to be minimized is given by (5.12) below. In (5.12) the distance between the new desired location for each eigenvalue and the predicted value from the sensitivity calculation has been normalized by dividing it by the distance between the open-loop and the closed-loop eigenvalues.

$$f_1(\phi) = \sum_{i=1}^m \frac{|\lambda_i - \tilde{\lambda}_i|}{|\lambda_i - \bar{\lambda}_i|} \quad (5.12a)$$

$$f_2(\phi) = \sum_{j=m+1}^n \sum_{i=1}^m \frac{|\lambda_i - \bar{\lambda}_j|}{|\lambda_i - \tilde{\lambda}_j|} \quad (5.12b)$$

5.4.3 Selection of the Optimal Left Eigenvector to Minimize Excitation of Problem Modes

From (5.6), the magnitude of excitation of a mode is the dot product of the initial condition immediately after clearing a disturbance and its left eigenvector. As the initial condition is not predictable, an approach that minimizes the weighted sum of the left eigenvector elements is used. The idea behind this approach is that if all the elements of (5.6) are reduced, then the excitation of the mode c_k is also likely to be small, regardless of the values of $x_k(0)$. Instead of using equal weights for all the elements, the participation factors can be effectively used for this purpose because they reflect the proportion of how much a given state contributes to the mode. Hence, the sub-objective function to be minimized to achieve assignment of the optimal left eigenvector may be defined as the sum of dot products:

$$f_3(\phi) = \sum_{i=1}^m |w_i^T \cdot p_i| \quad (5.13)$$

where w_i is left eigenvector associated with the assigned eigenvalue λ_i calculated using (4.10), and p_i is the participation factor of the open-loop eigenvalue $\bar{\lambda}_i$ that is used as weight vector.

5.4.4 Controlling Unassigned Eigenvalues

The above procedures discuss how to formulate the optimization problem to ensure that all targeted eigenvalues move to their designated new locations. However, this objective should not result in the unassigned eigenvalues moving to problematic (poorly damped) locations as discussed in § 5.3.3.

Hence, all unassigned eigenvalues must be constrained to the un-hatched region in Fig. 5.4. In this region, the damping ratio of any complex pair of eigenvalues $\zeta (\triangleq -\text{Re}(\lambda)/|\lambda|)$ is greater than a pre-specified design limit ζ_{min} . Additionally, no eigenvalue has a real part that is greater than a pre-assigned limit α_{min} . These require-

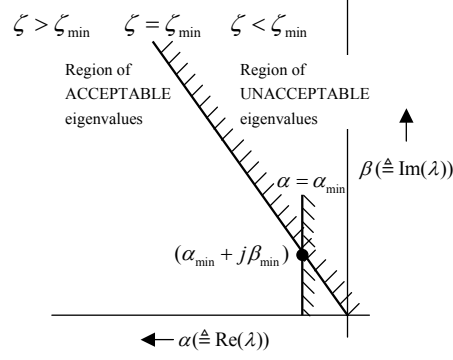


Figure 5.4: Acceptable and unacceptable region of the closed-loop eigenvalues.

ments can be incorporated into the optimization problem in the form of additional constraint defining sub-objectives as shown in (5.14) and (5.15). In the equations, $\tilde{\zeta}_j$ and $\tilde{\alpha}_j$ are the damping factor and the real part of the estimated location of a typical unassigned eigenvalue calculated from a sensitivity analysis, as in § 5.4.2. Note that $f_4(\phi)$ and $f_5(\phi)$ have a zero value if the objective is met, and have a penalizing positive value that increases with the degree of violation of the objective.

$$f_{4j}(\phi) = \begin{cases} (\tilde{\zeta}_j - \zeta_{\min})^2 & \text{if } \tilde{\zeta}_j < \zeta_{\min} \\ 0 & \text{otherwise} \end{cases} \quad (5.14a)$$

$$f_4(\phi) = \sum_{j=m+1}^n f_{4j}(\phi) \quad (5.14b)$$

and

$$f_{5j}(\phi) = \begin{cases} (\tilde{\alpha}_j - \alpha_{\min})^2 & \text{if } \tilde{\alpha}_j > \alpha_{\min} \\ 0 & \text{otherwise} \end{cases} \quad (5.15a)$$

$$f_5(\phi) = \sum_{j=m+1}^n f_{5j}(\phi) \quad (5.15b)$$

5.4.5 Minimizing Controller Effort

Because K is the feedback gain, the magnitude of the feedback signal components is proportional to the elements of K . If the problem is properly scaled, selecting

the largest element (in magnitude) of K to be less than a certain limit k_{lim} permits the minimization of the control effort. The sub-objective given in (5.16) provides a penalty component if the largest component of K lies outside the limits.

$$f_6(\phi) = \begin{cases} (k_{\max} - k_{\lim})^2 & \text{if } k_{\max} > k_{\lim} \\ 0 & \text{otherwise} \end{cases} \quad (5.16)$$

where $k_{\max} = \max(|K|)$.

5.5 MONLOP and the Solution[4]

With the sub-objective functions as defined in the previous sections, the MONLOP problem can be now be transformed into a single-objective nonlinear optimization problem (SONLOP) in which the single objective is a weighted sum of the individual sub-objectives as

$$\text{minimize } F(\phi) = \sum_{i=1}^6 \beta_i f_i(\phi) \quad (5.17)$$

where β_i is a suitable positive weight for the i th sub-objective. The scalar weight β_i is increased if more importance is assigned to the achievement of the i th sub-objective in comparison to the others. Some experimentation is usually required to arrive at a suitable set of weights because not all the objectives are equally important, and additionally, because the objectives are measured in different units. It should be noted that if ϕ can be selected so that $F(\phi) = 0$ all sub-objectives are perfectly achieved, and hence the design is ideal. If this ideal is not achievable, the next best course of action is to select values for variables ϕ that result in the smallest possible value for $F(\phi)$, thereby yielding the best achievable design. The Nelder and Mead nonlinear simplex method is used in this thesis to conduct the minimization process. Details of this nonlinear optimization (NLO) algorithm can be found in [37] and the underlying concept of the algorithm is shown in Appendix D. As described in § 5.4.1, the design vector ϕ contains the real and imaginary parts of the parametric vector G_p . In the first optimization step, the NLO selects a starting value for the vector ϕ .

Note that the choice of ϕ is essentially the choice of G_p . The eigenvalues are moved to the new locations as described in § 4.3.1 and the functions $f_1(\phi), f_2(\phi), \dots, f_6(\phi)$, which determine how successful the move was in meeting the various sub-objectives described in § 5.4, are evaluated. Then, using (5.17), the single combined objective function $F(\phi)$ is calculated. In any given optimization step, the NLO observes the value of $F(\phi)$ and by comparing it to the previous optimization steps, strategically selects a new candidate value for ϕ that has a high likelihood of further reducing the value of $F(\phi)$. The procedure converges when the change in $F(\phi)$ from the previous iteration falls below an exit threshold. This finds a ‘local’ best for the starting search vector ϕ and hence for the free parameter G_p , from which the controller gain K can be determined (§ 4.3.1). Although the Nelder and Mead method is utilized here, any other suitable NLO algorithm could have been used. Nonlinear functions often exhibit multiple local minima. By selecting a different starting point for the above optimization search, it is often possible to converge to a different local minimum. The different controllers generated from several of these starting choices can be further compared amongst themselves to see if any of them provide additional benefits, such as robustness or some other design criteria.

5.6 Power System Controller Design Procedure

The complete procedure for designing controllers using the proposed eigenstructure assignment based algorithm can be described as follows.

1. Calculate the plant matrix of the power system

The design procedure begins with the linearization of the non-linear power system around an operating point to yield the linear differential equations of n_s state variables as

$$\dot{x}_s = A_s x_s \tag{5.18}$$

where

$$x_s \in \mathbb{R}^{n_s}, A_s \in \mathbb{R}^{n_s \times n_s}.$$

The vector x_s is the system state vector and A_s is the system plant matrix. At this stage the input-output matrices of the system need not be defined. The procedure to develop the plant matrix A_s using the general structure of each of the dynamic devices in the power system is described in Appendix A. The plant matrix can be developed explicitly for a small power system comprising up to several hundred states, but for a large scale power system it is implicitly expressed using several intermediate matrices.

2. Identification of Critical Eigenvalues

The objective of the controller considered in this thesis is to address the rotor angle stability of the power system, and it is assumed, for the sake of simplicity, that the system will exhibit only this kind of stability problem. The frequency of the electromechanical modes in a power system are usually in the range of 0.2 Hz to 2.0 Hz. Hence, the eigenvalues of A_s can be screened accordingly to identify critical modes.

The electromechanical modes having a damping ratio below 0.025 are usually considered critical modes, and a PSS is installed for such cases to apply corrective measures.

It is possible to perform a complete eigenanalysis, i.e., calculation of all the eigenvalues and eigenvectors, of a small system having several hundred states. For a complete eigenanalysis of a matrix, a QR algorithm and its variant are the most stable and commonly used algorithms. For a large scale power system, the number of states can easily be tens of thousands. For such a system, few eigenvalues around a point in the complex plane may be computed using the well known Implicitly Restarted Arnoldi method. This algorithm has been implemented in the freely available software package ARPACK [38]. The

implementation of the program for the case of a power system is shown in Appendix C.

3. PSS location and output variables

The next step is to identify the most suitable generator to equip with a PSS to improve the damping of the critical mode(s) identified in the previous step. The most commonly used procedures for this are analyzed in § 3.2. The method suggested in [13] is practical at the same time is the most accurate, which can be summarized as: using the participation factor between the speed of the generators and poorly damped modes, screen the potential locations for the PSS, and then select the most suitable location by further evaluating them using residues.

Input and output matrices for various candidate generators are computed at this stage in order to carry out the residue analysis. The residues between as many system outputs as possible that are local to the candidate generators and local input are computed in order to identify their effectiveness in improving the damping of the critical mode(s). In this manner the system outputs most suitable to be employed as PSS inputs can readily be identified.

During sensitivity analysis, the dynamics of the filters can be excluded. Since the filters are designed to provide a gain close to unity and close to zero phase shift at the frequency of interest, the impact of filters on the sensitivity results will be negligible.

After choosing the PSS location and the number and type of outputs, the input and output matrices of the system are calculated and included in the linearized system (5.18). The resulting n_s -state, \bar{m} -input, and r_s -output linearized power system is given by

$$\begin{aligned} \dot{x}_s &= A_s x_s + B_s \bar{u} \\ y_s &= C_s x_s \end{aligned} \tag{5.19}$$

where

$$x_s \in \mathbb{R}^{n_s}, \bar{u} \in \mathbb{R}^{\bar{m}}, y_s \in \mathbb{R}^{r_s}$$

and the matrices are of appropriate dimensions.

4. Critical eigenvalues and their new location

The next step is the selection of the critical open-loop eigenvalues, those are to be assigned new locations. The set will comprise m such critical eigenvalues, $\{\bar{\lambda}_1, \dots, \bar{\lambda}_m\}$. There is no restriction on the number of eigenvalues to be included in the set; however, the eigenvalues included should be observable and controllable (i.e., should be sensitive to the PSS inputs and outputs), and their relocation should be justifiable based on some or all of the potential benefits described below.

The set will definitely include the critical eigenvalues identified in Step 2, as those have warranted corrective measures in the first place. Additionally, the eigenvalues having higher sensitivities to the selected input-output pair(s) will be included in the set. For example, when a PSS is installed on a generator to improve the damping of an inter-area mode, then the local mode of the generator is also likely to be very sensitive to the PSS. As described earlier, the algorithm will try to move the open-loop eigenvalues to the prescribed locations. Hence, the inclusion of such sensitive eigenvalues (in this case plant mode) in the set of critical eigenvalues will ensure that they are moved precisely to a desirable location when MONLP is solved, and the uncertainty regarding the movement of sensitive eigenvalues can be avoided.

After identifying the set of critical eigenvalues, $\{\bar{\lambda}_1, \dots, \bar{\lambda}_m\}$, new locations to be assigned to each of them $\{\lambda_1, \dots, \lambda_m\}$ are selected. While moving an eigenvalue

to a new location, its real part is usually made more negative without altering its imaginary part. The real part may be made sufficiently small (i.e., sufficiently more negative) so that the damping ratio satisfies the criteria. The controllers will be designed subsequently using the proposed algorithm to assign the set of eigenvalues $\{\lambda_1, \dots, \lambda_m\}$ to the close-loop system.

The set of eigenvalues to be assigned should comprise either real eigenvalues or complex conjugate pairs of eigenvalues. This condition is imposed by the fact that assignment of only real eigenvalues or complex conjugate pairs of eigenvalues will yield a real valued controller.

5. Filter Design

The outputs of the system y_s in (5.19) are usually filtered using high pass washout before supplying them to the PSS. The purpose of the filter and the design method are described in § 3.3.1. Additional filters may be employed (e.g., band pass, low pass) to generate more signals from a given system output in order to make the controller selectively respond to the problem modes. Thus, the dimension of output \bar{y} that is available to the PSS can be higher than the dimension of the system output y_s .

The dynamics of the filter can be expressed in state space form having n_f -states; r_s -input and \bar{r} -output as

$$\begin{aligned}\dot{x}_f &= A_f x_f + B_f y_s \\ \bar{y} &= C_f x_f + D_f y_s\end{aligned}\tag{5.20}$$

where

$$x_f \in \mathbb{R}^{n_f}, y_s \in \mathbb{R}^{r_s}, \bar{y} \in \mathbb{R}^{\bar{r}}$$

and the matrices those described dynamics of filter are of appropriate dimensions. The output of the filter \bar{y} will then be supplied to the SS type PSS.

6. Dynamic compensator states [4]

As noted in § 4.3.1, the maximum eigenvalues that can be assigned to the closed-loop system are equal to the number of inputs to the system when using the partial left eigenstructure assignment technique in the design of a proportional output feedback controller. A power system stabilizer normally controls the power network through one output signal, typically through the reference voltage setting of the exciter. Hence, from the point of view of the controller, the power system appears to be a single input system. However, it is usually necessary to relocate at least one complex conjugate pairs of eigenvalues, (i.e., at least two eigenvalues), to more favorable locations. Thus, assignment of the desired number of eigenvalues is not possible by employing a strictly proportional output feedback controller. Nonetheless, as described in § 4.2, employing a dynamic compensator type controller having a states will increase the effective number of system inputs (and outputs as well) by a when the system is transformed into its equivalent proportional output feedback control system. This will permit assignment of additional a eigenvalues. Hence, if m eigenvalues are to be assigned and system inputs are \bar{m} , then the required minimum number of dynamic compensator states is given by $a = m - \bar{m}$.

Of course, a dynamic compensator can be employed with states greater than $(m - \bar{m})$; however, this will not provide any additional benefits. In such a situation, the number of inputs of the equivalent system will be $(\bar{m} + a)$ greater than the number of assigned eigenvalues (m). Moreover, the resulting increased number of outputs will not be beneficial in improving the left eigenvector of the eigenvalues to be assigned.

Therefore, the number of dynamic compensator states must be selected to be the minimum number that will enable assignment of m eigenvalues, i.e., $a = m - \bar{m}$.

7. Control system

The control system resulting from the combination of linearized power system

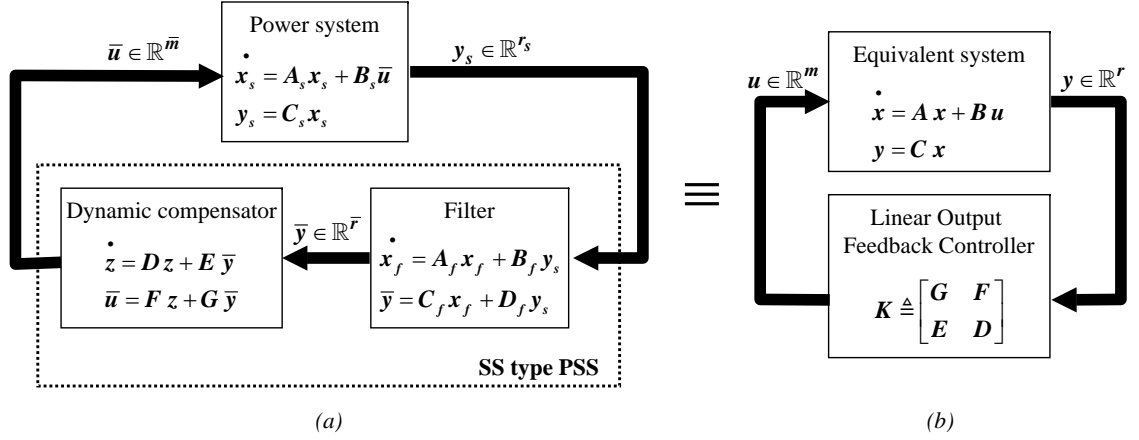


Figure 5.5: (a) Schematic of the control system comprising a linearized power system, a filter and a dynamic compensator. (b) Equivalent linear proportional output feedback control system.

in (5.19), the filter in (5.20), and the dynamic compensator in (5.2) is described schematically in Fig. 5.5.a. The eigenstructure assignment technique is suitable for the proportional output feedback controller. Hence, for the purpose of the design of the dynamic compensator parameters using the eigenstructure assignment technique, the system can be transformed into its equivalent linear output feedback control system shown Fig. 5.5.b. The equivalent system is given by

$$\begin{aligned}
 \dot{x}(t) &= A x(t) + B u(t) \\
 y(t) &= C x(t) \\
 u(t) &= K y(t)
 \end{aligned} \tag{5.21}$$

where

$$\begin{aligned}
x &= \begin{pmatrix} x_s \\ x_f \\ z \end{pmatrix}, u = \begin{pmatrix} \bar{u} \\ \dot{z} \end{pmatrix}, y = \begin{pmatrix} \bar{y} \\ z \end{pmatrix} \\
A &= \begin{pmatrix} A_s & 0 & 0 \\ B_f C_f & A_f & 0 \\ 0 & 0 & 0 \end{pmatrix}, B = \begin{pmatrix} B_s & 0 \\ 0 & 0 \\ 0 & I_a \end{pmatrix}, C = \begin{pmatrix} D_f C_s C_f & 0 \\ 0 & 0 & I_a \end{pmatrix} \\
K &= \begin{pmatrix} G & F \\ E & D \end{pmatrix} \\
x &\in \mathbb{R}^n, u \in \mathbb{R}^m, y \in \mathbb{R}^r \\
n &= n_s + n_f + a, m = \bar{m} + a, r = \bar{r} + a
\end{aligned} \tag{5.22}$$

8. Optimizing the parametric vector

After formulating the control system as above, a single objective function defined by (5.17) shall be optimized using a suitable optimization algorithm. The nonlinear simplex algorithm described in Appendix E is used in this thesis.

A PSS or a controller can now be designed using the above described procedure to optimally assign partial left eigenstructure to the closed-loop system so that excitation of selected critical modes is minimized in addition to moving them to a preselected location in the $X - Y$ plane.

5.7 Proposed Algorithm and Practical Controller Design

In a practical environment often coordinated and robust design of controllers are required [39]. Whereas, using the proposed algorithm only one controller can be designed for a given operating point. The proposed algorithm is reviewed from the robustness and coordinated design perspective in the following.

For a practical application, the controllers are required to be robust, i.e., they should work effectively over a range of operating conditions, because the operating point of a power system can change significantly over a period of time. For example, the generator dispatches and loads during summer time and during winter time can be significantly different. The robustness criteria is not included in the proposed algorithm. However, it is still possible to design a robust controller in an indirect method using the proposed algorithm. As described in §5.5, the optimization process using a different starting point may converge to a different local minimum resulting in a different controller solution. The different controllers generated from several of these starting choices can be further compared amongst themselves in order to select the robust controller that works well over a range of operating points. A robust controller will be designed in such a manner for a wind-turbine generator in the following chapter.

A typical power system usually comprises more than one controller that are employed to address small signal stability problems. By means of coordinated design of such controllers, the parameters for all the controllers can be designed simultaneously to optimally realize collective small signal stability enhancement objectives. In the proposed algorithm, the problem of design of only one controller is considered. However, the coordinated design of multiple controllers can be implemented with little modification.

Thus, the proposed method has some limitations for the practical application that are not addressed in this thesis. Yet, the research work presented in this thesis is the first successful step in the direction of practical application of eigenstructure assignment in the design of power system controllers.

Chapter 6

Application of Proposed PSS Design Algorithm

The PSS design algorithm that will assign the optimal left eigenstructure was presented in the previous chapter. Practical applications of the proposed technique and its superiority over the conventional frequency domain method are demonstrated in this chapter by designing PSSs for three different systems having small-signal stability problems:

1. Two-Area, Four-Generator System: The system exhibits a poorly damped inter-area mode.
2. Doubly Fed Induction Generator (DFIG) System: The system exhibits unstable blade and turbine oscillation modes.
3. Mid-continent Area Power Pool (MAPP) System: The system has an unstable local plant mode.

As discussed in Chapter 4, the output of the system (the number of system outputs and output variables) is one of the important factors that define the subspace where the assignable left eigenvector lies. Thus, the system outputs will be a key factor in determining the possible excitation minimization of the assigned critical modes.

Hence, different system outputs are explored when designing the PSSs using the proposed method, and their effectiveness in minimizing undesirable oscillations is evaluated using transient simulations. Additionally, the dynamic performances of the PSSs designed using the proposed technique are compared against the PSSs designed using the conventional method.

6.1 Two-Area, Four-Generator System

In Chapter 3, the conventional frequency domain PSS design method was demonstrated using a two-area, four-generator system. The same system with a slightly different value of power flow and dynamic data is used here. The single-line diagram of the system is shown in Fig. 6.1, and the line impedances and load flow are marked in the figure, and the dynamic data of the devices are shown in Appendix D. Power transfer of 400 MW from Area-1 to Area-2 is considered. The modeling details of the system are described in detail in § 3.4.

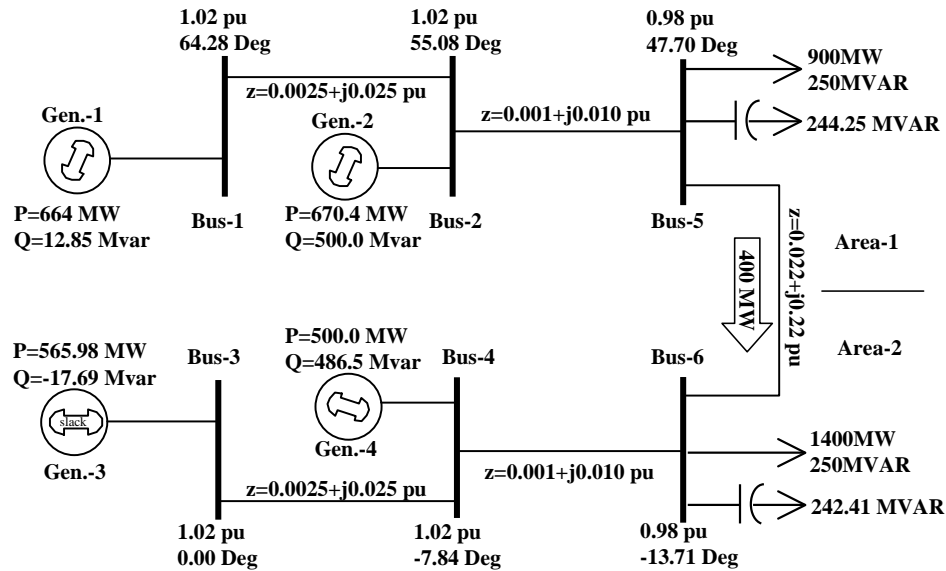


Figure 6.1: One line diagram of 2-Area, 4-generator system.

Possible advantages of using generator speed and electrical power, two locally and conveniently available signals, as input(s) to the PSS for the eigenstructure assignment based design methods are investigated in this sections.

6.1.1 Open Loop System Analysis

The eigenanalysis of the system without PSS reveals three electromechanical modes of oscillations. Table 6.1 shows the frequency and damping ratio of the modes; the magnitude of the participation factors between the modes and the state variable generator speeds; and mode shapes of generator speeds.

For the first mode (0.335 Hz), all the generators have high participation and the mode shape angle suggests oscillation of generators in Area-1 against Area-2, which indicates that it is an inter-area mode. The second mode is a plant mode for Area-1 because Gen-1 and Gen-2 in the area have high participation in the mode, and they oscillate against each other according to the mode shape angle. Similar analysis of third mode suggests it is a plant mode for Area-2.

The plant modes are well damped, but the inter-area mode is poorly damped. In order to assess the transient performance of the system, the system was simulated for a three phase fault at Bus 4 that was removed after 0.2 s. The transient response of the speed of the four generators are shown in Fig. 6.2. It can be seen that the high frequency transients die out within 2.5 s of removal of the fault. Subsequently, a poorly damped 0.3 Hz frequency inter-area mode dominates the responses. The speed of the generators are oscillating even after about 30.0 s from removal of the fault.

In order to improve the transient performance of the system, PSSs are designed using the conventional frequency domain method and designed using the proposed algorithm in the sections that follow.

Table 6.1: Electromechanical modes of the system without a PSS.

Mode	M1 ($\bar{\lambda}_1, \bar{\lambda}_1^*$)		M2 ($\bar{\lambda}_2, \bar{\lambda}_2^*$)		M3 ($\bar{\lambda}_3, \bar{\lambda}_3^*$)	
Eigenvalue	$-0.06 \pm j2.1$		$-1.3 \pm j7.7$		$-1.5 \pm j7.5$	
Freq. (Hz)	0.335		1.23		1.2	
Damp. Ratio(%)	2.8		16.13		19.08	
Generator	$ pf $	Mode Shape	$ pf $	Mode Shape	$ pf $	Mode Shape
G1	0.43	$0.41 \angle 26^\circ$	0.92	$0.92 \angle -172^\circ$	0.00	$0.02 \angle 27^\circ$
G2	0.35	$0.43 \angle 27^\circ$	1.00	$1.00 \angle 0^\circ$	0.00	$0.02 \angle -54^\circ$
G3	1.00	$1.00 \angle -2^\circ$	0.00	$0.09 \angle 111^\circ$	0.86	$0.88 \angle -175^\circ$
G4	0.88	$1.00 \angle 0^\circ$	0.00	$0.10 \angle -109^\circ$	1.00	$1.00 \angle 0^\circ$

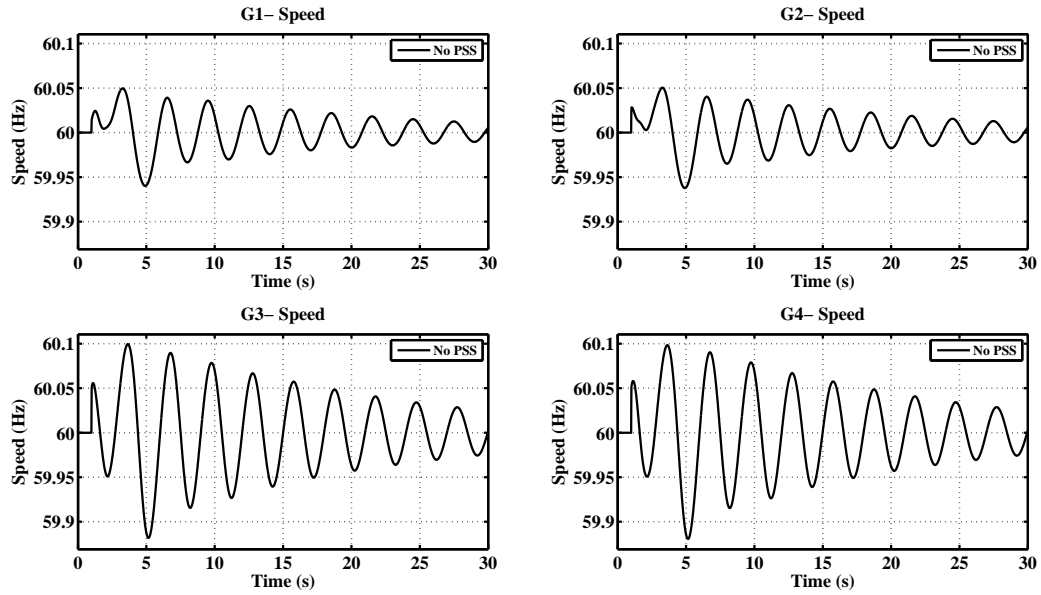


Figure 6.2: Transient response of the speed of generators without a PSS.

6.1.2 Selection of PSS Location

The procedure for selection of the PSS location was described in § 3.2, and the residues of the critical inter-area mode are used for that purpose.

Generator speed is the most commonly used input for a conventional PSS. Local generator power is another easily accessible variable. For a controller designed using the eigenstructure assignment method, speed and power are considered as candidate input to the PSS in order to investigate the possible advantages of using different system output and more than one system output. The output of the PSS will then be used to modulate the voltage reference signal V_{ref} of the local excitation system.

Therefore, the residues are evaluated for each generator between the local exciter input V_{ref} and the local outputs speed and electrical power. The magnitude of the calculated residues are shown in Table 6.2 and their arguments are shown in Table 6.3.

Table 6.2: Magnitude of the residues between the generator speed and power output and the exciter V_{ref} input of different generators for the critical inter-area mode.

Generator	M1 ($-0.06 \pm j2.1$)		M2 ($-1.3 \pm j7.7$)		M3 ($-1.5 \pm j7.5$)	
	speed	power	speed	power	speed	power
G1	0.0073	0.2107	0.0072	0.7231	0.0000	0.0015
G2	0.0138	0.3773	0.0054	0.5509	0.0000	0.0009
G3	0.0134	0.3738	0.0000	0.0005	0.0067	0.6633
G4	0.0258	0.7057	0.0000	0.0025	0.0053	0.5229

Table 6.3: Argument of the residue between the generator speed and power output and the exciter V_{ref} input of different generators for the critical inter-area mode.

Generator	M1		M2		M3	
	$(-0.06 \pm j2.1)$		$(-1.3 \pm j7.7)$		$(-1.5 \pm j7.5)$	
	speed	power	speed	power	speed	power
G1	-26.1°	-134.8°	85.9°	-0.5°	0.2°	-84.5°
G2	-21.0°	-111.5°	68.2°	-13.1°	136.5°	57.0°
G3	120.9°	19.0°	127.1°	42.7°	82.3°	-0.4°
G4	126.6°	35.6°	0.2°	-81.2°	70.2°	-9.5°

The main objective of PSS design is to improve the damping of the least damped inter-area mode. Hence, for PSS siting purposes the residue of mode M1 will be examined. For mode M1, Generator-4 has the highest residue for the speed and power outputs of all the generators. Therefore, Generator 4 is the optimal location to install a PSS, irrespective of type of PSS employed.

6.1.3 Conventional PSS Designed in the Frequency Domain

As shown in Fig. 6.3, the lead-lag type PSS considered here comprises a filter and two lead-lag blocks. This PSS is designed using the conventional frequency domain method.

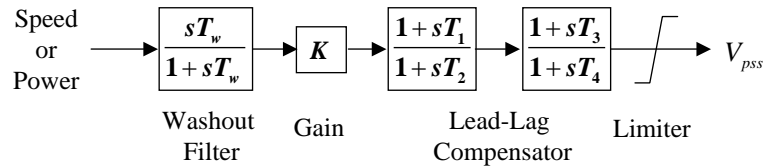


Figure 6.3: Single input PSS1A (lead-lag) type PSS.

For acceptable dynamical performance of the sample system it is necessary to improve the damping ratio of the inter-area modes to a certain minimum value. Here, a 5% damping ratio is considered acceptable; and accordingly, the objective of the PSS design is to improve the damping ratio of the inter-area mode to at least 5% by moving the associated complex conjugate pair of eigenvalues further left in the complex plane. This requires that the inter-area mode be relocated from $(-0.06 \pm j2.1)$ to somewhere about $(-0.105 \pm j2.1)$.

6.1.3.1 PSS Parameters

The purpose of the washout filter is to remove dc components present in the input signal, and it does not play a very critical role in PSS performance. The role of the washout filter and the guidelines for selection of the washout filter constant are described in § 3.3.1. Accordingly, the value of 10.0 s is selected for time constant T_W .

The PSS design procedure described in § 3.3.2.1 is used to design the lead-lag blocks of the PSS. Accordingly, the required phase compensations to improve damping of the inter-area mode ($\bar{\lambda}_1, \bar{\lambda}_1^* = -0.06 \pm j2.1$) for the speed input and the power input PSSs, are shown in Table 6.4. Each of the lead-lag blocks was designed so that it provides half of the required phase compensation with maximum gain at the inter-area mode frequency of 2.1 rad/s (0.33 Hz). The values of the lead-lag parameters calculated in this manner are shown in Table 6.4. The approximate gains, evaluated after determining the lead-lag parameters for speed input and power input PSSs are shown in Table 6.4 in the “Approximate Gain” column. If the PSS, when using approximate gain, has not improved the damping of the inter-area mode to the desired value of 5%, then the value of gain is adjusted until the desired damping is achieved. The final value of the gain is shown in Table 6.4 in the “Final Gain” column.

Table 6.4: The lead-lag type PSS parameters designed using the residue method.

Input	Phase Compensation	T1=T3	T2=T4	Gain (Ks)	
				Approximate	Final
Speed	50.7°	0.7582	0.3114	0.73	0.705
Power	141.6°	2.7495	0.091371	0.0019	0.0019

6.1.3.2 Results

Speed Input Lead-Lag Type PSS

A speed input lead-lag type PSS (simplified IEEE stabilizer type PSS1A) designed using the frequency domain method was incorporated into the system model for small-signal and nonlinear transient analysis purposes. The electromechanical modes of the oscillations of the system are shown in Table 6.5. By comparing the frequencies of the electromechanical modes of the closed-loop system with those of the open loop system shown in Table 6.1, it can be observed that implementation of the PSS has improved the damping of the inter-area mode without altering its frequencies or any other electromechanical modes.

Table 6.5: Electromechanical modes of the system with the speed input lead-lag type PSS.

No.	Eigenvalue	Freq. (Hz)	Damping (%)	Dominant state
1	$-0.1058 \pm j2.1063$	0.3352	5.01	δ_3
2	$-1.2632 \pm j7.7302$	1.2303	16.13	ω_2
3	$-1.4677 \pm j7.5552$	1.2024	19.07	ω_4

This is further confirmed using non-linear simulations of the system. The transient response of the speed of generators for the case without a PSS and for the case with the speed input PSS are compared in Fig. 6.4.

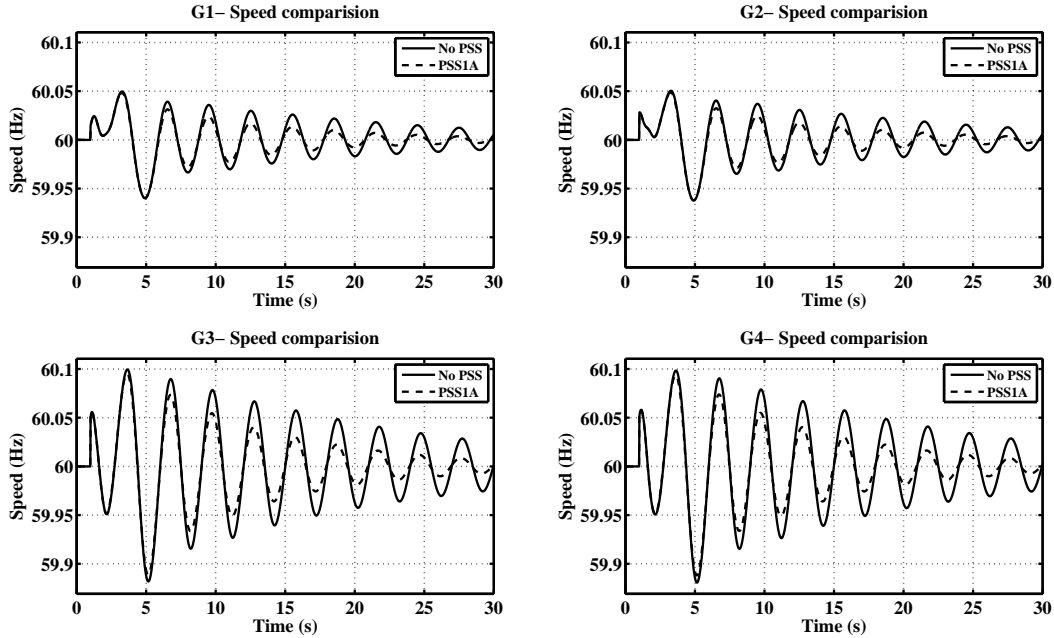


Figure 6.4: Transient response of the speed of generators for the case without a PSS and that for the case with the speed input PSS1A (lead-lag) PSS.

It is evident from the plot that 0.3 Hz is the dominant frequency (which is the inter-area mode frequency) in the speed transients in both cases, and it is also evident that there is better damping for the case with the PSS. Hence, the speed input PSS designed using the frequency domain method has improved the damping of the inter-area mode without altering its frequency. As mentioned earlier, the conventional design method does not attempt to alter the eigenstructure of the system. This is evident from the properties of the inter-area mode shown in Table 6.12. The table shows the right and left eigenvector entries corresponding to generator speed. Since the inter-area mode is dominant in the transients, only the properties of the inter-area mode are produced; and since the mode is electromechanical, only the entries corre-

sponding to the speed are produced. It can be seen from the table that the values of the eigenvectors for the system with the speed input lead-lag PSS are very similar to those of the open-loop system.

Power Input Lead-Lag Type PSS

The electromechanical modes of the oscillations of the system with the power input PSS are shown in Table 6.6. Similar to the previous case of a system with the speed input PSS, the power input PSS has improved the damping of the inter-area mode without altering its frequency or any other electromechanical mode. The comparison of the generator speed responses of the system with the power input PSS to those of the system without a PSS in Fig. 6.5 shows that the power input PSS, like the speed input PSS, has improved the damping of the inter-area mode.

The transient response of the speed of generators for the power input PSS cases are compared with those of the speed input PSS in Fig. 6.6. The identical response suggest that the eigenstructure of the electromechanical modes (the dominant modes in transients) for both the systems are identical. This is due to the fact that no attempt is made to alter the associated eigenstructure of the mode. This is evident from the values of the generator speed entries of the eigenvectors of the inter-area mode shown in Table 6.12.

Table 6.6: Electromechanical modes of the system with the power input lead-lag type PSS.

No.	Eigenvalue	Freq. (Hz)	Damping (%)	Dominant state
1	$-0.1052 \pm j2.1042$	0.3349	5.00	δ_3
2	$-1.2638 \pm j7.73315$	1.2305	16.13	ω_2
3	$-1.6023 \pm j7.9486$	1.2651	19.76	ω_4

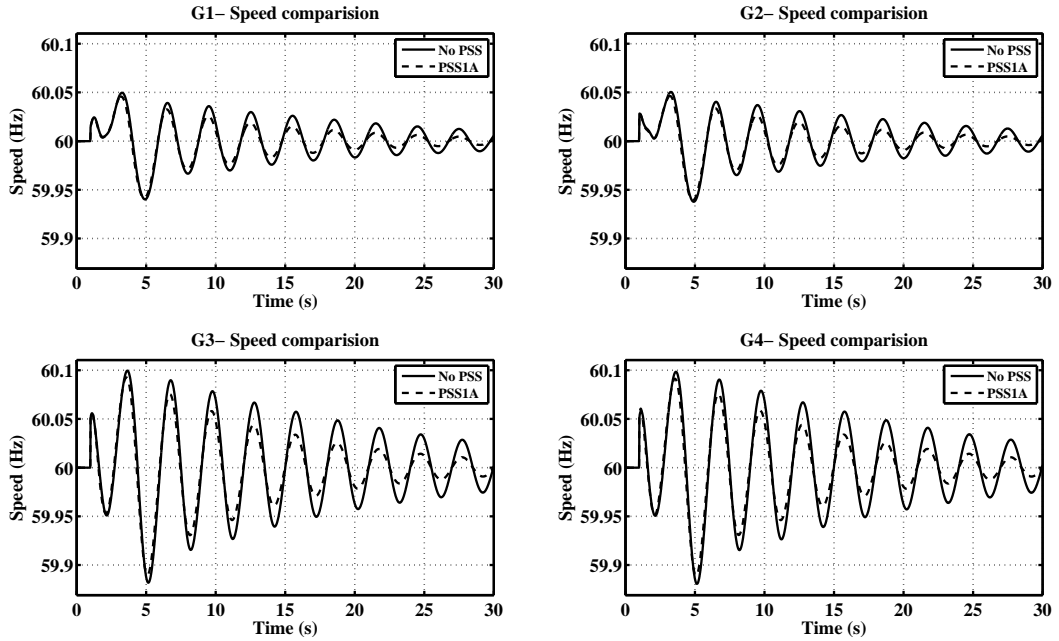


Figure 6.5: Transient response of the speed of generators for the case without a PSS and that for the case with the power input PSS1A (lead-lag) PSS.

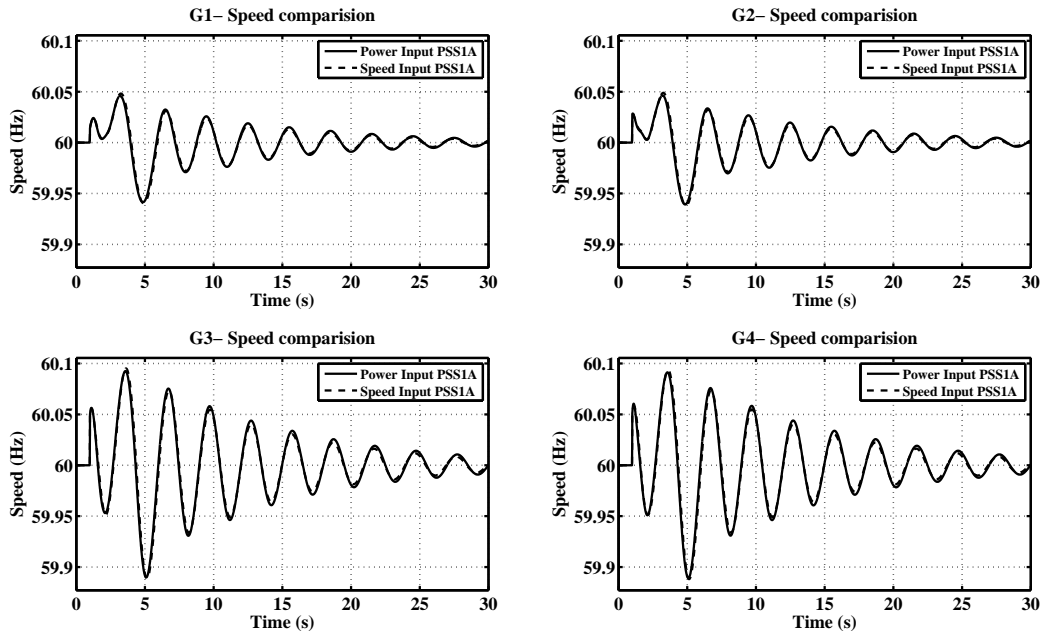


Figure 6.6: Transient response of the speed of generators for the case with the power input PSS1A (lead-lag) PSS and that for the case with the speed input PSS1A (lead-lag) PSS.

6.1.4 SS type PSS Design using the Eigenstructure Assignment Technique

The SS type PSSs in this section are designed to improve the damping of the critical mode and to assign an optimal left eigenvector using the algorithm developed earlier. The number of inputs and the signals used for inputs will play a critical role in the determination of the assignable left eigenstructure. Hence, in order to assess the improvement in eigenstructure made possible by employing alternate inputs signals and by employing more than one signal, the following three different PSSs were designed using the proposed technique:

- Speed input PSS
- Power input PSS
- Speed and power input PSS

6.1.4.1 Filters

An SS type PSS comprises a filter and a dynamic compensator, as described in § 5.1. The block diagram of the single input SS type PSS is shown in Fig. 6.7 and the block diagram for the dual input SS type PSS is shown in Fig. 6.8. The block diagrams show the detailed filter transfer functions.

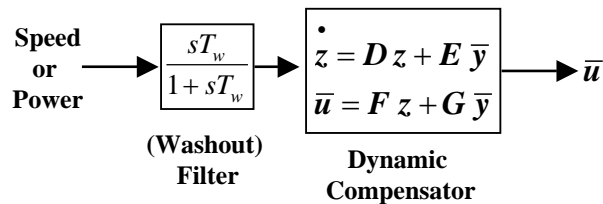


Figure 6.7: Block diagram of the single input state-space (SS) type PSS.

A simple high-pass washout filter, similar to the one used for the PSS1A type PSS in § 6.1.3, is considered for the single input type PSS; and the washout filter time

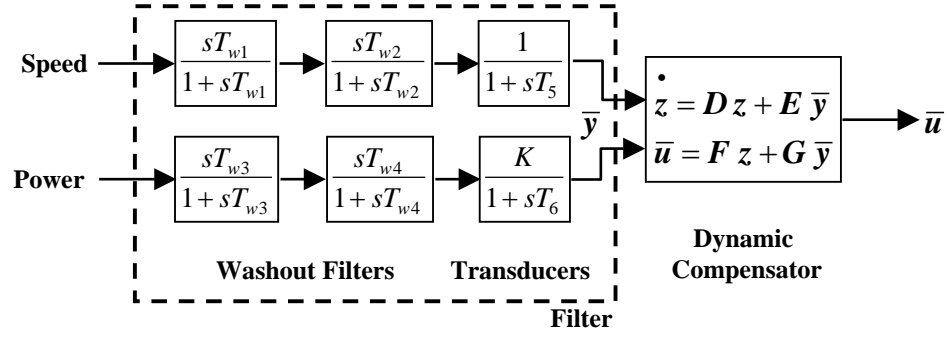


Figure 6.8: Block diagram of the dual input state-space (SS) type PSS.

constant of 10.0 s selected for the Stab1 type PSS is also chosen for the single input SS type PSS.

For the dual input SS type PSS, the detailed filter model used in the dual input IEEE type PSS2A type PSS [8] is selected. The Tw1-Tw4 control blocks are washout filters for the inputs, and the T4-T5 control blocks represent an output measurement transducer. The practical parameters of the filters and transducers presented in [5] were used here and are shown in Table 6.7.

Table 6.7: Filter and transducer parameters [5]
for the dual-input SS type PSS.

Tw1	Tw2	Tw3	Tw4	Tw5	Tw6	K
10.0	10.0	10.0	30.0	0.1	10.0	1.462

6.1.4.2 Critical Eigenvalues and Their New Locations

The main objective of the design is to improve the damping ratio of the critical inter-area mode to 5% without altering its frequency. Hence, as a first design criteria the inter-area mode $(-0.059 \pm j2.10)$ will be moved to $(-0.1058 \pm j2.10)$. The PSS

is to be installed on Gen-4 as determined in § 6.1.2. It is evident from Table 6.2 that the Area-2 plant mode (Mode 3) is sensitive to the signals to be used as PSS input. In order to ensure it moves to a suitable well-damped location when MONLP is solved, the plant mode $(-1.463 \pm j7.5345)$ will be moved $(-1.6 \pm j7.5345)$.

Thus, one of the objectives of SS type PSS design is to move open-loop eigenvalues $\bar{\Lambda}_m = \{-0.059 \pm j2.10, -1.463 \pm j7.53\}$ to $\Lambda_m = \{-0.1058 \pm j2.10, -1.6 \pm j7.53\}$.

6.1.4.3 Selection of the Dimension of the Dynamic Compensator

According to the design criteria established in the previous step, four eigenvalues (two sets of complex conjugate pairs of eigenvalues) along with their left eigenvectors are to be assigned to the closed-loop system. In order to make this possible, at least four system inputs ($m = 4$) are required (§ 4.3). However, the linearized system offers only one input (i.e., $\bar{m} = 1$), V_{ref} of the excitation system of Gen-4. In order to be able to assign the desired number of eigenvalues, the dynamic compensator with the minimum required dimension $a = m - \bar{m} = 4 - 1 = 3$ (§ 5.6) for the state vector is selected.

6.1.4.4 SS type PSS Parameters

After selecting the eigenvalues to be assigned to the closed-loop system and the dimension of the dynamic compensator, the PSSs were designed to optimally assign the left eigenstructure by solving MONLOP, as described in § 5.4. The designed PSS parameters for the three SS type PSSs are shown in Table 6.8.

PSS Input	D	E	F	G
Speed	$\begin{pmatrix} 1.8 & 3.34 & 4.99 \\ -10.73 & -3.57 & 6.81 \\ -3.89 & -2.0 & -2.78 \end{pmatrix}$	$\begin{pmatrix} 0.42 \\ 2.13 \\ 1.32 \end{pmatrix}$	$\begin{pmatrix} 2.97 & 3.62 & 1.28 \end{pmatrix}$	$\begin{pmatrix} 0.68 \end{pmatrix}$
Power	$\begin{pmatrix} -14.55 & -46.51 & -52.38 \\ 13.45 & -30 & 7.90 \\ -3.92 & 21.95 & 16.2 \end{pmatrix}$	$\begin{pmatrix} 1.02 \\ 1.28 \\ -1.40 \end{pmatrix}$	$\begin{pmatrix} -0.77 & -1.31 & -1.89 \end{pmatrix}$	$\begin{pmatrix} 0.22 \end{pmatrix}$
Speed & Power	$\begin{pmatrix} -4.59 & 5.70 & 17.75 \\ -4.58 & -8.42 & -11.62 \\ 10.96 & 4.00 & -7.12 \end{pmatrix}$	$\begin{pmatrix} -7.33 & -11.46 \\ -3.35 & 1.16 \\ 13.04 & 12.51 \end{pmatrix}$	$\begin{pmatrix} -65.71 & -39.95 & 16.06 \end{pmatrix}$	$\begin{pmatrix} -48.84 & -52.87 \end{pmatrix}$

Table 6.8: Parameters of the speed input, power input and speed-power (dual) input SS type PSSs.

6.1.4.5 Results

In the previous section, the following three PSSs were designed using the proposed eigenstructure assignment algorithm:

- Speed input PSS
- Power input PSS
- Speed and power input PSS

The transient performance of the system and the eigenstructure of the inter-area mode of the system with above PSSs implemented as separate cases are analyzed in this section.

Speed input SS type PSS

The electromechanical modes of the oscillations of the system are shown in Table 6.9. Note that the eigenvalues associated with Modes 1 and 3 are the eigenvalues assigned to the closed-loop system during design. Fig. 6.9 shows the trace of the open-loop electromechanical modes ($M_1 = -0.059 \pm j2.1062$ and $M_2 = -1.463 \pm j7.534$) for a gradual increase in the F and G gains of the PSS from zero to their final values (the corresponding values in first row of Table 6.8). The trace shows that the PSS has moved the open-loop eigenvalues to their assigned locations, as desired, (i.e., $\bar{\Lambda}_m = \{-0.059 \pm j2.1062, -1.463 \pm j7.5345\}$ are moved to $\Lambda_m = \{-0.1058 \pm j2.1063, -1.6 \pm j7.5345\}$).

The generator speed transients with the speed input lead-lag PSS and an SS type PSS are compared in Fig. 6.10. It is evident that the transient responses of the two systems are identical, which suggests that the eigenstructure of the inter-area mode could not be altered by the speed input SS type PSS. This can be ascertained from the entries of the eigenvectors of the inter-area mode shown in Table 6.12.

Table 6.9: Electromechanical modes of the system with the speed input SS type PSS.

No.	Eigenvalue	Freq. (Hz)	Damping (%)	Dominant state
1	$-0.1058 \pm j2.1073$	0.3354	5.01	δ_3
2	$-1.2624 \pm j7.7335$	1.2308	16.11	ω_2
3	$-1.600 \pm j7.5345$	1.1992	20.77	ω_4

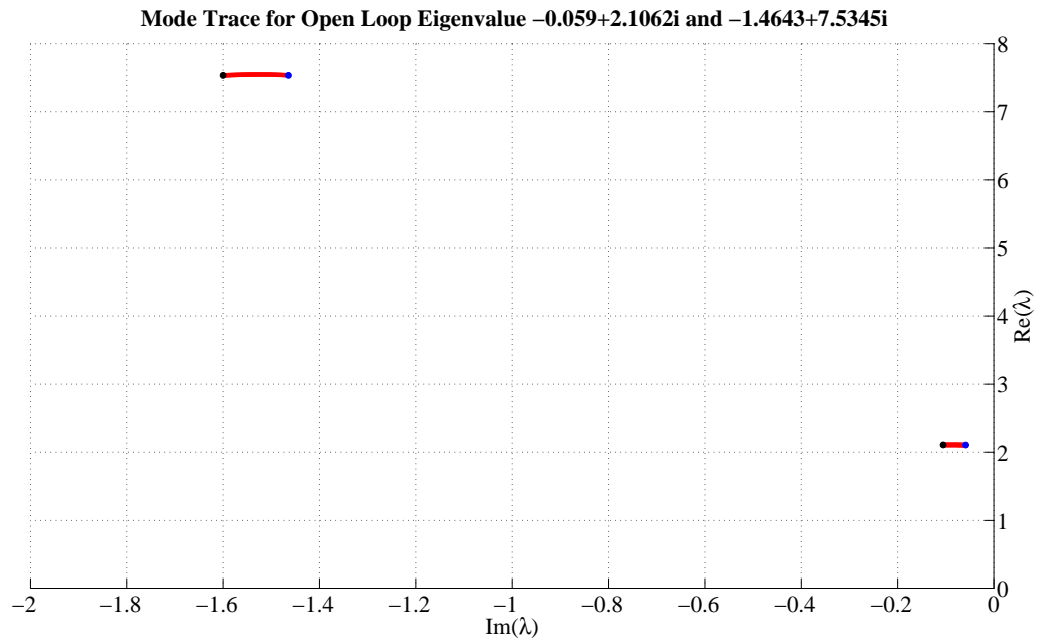


Figure 6.9: Mode traces of the system with the speed input SS type PSS for increasing gain from zero to the designed value.

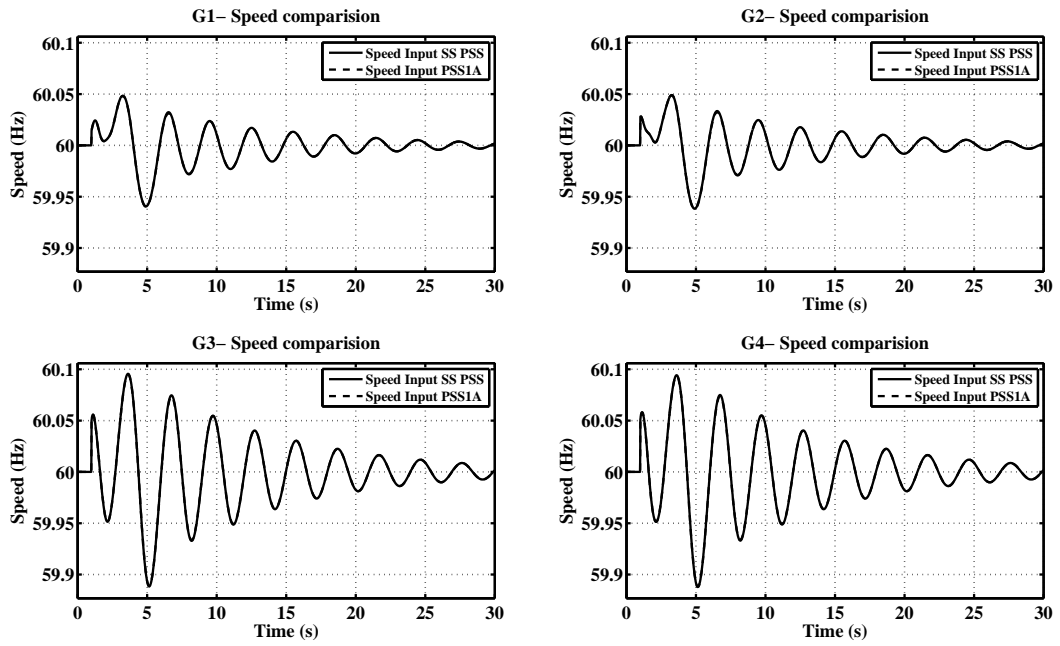


Figure 6.10: Transient response of the speed of generators for the case with the speed input SS PSS and that for the case with the speed input PSS1A (lead-lag) PSS.

Power input SS type PSS

In § 6.1.4, the power input SS type PSS was designed by assigning the optimal eigenstructure. The electromechanical modes of the oscillations of the system with this PSS are shown in Table 6.10.

Fig. 6.11 shows the trace of the open-loop electromechanical modes ($M_1 = -0.059 \pm j2.1062$ and $M_2 = -1.463 \pm j7.534$) for a gradual increase in the gains of the PSS, F and G in Fig. 6.7, from zero to their final values (the values in the second row of Table 6.8). The trace shows that the PSS has moved the open-loop eigenvalues to their assigned locations, as desired.

The generator speed transients with the power input SS type PSS are compared with those of a power input lead-lag type PSS in Fig. 6.12. The smaller magnitude of the low frequency oscillation is evident from the plots and suggests a somewhat improved eigenstructure of the system with the power input SS type PSS. This can be ascertained from the eigenstructure of the inter-area mode shown in Table 6.12. It can be seen that in this case, the magnitude of the left eigenvector entries corresponding to speed have smaller magnitudes compared to those of the system without a PSS, with the speed input lead-lag PSS, with the power input lead-lag PSS, and with the speed input SS type PSS.

Table 6.10: Electromechanical modes of the system with the power input SS type PSS.

No.	Eigenvalue	Freq. (Hz)	Damping (%)	Dominant state
1	$-0.1058 \pm j2.1073$	0.3354	5.01	ss_3
2	$-0.3082 \pm j1.9081$	0.3037	15.94	ss_3
3	$-1.2635 \pm j7.7306$	1.2304	16.13	ω_2
4	$-1.600 \pm j7.5345$	1.1992	20.77	ω_4

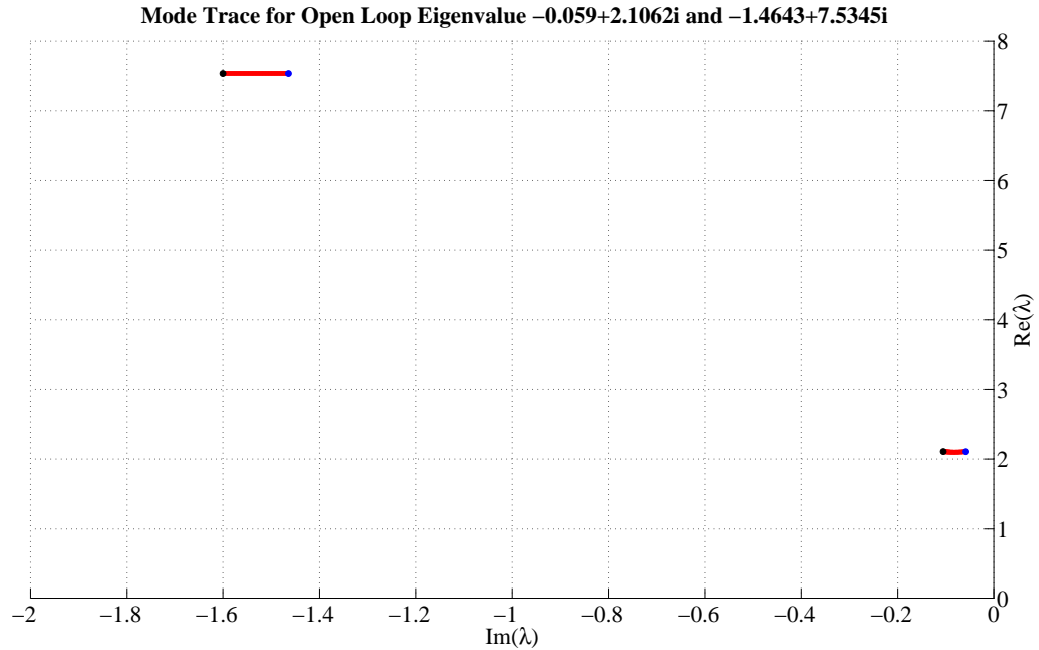


Figure 6.11: Mode traces of the system with the power input SS type PSS for increasing gain from zero to the final design value.

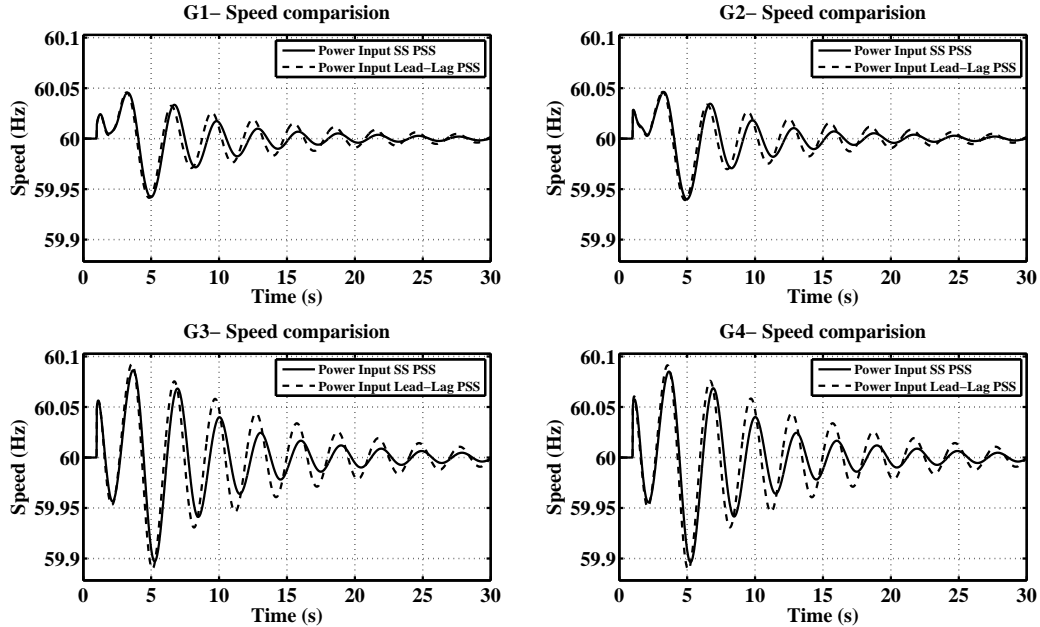


Figure 6.12: Transient response of the speed of generators with the power input SS PSS and that for the case with the power input PSS1A (lead-lag).

Speed and Power, Dual Input, SS Type PSS

The electromechanical modes of the oscillations of the system with the dual input SS type PSS are shown in Table 6.11. Note that the eigenvalues associated with Modes 1 and 4 are the eigenvalues assigned to the closed-loop system during design.

Fig. 6.13 shows the trace of the open-loop electromechanical modes ($M_1 = -0.059 \pm j2.1062$ and $M_2 = -1.463 \pm j7.534$). The trace shows that the PSS has moved the open-loop eigenvalues to their assigned locations: $\Lambda_m = \{-0.1058 \pm j2.1063, -1.6 \pm j7.5345\}$.

The speed transients of the system with the dual input SS type PSS are compared with those of the system with the power input lead-lag type PSS in Fig. 6.14. The substantially smaller magnitude of the low frequency oscillation is evident from the figure, and is a direct consequence of the significantly altered eigenstructure of the inter-area mode due to implementation of the speed-power input SS type PSS. This can be ascertained from the eigenstructure of the inter-area mode shown in Table 6.12. It can be seen that the entries of the left eigenvector and the participation factor for Gen-1 to Gen-3 speed are significantly smaller. The combined effect is the negligible excitation of the inter-area mode.

Table 6.11: Electromechanical modes of the system with the dual-input SS type PSS.

No.	Eigenvalue	Freq. (Hz)	Damping (%)	Dominant state
1	$-0.1068 \pm j2.1063$	0.3352	5.06	ω_4
2	$-1.2635 \pm j7.7307$	1.2305	16.13	ω_2
3	$-0.3522 \pm j2.0348$	0.3239	17.05	ω_4
4	$-0.0171 \pm j0.0818$	0.0130	20.47	ω_4
5	$-1.6200 \pm j7.6000$	1.2096	20.85	δ_4
6	$-0.5029 \pm j1.1707$	0.18636	39.47	ω_4

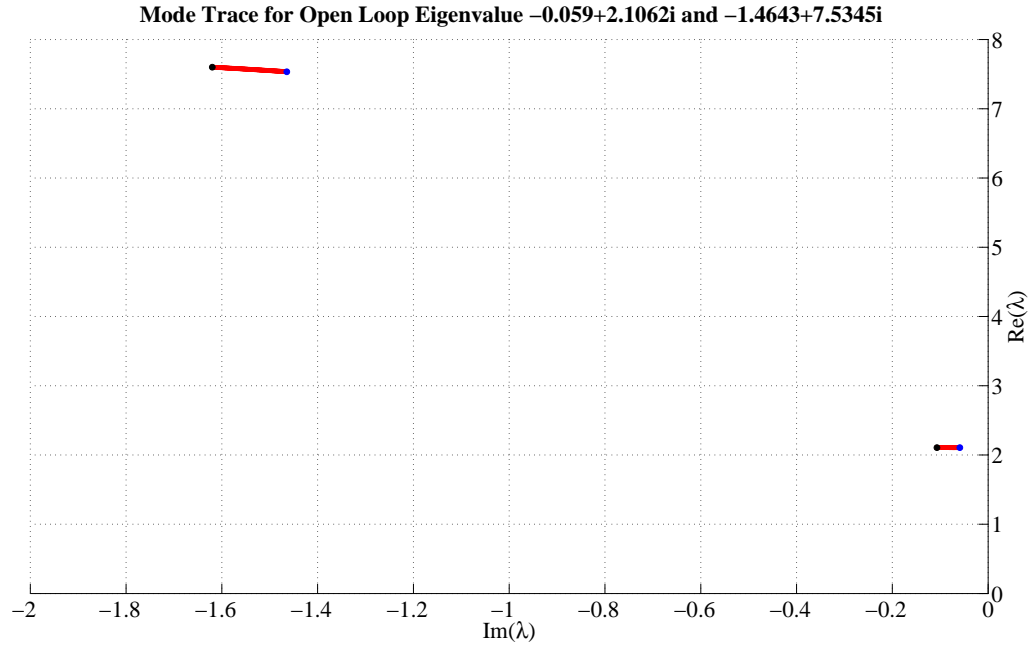


Figure 6.13: Mode traces of the system with the dual input SS type PSS for increasing gain from zero to the final design value.

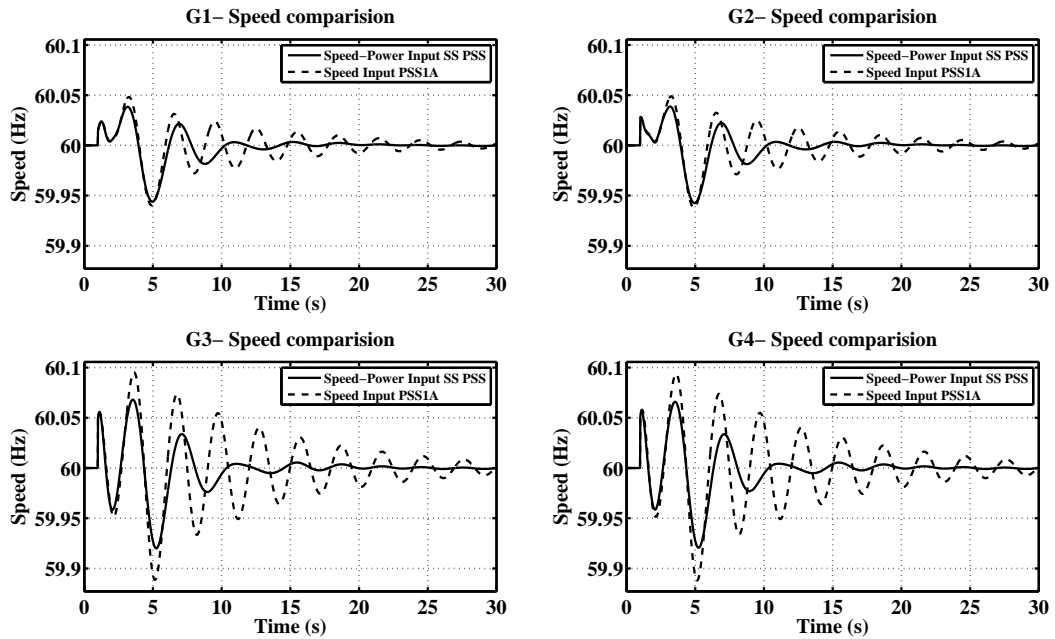


Figure 6.14: Transient response of speed of generators for the case with the speed-power (dual) input SS PSS and that for the case with the speed input PSS1A (lead-lag) PSS.

Table 6.12: Modal Properties of the inter-area mode and the Area-2 plant mode of the system without any PSS and of the system with different types of PSS.

	State	No PSS	Speed, lead-lag	Power, lead-lag	Speed, SS	Power, SS	Speed-power, SS
LEV	ω_1	0.6678	0.7085	0.7084	0.7133	0.4435	0.0713
	ω_2	0.5284	0.557	0.5571	0.5607	0.3486	0.056
	ω_3	0.6481	0.6934	0.6924	0.6986	0.4343	0.0698
	ω_4	0.5658	0.6011	0.5875	0.6054	0.3667	4.1365
REV	ω_1	0.2425	0.2462	0.2464	0.2461	0.2447	0.2463
	ω_2	0.2514	0.2552	0.2554	0.255	0.2536	0.2552
	ω_3	0.5862	0.5861	0.5858	0.5862	0.5829	0.5861
	ω_4	0.5887	0.5859	0.5857	0.5859	0.5826	0.5858
pf	ω_1	0.1619	0.1744	0.1746	0.1755	0.1085	0.0175
	ω_2	0.1328	0.1421	0.1423	0.143	0.0884	0.0143
	ω_3	0.3799	0.4064	0.4056	0.4095	0.2531	0.0409
	ω_4	0.3331	0.3521	0.3441	0.3547	0.2136	2.4232

¹ The right eigenvectors are normalized by their L2-Norm. Left eigenvectors are normalized such that the dot product of the right and left eigenvectors is unity.

6.2 System with a Wind Turbine Generator[4]

6.2.1 System Description

The eigenstructure assignment procedure was used to design a combined power system stabilizer and active damping controller for a very large DFIG wind turbine generator in a projected wind power scenario in Scotland [40]. This unit is connected to a large power system, as shown in Fig. 6.15. The generators G1 and G3 are steam turbine driven round rotor synchronous generators rated at 2,800 MVA and 21,000 MVA, respectively [40]. They form a lumped equivalent of the network in the south of Scotland and the networks of England and Wales, respectively. Generator G2 represents a large 2400 MW wind turbine park in northern Scotland equipped with doubly fed induction generators (DFIG). The schematic diagram of the DFIG system is shown in Fig. 6.16.

The model of the generators, the generator data, and the network data used in this thesis are essentially identical to the model presented in[40]. The principal difference of the model used in this thesis is the use of a more detailed three mass model for the wind turbine, which allows investigation of the blade vibrations.

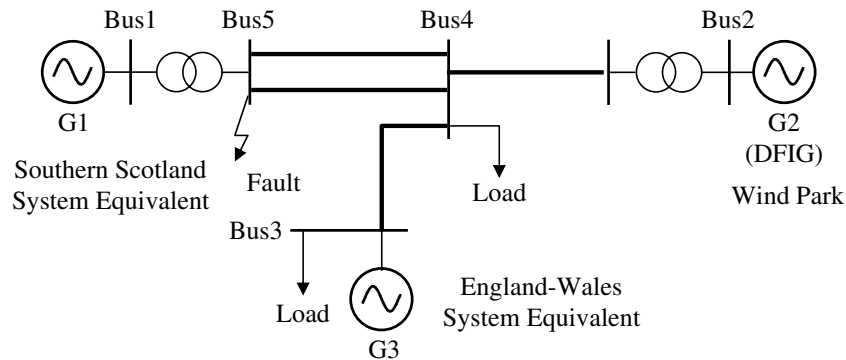


Figure 6.15: One line diagram of the system comprising DFIG wind generation.

Each synchronous generator is represented using a sixth order model. Exciters

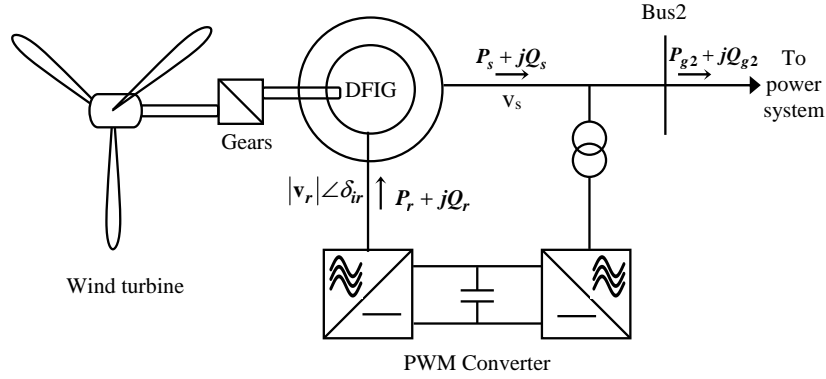


Figure 6.16: Schematic of the wind turbine and the doubly fed induction generator system.

and governors are also modeled. The loads are modeled as constant impedances, and the DFIG system is represented using a third order model. The wind turbine system is modeled using a three mass model, as shown in Fig. 6.17. In this model, at one end the generator rotor is connected to the turbine hub via a shaft (including the gearbox). The blades are mounted on the hub; they are not rigid, and for the purposes of the model all the blades are assumed to oscillate in unison. The turbine hub-blade system is represented by considering the hub to be connected to a third mass via a flexible shaft. The oscillations in the speed of this third mass are considered to represent the oscillations of the blades. Various constants of the three mass model are shown in Table 6.13. The adequacy of lumped mass model of wind turbine considered in this example is explained below.

In a typical wind turbine system, the forces generated by wind on the turbine results in multitude of structural oscillatory modes. These oscillatory modes can be studied using higher order representations of the structural dynamics [41]. Analysis using detailed structure dynamics would provide useful information about stability of a wind turbine and structure due to forces generated by wind.

On the other hand the transients generated in the electric system can also excite certain oscillation modes of wind turbine. Usually the interaction between the electri-

cal system and the turbine through subsynchronous oscillatory modes of turbine are of chief concern. In order to study small signal stability of wind turbine-generator at subsynchronous frequency, two or three lumped mass model of turbine is considered adequate.

In this example case, the focus of the study is to examine the small signal stability of a wind turbine and its structure during disturbances in the electrical system rather than due to wind force. Hence, three lumped mass model of wind turbine has been used in this case.

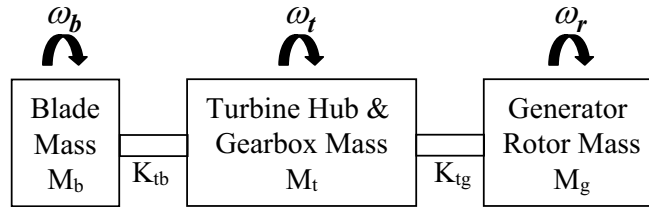


Figure 6.17: Three mass model of DFIG wind turbine.

Table 6.13: DFIG three mass model data.

Inertia constants (MW·sec/MVA)			Torsional stiffness (pu torque/electrical rad)	
H_b	H_t	H_g	K_{tb}	K_{tg}
7.6416	1.2749	1.9250	5.6184	6.3912

The desired DFIG terminal voltage \mathbf{v}_s and stator power P_s are achieved by giving the appropriate rotor voltage magnitude $|\mathbf{v}_r|$ and phase angle $\angle \mathbf{v}_r$ orders to the PWM inverter. The signals are produced by the flux magnitude-angle controller (FMAC) shown in Fig. 6.18 [40]. The power and voltage control loops of the DFIG produce variations in generator torque that introduce negative damping at the turbine shaft and rotor blade natural oscillation frequencies. To avoid instability, an active damping

controller needs to be introduced into the DFIG control scheme to provide damping of these oscillations in order to permit stable DFIG operation. The same controller can be augmented so that it also provides a positive contribution to the damping of network electromechanical oscillations by modulating the current injected into the network by the stator of the DFIG. The designed PSS controller then performs the dual task of stabilizing the low-frequency electromechanical oscillations and providing the necessary damping to the DFIG shaft oscillations.

The controller designed using the proposed approach affects the system by adding its output u_c to the power reference order P_{s-ref} of the FMAC controller, as shown in Fig. 6.18.

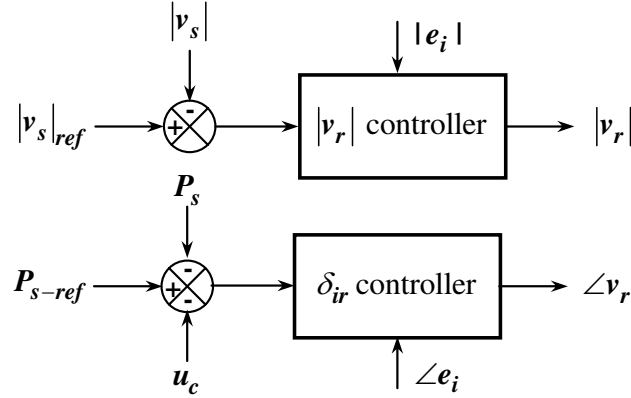


Figure 6.18: Block diagram of flux magnitude-angle controller (FMAC).

A comprehensive range of operating conditions (slip and DFIG output power) for the wind park are considered, as listed in Table 6.14. The components of output power provided by the stator and rotor circuits are also listed in the table. The controller is designed for the base case operating condition of a slip of -0.1 pu. As discussed earlier in § 5.5, the nonlinear optimization problem has multiple solutions. The most robust amongst these multiple controller designs (i.e., the one that provides the best average transient performance at the other three operating conditions) is selected as the final design.

Table 6.14: Various operating conditions of the DFIG system.

Slip	DFIG stator power (P_s) (MW)	DFIG rotor power (P_r) (MW)	DFIG output power (P_{g2}) (MW)
-0.2	1928	-375	2303
-0.1	1622	-153	1775
0.1	1085	119	966
0.2	857	182	675

6.2.2 Controller Design Specifications

Three critical modes, M1, M2, and M3 of frequencies 4.81, 1.87, and 0.98 Hz, respectively, are identified using eigenanalysis of the system. Two of these modes, M1 and M2, are unstable modes, and the third mode, M3, is stable but has a small real part. The damping and oscillation frequencies of the modes are shown in Table 6.15. Analysis of the participation factor and the mode shape suggest modes $M1$ (4.81 Hz), $M2$ (1.87 Hz), and $M3$ (0.98 Hz) are DFIG turbine oscillation, DFIG blade oscillation, and conventional electromechanical oscillation modes, respectively.

As the controller is located on the DFIG (Generator 2), conveniently available local signals - generator speed ω_2 and power P_{g2} - are selected as controller inputs. These signals are effective in controlling the modes, which can be seen from the large sensitivities (residues) between these modes and these signals, as shown in Table 6.16. In order to make the controller selectively respond to the problem modes, these inputs are first passed through signal-conditioning filters. Modes M2 and M3 fall in the pass-band of the (2-15 rad/s) first filter whereas the 20 rad/s cutoff frequency high pass filter allows $M1$ to pass unchanged. Thus, the presence of two filters in each of the system outputs, (i.e., ω_2 and P_s), increases the effective number of outputs of

Table 6.15: Critical Modes of the system without controller.

Mode	Eigenvalue, $\bar{\lambda} = \bar{\alpha} \pm j\bar{\beta}$	Damping ratio, $\bar{\zeta}^a(\%)$	Frequency, $\bar{\omega}^b(\text{Hz})$
M1	$0.0885 \pm j30.231$	-0.29	4.81
M2	$0.2692 \pm j11.727$	-2.23	1.87
M3	$-0.5553 \pm j6.185$	8.94	0.98

$$^a \zeta \triangleq -\alpha 100.0/|\lambda|$$

$$^b \omega \triangleq \beta/(2\pi)$$

the system to four. The block diagram of the controller with filter and dynamic compensator as distinct functional blocks is shown in Fig. 6.19.

The required re-located positions of the critical modes are shown in Table 6.17. These positions correspond to the horizontal movements of the problem eigenvalues to well damped positions in the left-hand side of the complex plane.

Table 6.16: Residues between various DFIG outputs and P_{s-ref} as input for the critical modes.

Output	M1	M2	M3
Gen1 speed	0.0000	0.0006	0.0200
Gen2 (DFIG) speed	0.0083	0.0640	0.0039
Gen3 speed	0.0000	0.0000	0.0023
Gen1 power	0.0256	0.1628	2.5650
Gen2 (DFIG) power	0.0429	0.2176	1.0386
Gen3 power	0.0119	0.039	2.2471

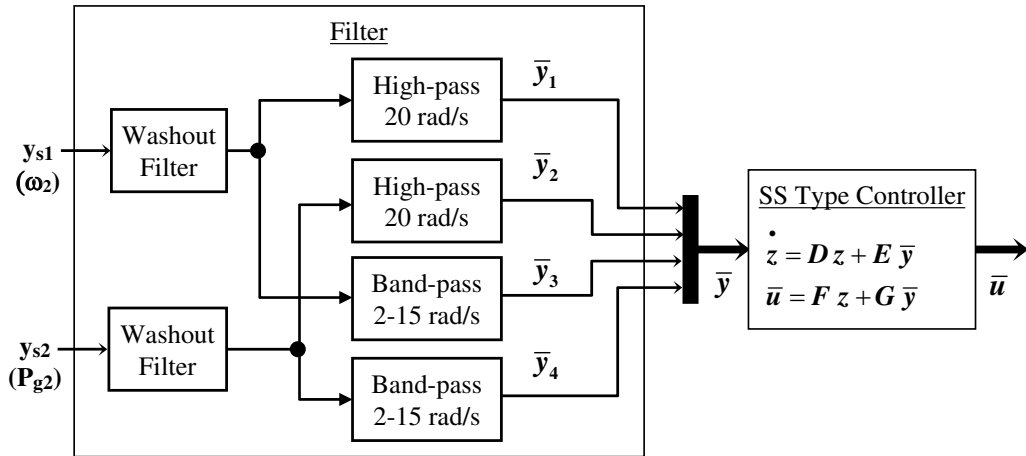


Figure 6.19: State-space (SS) type controller for the DFIG system.

Table 6.17: New locations of the critical modes.

Mode (Open-loop eigenvalue)	Assigned eigenvalue	Damping ratio (%)	Frequency (Hz)
M1 ($0.0885 \pm j30.231$)	$-1.6 \pm j30.2$	5.29	4.81
M2 ($0.2692 \pm j11.727$)	$-2.1 \pm j11.7$	17.67	1.86
M3 ($-0.5553 \pm j6.185$)	$-1.5 \pm j6.2$	23.51	0.99

6.2.3 Controller Design Results

The dynamic compensators were designed using the proposed algorithm, which moves the critical modes horizontally to well-damped locations in the left-hand complex plane. As discussed in § 5.4.3, this procedure also selects the optimal associated left eigenvector to minimize possible adverse excitation of the problem modes. *Controller*₁ is a design obtained using the proposed method. The parameters of the *Controller*₁

are

$$\begin{aligned}
 D &= \begin{pmatrix} -7.02 & -1.27 & 7.71 & 10.64 & 0.91 \\ -4.97 & -2.47 & -3.09 & 6.18 & -7.63 \\ -10.58 & -5.53 & 1.86 & -15.93 & 8.11 \\ -17.44 & -11.18 & 12.42 & -2.43 & -12.50 \\ -10.86 & 10.63 & -4.4 & 15.93 & -1.32 \end{pmatrix} \\
 E &= \begin{pmatrix} 3.37 & -16.41 & 0.12 & 0.29 \\ 1.99 & -12.95 & 0.03 & -0.18 \\ 9.78 & -12.30 & 0.03 & -0.01 \\ 0.12 & -15.33 & 0.05 & 0.37 \\ -9.81 & 14.01 & -0.08 & -0.06 \end{pmatrix} \\
 F &= \begin{pmatrix} -16.79 & -20.14 & -26.58 & -22.20 & 26.34 \end{pmatrix} \\
 G &= \begin{pmatrix} 15.45 & 12.66 & 0.44 & 2.37 \end{pmatrix}. \tag{6.1}
 \end{aligned}$$

A second design, *Controller*₂, was designed using the same procedure as that used for *Controller*₁, except that the weight associated with the sub-objective function quantifying optimal left eigenvector β_3 in (5.17) was set to zero. This is somewhat similar to using the conventional pole-placement algorithm normally employed for control system design. The controller designed in such manner ensures that critical modes move to their assigned (better damped) locations. Additionally, in contrast to conventional pole placement, the method used to develop *Controller*₂ ensures that the unassigned closed-loop eigenvalues are also acceptable. However, unlike *Controller*₁,

the associated left eigenvectors are not optimized. The parameters of *Controller*₂ are

$$\begin{aligned}
 D &= \begin{pmatrix} -9.45 & 2.57 & 9.55 & 15.02 & -1.96 \\ -8.37 & 0.10 & -3.03 & 8.93 & -9.35 \\ -12.25 & -3.48 & 2.20 & -13.45 & 6.49 \\ -14.44 & -13.24 & 13.14 & -4.34 & -11.57 \\ 14.49 & 6.07 & -5.25 & 10.61 & -7.90 \end{pmatrix} \\
 E &= \begin{pmatrix} 0.97 & -16.86 & 0.10 & -0.06 \\ 2.05 & -14.23 & -0.10 & -0.07 \\ 8.96 & -12.89 & -0.09 & -0.09 \\ -1.51 & -13.80 & -0.25 & -0.12 \\ -8.00 & 15.18 & 0.12 & 0.12 \end{pmatrix} \\
 F &= \begin{pmatrix} -13.74 & -9.80 & -17.15 & -9.23 & 17.73 \end{pmatrix} \\
 G &= \begin{pmatrix} 1.95 & 15.91 & 0.22 & 0.08 \end{pmatrix}.
 \end{aligned} \tag{6.2}$$

The effectiveness of the PSSs in improving the transient performance was evaluated by nonlinear simulation of a 4-cycle 3-phase fault at the location shown in Fig. 6.15. Fig. 6.20 shows the transient response of the rotor speed deviation of generators G1 (ω_1) and DFIG (ω_2), and the DFIG turbine hub speed deviation (ω_h). The superiority of *Controller*₁, which is based on eigenstructure assignment, is clearly evident. The magnitudes of the low frequency oscillation in the speed signal ω_1 , and the high frequency oscillation in signals ω_2 and ω_h , are smaller with *Controller*₁ than with *Controller*₂.

Although *Controller*₁ and *Controller*₂ were stable at the designed operating point, they were unstable at the other operating point where *slip* = 0.2 (row 4 of Table 6.14). This is evident from the transient response of ω_1 , ω_2 , and ω_h shown in Fig. 6.21. A solution to this problem is possible by realizing that the MONLOP optimization procedure produces several locally-optimal solutions depending on the starting point for optimization, as discussed in § 5.5. Each of the multiple solu-

tions can be evaluated as to its effectiveness in achieving good transient performance at operating points different from the operating point for which the controller was designed. This selection allows the design of a more ‘robust’ controller. In this example, *Controller*₃ is another such design obtained with a different optimization starting point than the one used for obtaining *Controller*₁. The parameters of *Controller*₃ are

$$\begin{aligned}
 D &= \begin{pmatrix} -8.14 & 1.40 & 12.65 & 12.50 & -3.6 \\ -7.06 & -0.57 & 0.11 & 6.95 & -11.14 \\ -1.73 & -4.03 & 4.29 & -15.11 & 5.74 \\ -14.86 & -12.34 & 10.13 & -2.56 & -9.92 \\ 13.19 & 7.40 & -9.69 & 14.07 & -5.99 \end{pmatrix} \\
 E &= \begin{pmatrix} 1.00 & -16.65 & 0.14 & -0.11 \\ 1.58 & -13.99 & 0.06 & -0.56 \\ 9.09 & -12.63 & -0.21 & -0.30 \\ -0.33 & -13.99 & -0.08 & 0.73 \\ -8.00 & 14.74 & 0.19 & 0.54 \end{pmatrix} \\
 F &= \begin{pmatrix} -14.14 & -13.90 & -13.54 & -15.32 & 17.58 \end{pmatrix} \\
 G &= \begin{pmatrix} 4.36 & 16.27 & -0.15 & 1.63 \end{pmatrix}.
 \end{aligned} \tag{6.3}$$

As seen in Fig. 6.22, the dynamic response of *Controller*₁ and *Controller*₃ are very similar at the designed operating point. However, in contrast to *Controller*₁ and *Controller*₂, *Controller*₃ is stable with good transient response at the other operating points also (Fig. 6.23), and is hence selected as the final design.

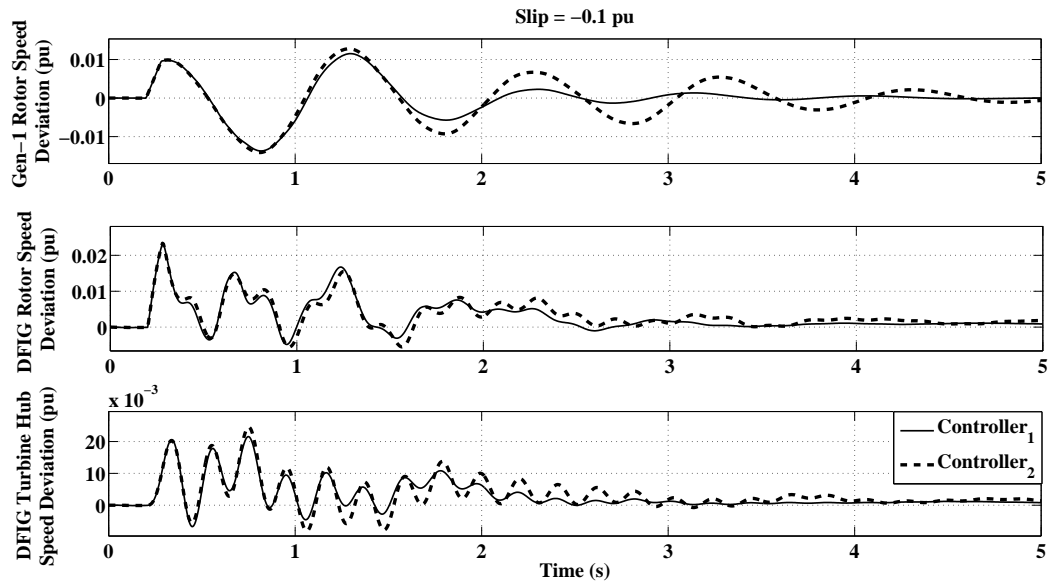


Figure 6.20: Transient response of speeds for the case with *Controller*₁ and that for the case with *Controller*₂ when operating at *slip* = -0.1 pu.

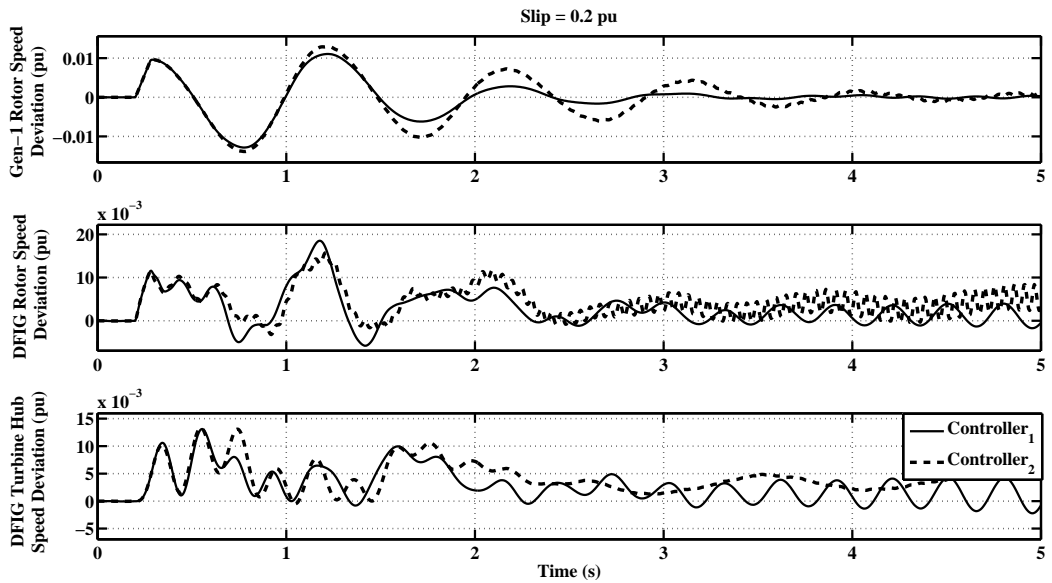


Figure 6.21: Transient response of speeds for the case with *Controller*₁ and that for the case with *Controller*₂ when operating at *slip* = +0.2 pu.

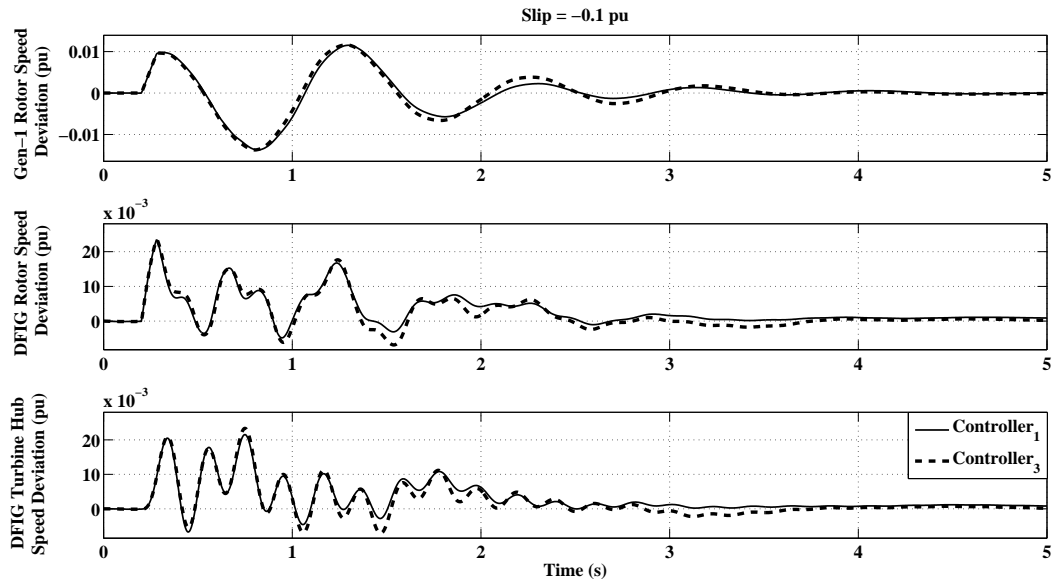


Figure 6.22: Transient response of speeds for the case with *Controller*₁ and that for the cases with *Controller*₃ when operating at *slip* = -0.1 pu.

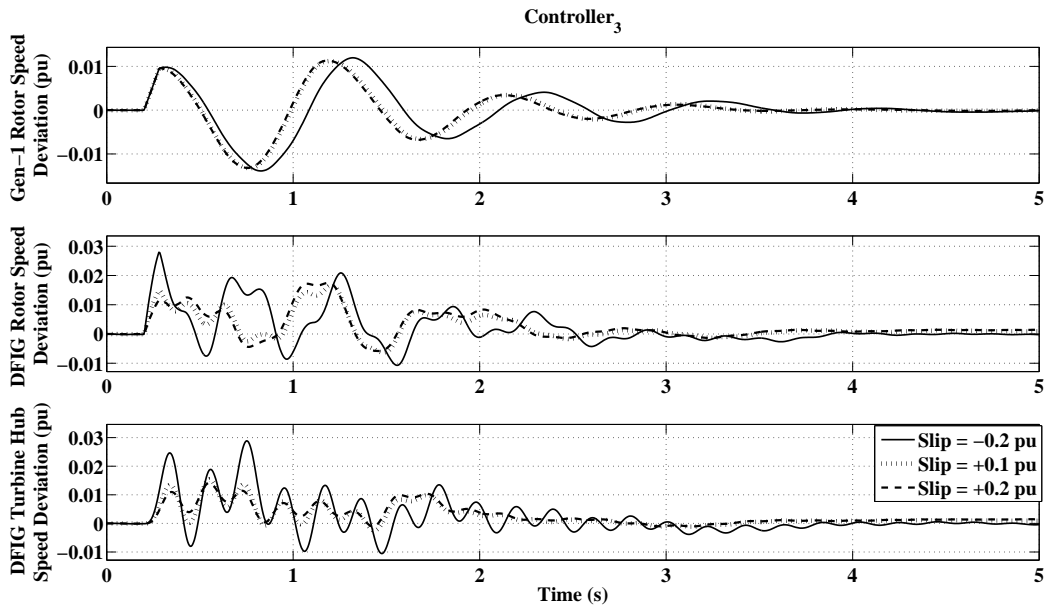


Figure 6.23: Transient responses of speeds for the case with *Controller*₃ when operating at different slips.

6.3 Large Power System

In previous sections, the proposed eigenstructure assignment based algorithm was used in the design of controllers for small systems. The results clearly show the advantage of the proposed technique over the conventional frequency domain method. In this section, the PSS is designed for a large power system. The results demonstrate that the proposed algorithm is equally suitable in the design of controllers for a practical large power system, and that, it is possible to achieve better dynamical performance for a large-scale systems by employing a controller designed using the algorithm compared to that obtained by employing a PSS designed using the conventional design technique .

The application of the proposed technique involves various mathematical operations on matrices. The computations involving small matrices, such as those associated with the relatively smaller systems described in previous sections, can be carried out in a relatively straightforward manner using the basic subroutines available in commercial programs. The use of such techniques and programs for a large power system is computationally prohibitive. The available techniques and programs suitable specifically for large matrices and used in the design of controllers for large power systems are shown in Appendix C.

6.3.1 System Description

In this section, a PSS for the Manitoba Hydro system is designed using the proposed algorithm. The Manitoba Hydro system is an integral part of the mid-continent area power pool (MAPP) system, which is inter-connected electrical system of upper Midwest North American area and comprise electrical utilities of Manitoba, Minnesota, Nebraska, North Dakota, Wisconsin, Montana, Iowa, and South Dakota. The model comprises the generation, load, and transmission network of the complete upper mid-western part of North America. The summary of the power system model is shown

in Table 6.18 to Table 6.19. The case considered here represents the peak load flow during summer. The total number of state variables of the system is 28,883. As described in Appendix A, calculation of intermediate matrices is the first step in the small-signal study of the system. The required intermediate matrices for controller design purposes were obtained using a small-signal analysis tool (SSAT), a component of the commercial program DSATool by Powertech Labs Inc.

Table 6.18: MAPP power system summary.

Component	Numbers
Buses	21747
Areas	138
Zones	358
Generating units	3847
Loads	14930
Fixed shunts	4310
Switched shunts / SVCs	1644
Lines	24500
Adjustable transformers	8466

Table 6.19: Summary of powerflow of the MAPP power system.

		MW	Mvar
System	Generation	577393.9	136509.6
	Total Load	564924.1	37436.49
Manitoba	Generation	4755.7	2974.1
Hydro	Load	2354.4	516.4
Area	Export	2097.3	187.8

Table 6.20: Summary of EHV and HV bus and branch in the MAPP power system.

Voltage Level (kV)	Number of Branches	Number of Buses
765	44	31
500	341	253
345	1363	781
230/220	3331	1888
138	6160	3497
120/115/110	6225	3457
DC	12	24

6.3.2 System Open Loop Analysis

The system is unstable, as shown in Fig. 6.24, due to the loss of 50% of 120 MW load for a duration of 50 ms at 138 kV bus 67703. The system instability is the result of negatively damped electromechanical mode ($0.095 \pm j3.75$) of the system. The participation factors and right eigenvector analysis shown in Table 6.21 suggest that the electromechanical mode is a local plant mode. The generators close to each other - two equally rated Kettle generators and a Kelsey generator - will oscillate in unison against the rest of the system. Related to these generators is another electromechanical mode ($-0.25 \pm j8.18$) that has higher frequency and is relatively well damped. The participation factors and the mode shape of the generators in the mode are also shown in Table 6.21. The mode shape suggests that the higher frequency electromechanical mode is an interplant mode where the two Kelsey generators will oscillate against Kettle generator.

As the first step in PSS design, the most suitable location for the PSS is determined using the procedure described in § 3.2. Accordingly, the Kettle and Kelsey generators are selected for residue analysis because they participate most in this electromechanical mode. The other generators have a participation factor of 0.01 or less.

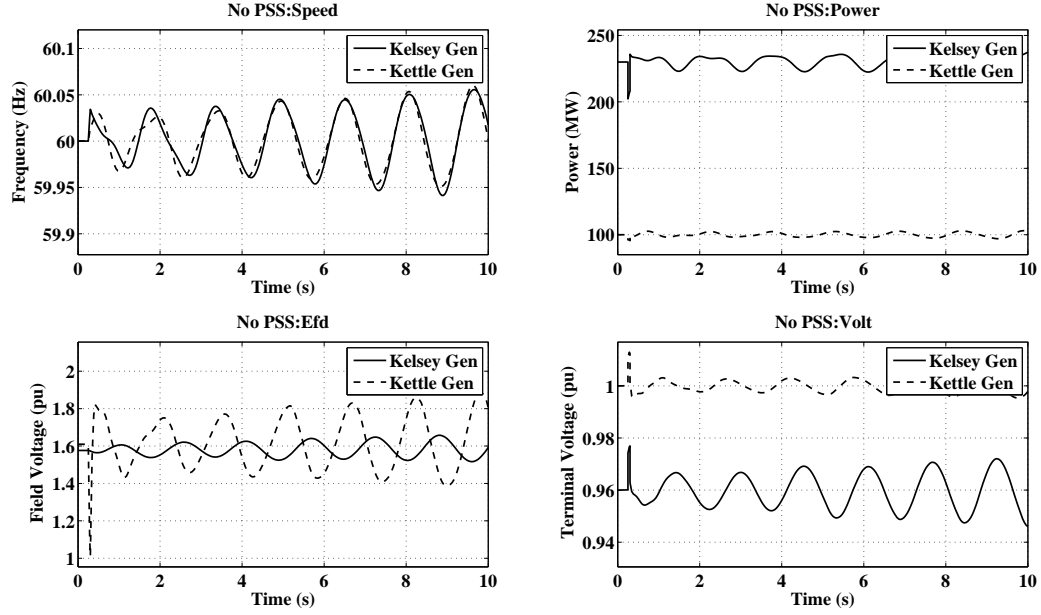


Figure 6.24: Transient response of variables of generators without a PSS.

Table 6.21: Modal analysis of critical plant and local plant modes.

	Plant mode		Local mode	
Eigenvalue	$\bar{\lambda}_1, \bar{\lambda}_1^* = 0.0951 \pm j3.7464$		$\bar{\lambda}_2, \bar{\lambda}_2^* = -0.25 \pm j8.18$	
Frequency	0.60		1.30	
Damping	-2.54		3.05	
Generator	Participation Factor	Mode Shape	Participation Factor	Mode Shape
Kelsey	1.00	$1.00 \angle 0^\circ$	1	$0.96 \angle -173.8^\circ$
Kettle	0.43	$0.43 \angle 5.47^\circ$	0.45	$1 \angle 0^\circ$

The one line diagram of the system around Kettle and Kelsey generating stations, which are in the northern part of the Manitoba Hydro system, are shown in Fig. 6.25.

The experience with the small sample system presented in previous sections suggests that using more than one signal as input for the PSS would result in improved

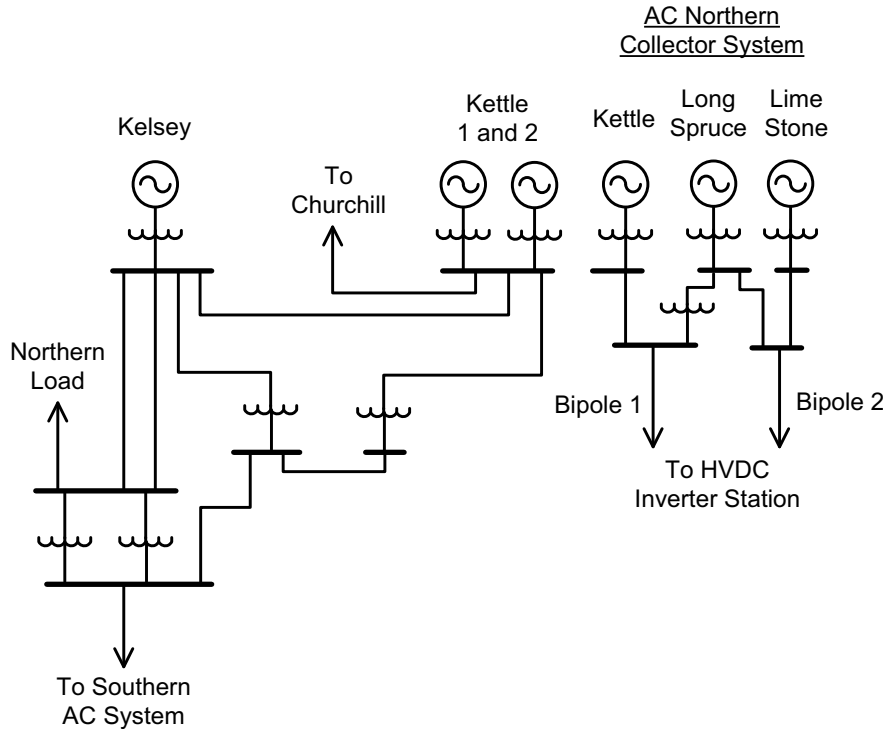


Figure 6.25: Manitoba Hydro northern area power system.

dynamical performance when an SS type PSS is designed using the proposed eigenstructure assignment based algorithm. Therefore, generator power, speed, and voltage, the locally available and easily measurable signals, are selected as candidate inputs for the PSS. The residue of the plant mode between the output variables and the local exciter voltage reference input are shown in Table 6.22.

The residues of speed and power for the three generators are comparable, whereas the residue of the voltage of the Kelsey generator is almost twice that of the Kettle generators. Hence, the Kelsey generator was selected for equipping with a PSS.

Note that if only a speed input PSS is to be employed, then, ideally, the most suitable location for the PSS will be Kettle according to the selection based on residue analysis; whereas, it will be Kelsey according to selection based on participation factor. This provides another example that selection of the location based on only the participation factor may not be an optimal location (a similar example was provided

in § 3.4.1).

The residue of the Kelsey generator outputs for the interplant mode is shown in Table 6.23. The interplant mode is somewhat sensitive to Kelsey generator power, and is almost insensitive to the generator speed and voltage. This necessitates some measure to ensure that the interplant mode remains well damped when a PSS is designed using the proposed algorithm. The measures implemented during the design are described later in this section.

Table 6.22: Residues of critical plant mode, $\bar{\lambda}_1, \bar{\lambda}_1^* = 0.0951 \pm j3.7464$ between various outputs and exciter *V_{ref}* input of Kelsey and Kettle generators.

Generator	Speed	Power	Voltage
Kelsey G1	$0.015 \angle 30.3^\circ$	$0.46 \angle -57.6^\circ$	$0.146 \angle -49.6^\circ$
Kettle G1 and G2	$0.019 \angle -14.8^\circ$	$0.485 \angle 78.7^\circ$	$0.072 \angle -35.9^\circ$

Table 6.23: Residues of interplant mode, $\bar{\lambda}_2, \bar{\lambda}_2^* = -0.25 \pm j8.18$ between various outputs and exciter *V_{ref}* input of Kelsey and Kettle generators.

Generator	Speed	Power	Voltage
Kelsey G1	$0.003 \angle -62.4^\circ$	$0.201 \angle 29.8^\circ$	$0.003 \angle 5.0^\circ$
Kettle G1 and G2	$0.030 \angle -64.7^\circ$	$1.689 \angle 28.4^\circ$	$0.123 \angle 76.3^\circ$

6.3.3 Conventional PSS Designed in Frequency Domain

The speed input lead-lag type stabilizer (used earlier for a two-area four-generator system in § 6.1.3) was designed to improve the small-signal stability of the system. The objective of PSS design is to make the plant mode ($\bar{\lambda}, \bar{\lambda}^* = 0.095 \pm j3.75$) stable and push it further to the left in the $X - Y$ plane until acceptable damping is achieved.

Here, 3.0% is considered as the desired damping ratio. This corresponds to relocation of the plant mode $\bar{\lambda}, \bar{\lambda}^*$ to $\lambda, \lambda^* = -0.115 \pm j3.75$ when moved parallel to the X -axis.

6.3.3.1 PSS Parameters

The value of 10.0 s is selected for washout filter time constant T_w ; and the lead-lag parameters are designed using the residue method described in § 3.3.2.1. The required phase compensation, the lead-lag parameters, and the approximate and actual gain are shown in Table 6.24.

Table 6.24: Lead-lag type PSS parameters.

Phase Compensation	T1=T3	T2=T4	Ks	
			Approximate	Adjusted
149.7°	2.18	0.032	0.2162	0.25

6.3.3.2 Results

The new location of two critical electromechanical modes (plant and inter-plant modes) after implementation of the lead-lag PSS are compared against their original locations, (i.e., without a PSS) in Table 6.25. It can be seen from the table that the desired damping of almost 3.0% is achieved for the plant mode by moving it almost parallel to the X -axis. The damping of the interplant mode has worsened; however, it is stable, and its real part (which decides the rate of decay of the mode) is still more negative than the plant mode, which means that the interplant mode will still decay faster than the plant mode.

The transient performance of the system is evaluated by nonlinear simulation of the system with the speed input lead-lag type PSS. A disturbance due to the loss of 50% of the 120 MW load at the 138 kV bus 67703 for a duration of 50 ms was considered for the nonlinear simulations. The transient response of the speed, power, field voltage, and bus voltages of the Kelsey and Kettle generators with the PSS are

compared to those for the system without a PSS in Fig. 6.26 and Fig. 6.27. It is evident from the plots that the PSS has stabilized the system and that the transients are well damped.

Table 6.25: Comparisons of electromechanical modes with the lead-lag PSS and without a PSS.

	Interplant mode			Plant mode		
	Eigenvalue	Freq	Damping	Eigenvalue	Freq	Damping
Without PSS	$0.095 \pm j3.75$	0.600	-2.54	$-0.25 \pm j8.18$	1.30	3.05
With PSS	$-0.114 \pm j3.86$	0.616	2.95	$-0.142 \pm j8.3$	1.32	1.70

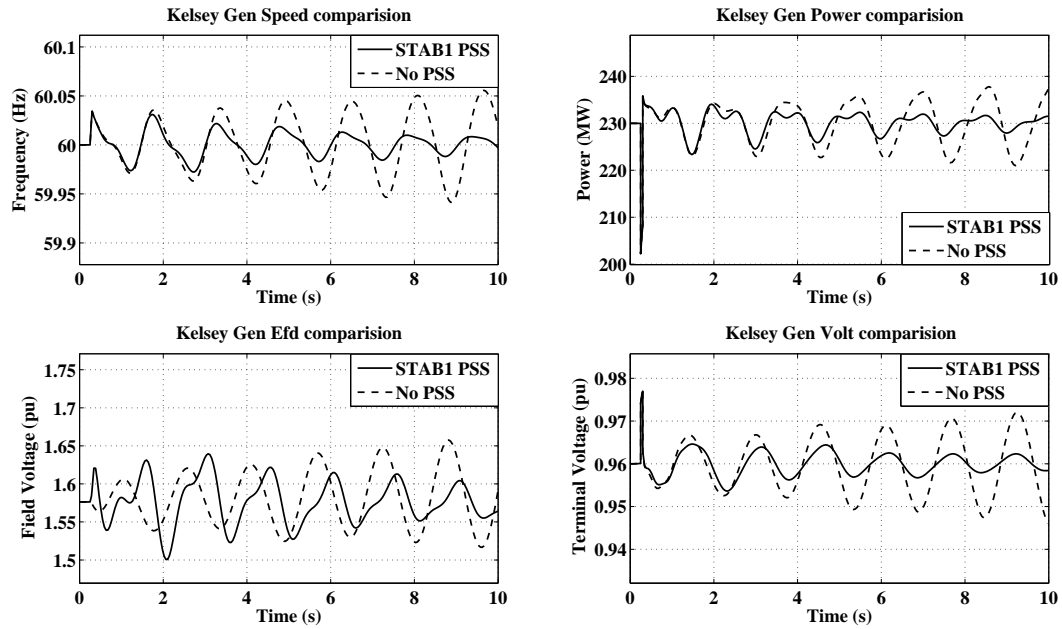


Figure 6.26: Transient response of Kelsey generator variables for the case with the speed input STAB1 (lead-lag) PSS and that for the case without a PSS.

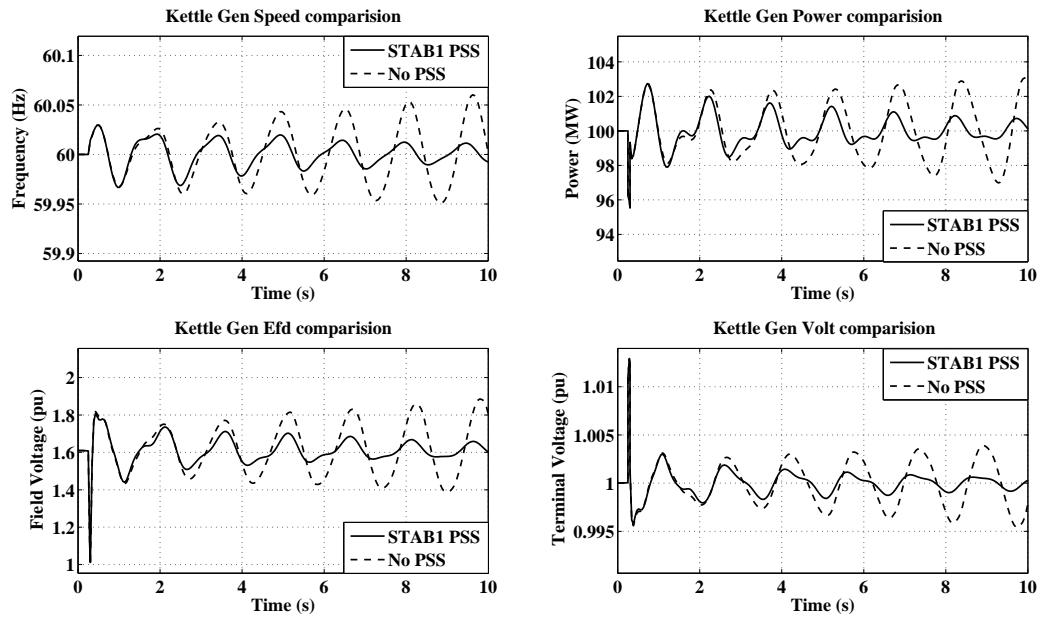


Figure 6.27: Transient response of Kettle generator variables for the case with the speed input STAB1 (lead-lag) PSS and that for the case without a PSS.

6.3.4 SS PSS Design Using the Proposed Technique

A state-space type PSS, shown in Fig. 6.28, was designed using the proposed technique in the following subsection. The SS type PSS is described in detail in § 5.1.

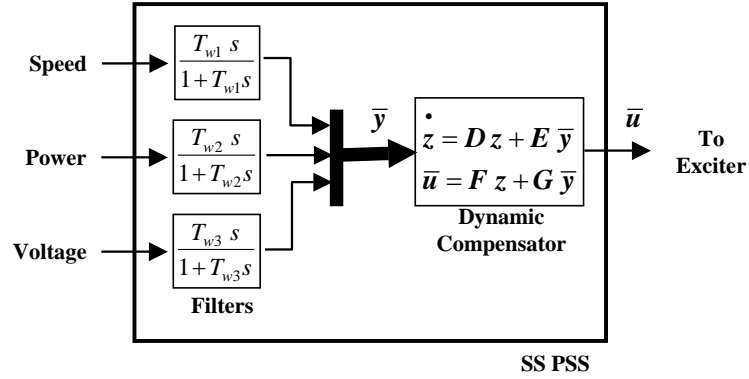


Figure 6.28: Block diagram of the three input SS type PSS.

6.3.4.1 Inputs to the SS type PSS

Here, the objective of PSS design using the proposed technique is to relocate the unstable critical plant mode to a suitable location in the $X-Y$ plane and, additionally, to assign the appropriate left eigenvector so that its excitation is minimized during disturbances. The subspace where the assignable left eigenvector lies depends on the number and type of the PSS inputs. The probability of assigning an improved eigenstructure increases as the number of system outputs increases. This concept was proven in § 6.1 by designing three PSSs, each having different inputs-speed input PSS, power input PSS, and speed and power (dual) input PSS. It was shown that using two inputs, speed and power, the excitation of the inter-area mode was suppressed almost completely. Therefore, in this case of large power system, local generator, speed, power, and voltage are employed as inputs to the SS type PSS.

6.3.4.2 Desired New Location of Electromechanical Modes

The system exhibits an unstable electromechanical plant mode. The main objective of installing a PSS is to improve damping of the plant mode to at least 3%. Therefore, the eigenvalues of the plant mode $\bar{\lambda}_1, \bar{\lambda}_1^* = 0.0951 \pm j3.746$ will be assigned eigenvalues $\lambda_1, \lambda_1^* = -0.115 \pm j3.75$.

As a secondary objective, the interplant mode is assigned a new, somewhat better-damped location for two reasons. The first reason is that the interplant mode has a large enough residue for Kelsey generator power, and hence, implementation of a PSS may reduce its damping, as observed in the previous section for the case in which a speed-input lead-lag type PSS was installed. The second reason is that, by assigning a new location provides an opportunity to improve its left eigenvector so that its excitation is minimized during a disturbance, thereby attaining further improved dynamical performance. The new location of the interplant mode is selected so that the distance to be moved is somewhat proportional to the distance the plant mode is to be moved and to the ratio of the residue of the interplant mode and the plant mode. Accordingly, the new location of the interplant mode $\bar{\lambda}_1, \bar{\lambda}_1^* = -0.25 \pm j8.18$ will be assigned an eigenvalue of $\lambda_1, \lambda_1^* = -0.28 \pm j8.18$.

6.3.4.3 Dynamic Compensator States

As decided in the previous subsection, there are four eigenvalues (two complex conjugate pairs) to be assigned to the closed-loop system. In order to be able to assign four eigenvalues using the left eigenstructure assignment technique, the system should have at least four inputs, (i.e., $m = 4$). However, the actual number of inputs to the system that will be used to modulate V_{ref} of an exciter for the Kelsey generator is one (i.e., $\bar{m} = 1$). Thus, the number of states of the dynamic compensator is selected to be $a = m - \bar{m} = 3$. This increases the number of inputs of the control system by three when the dynamic output feedback control system is transformed into its equivalent gain output feedback system (§ 4.2).

6.3.4.4 SS type PSS Parameters

Each of the measured signals is passed through a washout (high pass) filter, as shown in Fig. 6.28. The objective of the high pass filter is to remove the dc components present in the signals; a value of 10.0 s is selected for the washout filter time constants, T_{w1} , T_{w2} , and T_{w3} .

The PSS was designed to assign the eigenvalues determined in the previous section and optimally assign the left eigenstructure by solving the MONLOP described in § 5.4. The designed parameters of the SS type PSS are shown in (6.4).

$$\begin{aligned}
 D &= \begin{pmatrix} 2.69 & -1.07 & 26.84 \\ -4.96 & -13.63 & 6.61 \\ 4.27 & 23.26 & -25.87 \end{pmatrix} & E &= \begin{pmatrix} -11.63 & -7.9 & 6.76 \\ 15.29 & -9.83 & -19.27 \\ -20.91 & 13.06 & -11.45 \end{pmatrix} \\
 F &= \begin{pmatrix} -1.60 & -6.68 & 8.17 \end{pmatrix} & G &= \begin{pmatrix} 5.4 & -4.55 & 2.15 \end{pmatrix} \quad (6.4)
 \end{aligned}$$

6.3.5 Results

The optimization moved the open-loop electromechanical modes ($0.0951 \pm j3.746$ and $-0.25 \pm j8.18$) to their assigned locations ($-0.115 \pm j3.75$ and $-0.28 \pm j8.18$), as can be seen from their mode trace shown in Fig. 6.29. The mode traces were obtained by gradually increasing the gains F and G of the PSS.

The system was simulated for loss of 50% of a 120 MW load for a duration of 50 ms at the 138 kV bus 67703. The transient response of speed, power, voltage, and field voltage of the Kelsey and Kettle generators with the SS type PSS are compared with those of the system with the lead-lag type PSS in Fig. 6.30 and Fig. 6.31. The improved transients for the case of an SS type PSS compared to the case of a lead-lag PSS are visible. In order to quantify the improvement, the magnitude of the assigned modes ($-0.115 \pm j3.75$ and $-0.28 \pm j8.18$) obtained through prony analysis and the peak-to-peak values for the transient responses are compared in Table 6.26. The

peak-to-peak values of the variables shown in the table correspond for the transient after 0.5 s of clearing disturbance. As can be seen from the table, employment of an SS type PSS results in considerably reduced magnitudes of the interplant and plant modes and also of the peak-to-peak values compared to the magnitudes from the case with the lead-lag type PSS.

Table 6.26: Magnitudes of electromechanical modes in different generator variables due to disturbance.

Variable	Kelsey Generator			Kettle Generators		
	Lead-Lag	SS	Change	Lead-Lag	SS	Change
Mode M1 Magnitude						
Speed (Hz)	0.0301	0.0251	16.61%	0.0298	0.0251	15.77%
Power (MW)	4.444	3.5297	20.57%	1.6709	1.299	22.26%
Voltage (pu)	0.0062	0.0039	37.10%	0.0022	0.0014	36.36%
Field Voltage (pu)	0.0722	0.0277	61.63%	0.1277	0.0846	33.75%
Mode M2 Magnitude						
Speed (Hz)	0.0104	0.0096	7.69%	0.0098	0.0106	-8.16%
Power (MW)	3.2396	2.8709	11.38%	1.1381	1.1752	-3.26%
Voltage (pu)	0.0008	0.0004	50.00%	0.001	0.0007	30.00%
Field Voltage (pu)	0.0322	0.0051	84.16%	0.0548	0.0422	22.99%
Peak-to-Peak Magnitude						
Speed (Hz)	0.0588	0.049	16.67%	0.0536	0.056	-4.48%
Power (MW)	10.7525	9.1734	14.69%	4.1072	2.9436	28.33%
Voltage (pu)	0.011	0.0084	23.64%	0.0051	0.0041	19.61%
Field Voltage (pu)	0.139	0.0552	60.29%	0.2954	0.1837	37.81%

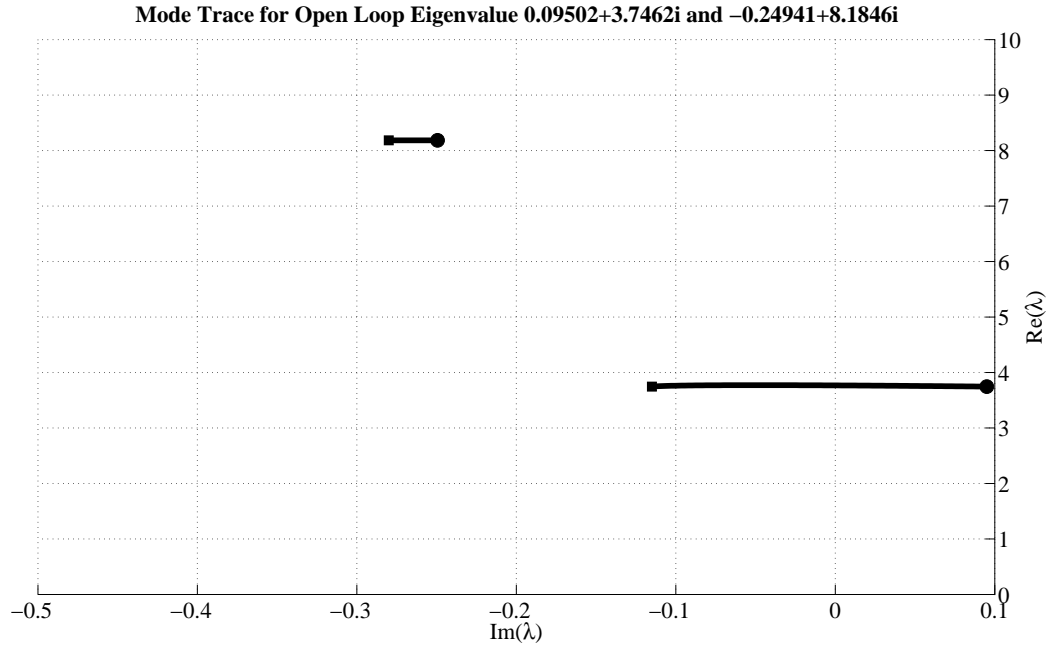


Figure 6.29: Mode trace of the system with the three input SS type PSS for varying gain from zero to the final value.

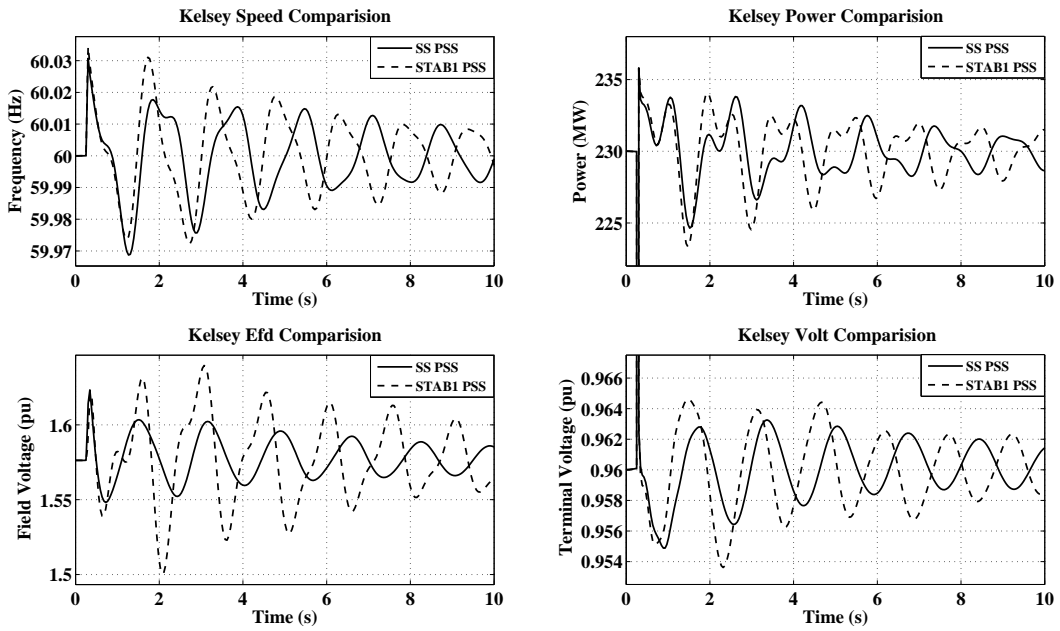


Figure 6.30: Transient response of Kelsey generator variables for the case with the three input SS type PSS and that for the case with the speed input STAB1 (lead-lag) PSS.

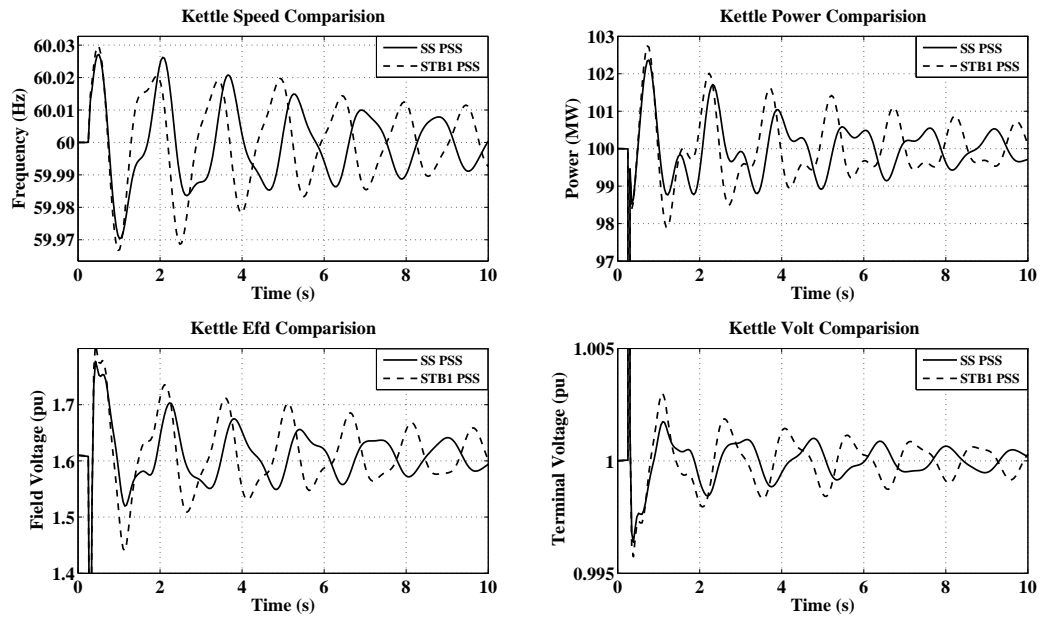


Figure 6.31: Transient response of Kettle generator variables for the case with the three input SS type PSS and that for the case with the speed input STAB1 (lead-lag) PSS.

6.3.6 Conclusions

In this chapter, PSSs were designed for three different systems, a two-area four-generator system, a system with a DFIG wind turbine, and a large power system, using the proposed optimization-based eigenstructure assignment PSS design algorithm.

For the case of the 2-area 4-generator system, three different PSSs were examined in order to assess the influence of employing alternate input signals and the influence of employing more than one signal. The signals considered for the SS type PSSs were speed input, power input, and speed-power dual input. Their small-signal and dynamic performances were evaluated by comparing them with those of the PSSs designed using the frequency domain method. The results show that PSS input signals affect the possible improvement in eigenstructure and dynamic performance. The speed input SS type PSS does not provide any benefit over the conventional PSS. However, somewhat improved eigenstructure, and therefore improved dynamic performance, is achieved by employing power as an input to the SS type PSS. Also, excellent performance is achieved when speed-power dual inputs are employed for the SS type PSS, excitation of the problematic inter-area mode is almost completely suppressed.

The proposed algorithm was successfully used to design a controller that greatly improved the system response for the system with a DFIG wind generator. Damping of critical shaft oscillations and electromechanical modes was improved by eigenvalue assignment, and the excitation of these modes was minimized through eigenvector assignment. The proposed controllers were validated through a time-domain transient solution. The nonlinear nature of the MONLOP algorithm developed in this thesis leads to multiple solutions depending on the initial values used. The resulting controllers can then be further evaluated for robustness, and the controller that provides universally good performance over the range of potential operating conditions can be selected as the final design.

Finally, the proposed algorithm was employed to design a PSS for a large power system to demonstrate the practical application of the algorithm. The SS type PSS with three inputs-speed, power, and voltage-was designed so that optimal eigenstructure is assigned to the system. It was demonstrated by a comparison of the transient performance of the system that significantly improved dynamic performance is achieved by employing an SS type PSS compared to that which can be achieved by employing a lead-lag type PSS designed using the conventional frequency domain method.

Chapter 7

Conclusions and Future Work

7.1 Summary and Conclusions

In this thesis an optimization based eigenstructure assignment algorithm is developed for power system controller design. This design method uses extra degrees of freedom to assign partial left eigenvector in addition to re-positioning the system eigenvalues to improve damping. Since this method permits optimization of the left eigenvectors, the excitation of the critical modes could be minimized. This possibility is not explored in the frequency domain design method that is widely used in power systems, and therefore the proposed method is superior.

The algorithm presented in this thesis is an improvement over previous eigenstructure assignment methods. These methods are suitable for small systems where the number of system inputs and outputs exceeds number of states; but these methods are not feasible in the much larger power networks where it is not practical to obtain system information from remote geographic locations. Hence, when these methods are employed for power system controller design, they do position the eigenvalues to the specified locations, but there is a risk that a non-critical eigenvalue will be moved instead of the critical one. Even in those cases where the critical eigenvalues are properly repositioned, there remains the possibility of the non-critical eigenvalues

moving to poorly damped or unstable locations.

These inadequacies have been addressed in the proposed algorithm presented in this thesis by formulating and solving an unconstrained multi-objective nonlinear optimization problem (MONLOP). The MONLOP comprises six sub-objective functions of parametric vectors to be minimized simultaneously. These functions are formulated to accomplish a number of objectives: ensure that the critical open-loop eigenvalues move to their assigned new locations; penalize inadvertent movement of open-loop eigenvalues that are not assigned new locations; quantify the weighted sum of the left eigenvectors associated with the assigned eigenvalues; and quantify the required controller efforts. After defining the sub-objective functions, the MONLOP problem is transformed into a single-objective nonlinear optimization problem (SONLOP) where the single objective is a weighted sum of the individual sub-objectives.

The Nonlinear Simplex Method of Nelder and Mead is used in this thesis to conduct the minimization process. The nonlinear nature of the MONLOP algorithm developed in this thesis leads to multiple solutions depending on the initial values. The resulting controllers can then be further evaluated to ensure that they meet all the design objectives and any additional performance criteria.

When the proportional output feedback controllers are designed using the partial left eigenstructure assignment technique, the maximum number of eigenvalues that can be relocated is the number of system inputs. For a typical case of PSS design, two or more eigenvalues are to be relocated to suitable locations, whereas only one system input is available in terms of the voltage reference signal of exciter. In such a case, a dynamic compensator with enough states can be employed so that the desired number of eigenvalues can be assigned.

The achievable optimal left-eigenvectors (and hence the extent to which the excitation of the modes could be minimized) depend on the system output variables and the number thereof. This aspect was explained theoretically and demonstrated by designing a PSS using the proposed algorithm for a two-area, four-generator system.

Using the example, it was shown that when a single system output is employed, the extent of minimization depends on the output variable employed; furthermore, by employing two system outputs, the excitation of the critical mode is reduced even further, resulting in even better dynamical performance.

The algorithm was applied to the design of two additional controllers: a combined PSS and active damping controller for a DFIG; and a PSS for a generator in the Manitoba Hydro system. Based on the earlier conclusion that increasing the number of system outputs results in superior dynamic performance, two conveniently available local outputs were employed. For the DFIG controller, the number of system outputs was further increased to four by passing the system outputs through additional filters. The proposed controllers were validated by comparing the time-domain transient performance of the system with the proposed controller to that of the system with a controller designed using either the conventional frequency domain method or a similar method. It was shown that not only was the damping of critical modes improved by eigenvalue assignment, but the excitation of these modes was minimized through partial eigenvector assignment resulting in significantly improved system response.

7.2 Recommendations

The proposed algorithm involves minimization of a single-objective nonlinear function where the single objective function is a weighted sum of the individual sub-objectives. In this thesis, the appropriate weights were determined by an iterative process. Using a given set of weights, a couple of controllers are obtained by minimizing the objective function from random starting points. The new values of the weights are then estimated based on the assessment of how successful these controllers are in achieving various design objectives. This process of weight adjustment is continued until the controllers are found to satisfy all the desired objectives. The assessment of

each of the controllers required eigenanalysis, mode trace, and (sometimes) transient simulations. Arriving at the appropriate weights in this manner is a time-consuming process.

Further research work can be undertaken to refine the above optimization process so that controllers can be designed in less time and with less designer intervention. Study of the nonlinear nature of the optimization problem and identification of a more suitable optimization technique are further avenues to explore.

An important aspect of the controller design is the robustness of the controller over a range of operating conditions. This aspect is not included in the proposed algorithm. Rather, a robust controller for a DFIG system was designed using the brute-force method. In this method, a robust controller was designed for the system by evaluating different controllers, which were obtained by carrying out optimization with different starting points, for a variety of operating conditions. The controller that performed universally well over the range of operating conditions was selected as the final robust controller. There are further avenues for research regarding the inclusion of the robustness aspect in the design process.

Bibliography

- [1] V. Arcidiacono, E. Ferrari, R. Marconato, J. Ghali, and D. Grandez, “Evaluation and improvement of electromechanical oscillation damping by means of eigenvalue-eigenvector analysis. practical results in the Central Peru Power System,” *IEEE Transactions on Power Apparatus and Systems*, vol. PAS-99, pp. 769–778, Mar 1980. vi, 27, 30
- [2] F. deMello and C. Concoridia, “Concept of synchronous machine stability as affected by excitation control,” *IEEE Trans. Power App. Syst.*, vol. Pas-88, pp. 316–329, Apr 1969. vi, 6, 32, 33
- [3] P. Kundur, M. Klein, G. Rogers, and M. Zywno, “Application of power system stabilizers for enhancement of overall system stability,” *Power Systems, IEEE Transactions on*, vol. 4, pp. 614–626, May 1989. vi, 7, 8, 29, 32, 33, 34
- [4] N. Kshatriya, U. Annakkage, F. Hughes, and A. Gole, “Optimized partial eigenstructure assignment-based design of a combined pss and active damping controller for a dfig,” *Power Systems, IEEE Transactions on*, vol. 25, pp. 866–876, May 2010. vii, viii, 69, 73, 78, 84, 111
- [5] B. Archer, L. Midford, and J. Davies, “Dual configuration, dual setting, digital power system stabilizer-simulation and tuning experience at manitoba hydro,” *Power Engineering Society Winter Meeting, 2002. IEEE*, vol. 2, pp. 741–746, 2002. xi, 100

- [6] P. Kundur, *Power System Stability and Control*. McGraw-Hill, Inc., 1994. 3, 4, 7, 17, 40, 65, 68, 163
- [7] P. Kundur, J. Paserba, V. Ajjarapu, G. Andersson, A. Bose, C. Canizares, N. Hatziargyriou, D. Hill, A. Stankovic, C. Taylor, T. Van Cutsem, and V. Vittal, “Definition and classification of power system stability IEEE/CIGRE joint task force on stability terms and definitions,” *IEEE Transactions on Power Systems*, vol. 19, pp. 387–1401, Aug 2004. 3, 17
- [8] “IEEE std 421.5 - 2005 IEEE recommended practice for excitation system models for power system stability studies,” *IEEE Std 421.5-2005 (Revision of IEEE Std 421.5-1992)*, pp. 1–85, 2006. 6, 62, 100
- [9] P. Kundur, L. Berube, G.R.and Hajagos, and R. Beaulieu, “Practical utility experience with and effective use of power system stabilizers,” *Power Engineering Society General Meeting, 2003*, vol. 3, pp. 1777–1785, July 2003. 7
- [10] E. Larsen and D. Swann, “Applying power system stabilizers part i, ii and iii,” *IEEE Transactions on Power Apparatus and Systems*, vol. PAS-100, pp. 3017–3046, June 1981. 7
- [11] I. Kamwa, R. Grondin, and G. Trudel, “IEEE PSS2B versus PSS4B: the limits of performance of modern power system stabilizers,” *Power Systems, IEEE Transactions on*, vol. 20, pp. 903–915, May 2005. 7
- [12] P. Kundur, D. Lee, and H. Zein El-Din, “Power system stabilizers for thermal units: Analytical techniques and on-site validation,” *IEEE Transactions on Power Apparatus and Systems*, vol. PAS-100, pp. 81–95, January 1981. 7
- [13] M. Klein, G. Rogers, S. Moorthy, and P. Kundur, “Analytical investigation of factors influencing power system stabilizers performance,” *Energy Conversion, IEEE Transaction on*, vol. 7, pp. 382–390, Sep 1992. 7, 28, 33, 45, 81

- [14] CIGRE Task Force 38.02.16, “Impact of interactions among power system controls,” *CIGRE Technical Brochure No. 166*, Aug 2000. 7
- [15] W. Wonham, “On pole assignment in multi-input controllable linear systems,” *Automatic Control, IEEE Transactions on*, vol. 12, pp. 660–665, December 1967. 10
- [16] E. Davison, “On pole assignment in linear systems with incomplete state feedback,” *Automatic Control, IEEE Transactions on*, vol. 15, pp. 348–351, June 1970. 10
- [17] E. Davison and R. Chatterjee, “A note on pole assignment in linear systems with incomplete state feedback,” *Automatic Control, IEEE Transactions on*, vol. 16, pp. 98–99, February 1971. 10
- [18] E. Davison and S. Wang, “On pole assignment in linear multivariable system using output feedback,” *IEEE Transactions on Automatic Control*, vol. 20, pp. 516–518, Aug 1975. 10
- [19] H. Kimura, “Pole assignment by gain output feedback,” *IEEE Transactions on Automatic Control*, vol. 20, pp. 509–516, Aug 1975. 10
- [20] S. Srinathkumar and R. Rhoten, “Eigenvalue/eigenvector assignment for multivariable systems,” *Electronics Letters*, vol. 11, pp. 124–125, March 1975. 10
- [21] B. Moore, “On the flexibility offered by state feedback in multivariable systems beyond closed-loop eigenvalue assignment,” *IEEE Transactions on Automatic Control*, vol. 21, pp. 689–692, October 1976. 10
- [22] S. Srinathkumar, “Eigenvalue / eigenvector assignment using output feedback,” *Automatic Control, IEEE Transactions on*, vol. 23, pp. 79–81, February 1978. 10

- [23] G. Liu and R. Patton, *Eigenstructure Assignment for Control System Design*. John Wiley & Sons Chichester, 1998. 11, 12, 48, 69
- [24] M.M.Fahmy and J.O'Reilly, "Multistage parametric eigenstructure assignment by output-feedback control," *International Journal of Control*, vol. 48, no. 1, pp. 97–116, 1988. 11, 48, 50, 52, 53, 54, 55, 56, 60
- [25] F. Brasch and J. Pearson, "Pole placement using dynamic compensator," *IEEE Transactions on Automatic Control*, vol. AC-15, pp. 34–43, Feb 1970. 11, 51
- [26] A. Andry, E. Shapiro, and J. Chung, "Eigenstructure assignment for linear systems," *Aerospace and Electronic Systems, IEEE Transactions on*, vol. AES-19, pp. 711–729, Sept 1983. 12
- [27] K. Sobel and E. Shapiro, "Eigenstructure assignment for design of multimode flight control systems," *Control Systems Magazine, IEEE*, vol. 5, pp. 9–15, May 1985. 12
- [28] M. Schulz and D. Inman, "Eigenstructure assignment and controller optimization for mechanical systems," *Control Systems Technology, IEEE Transactions on*, vol. 2, pp. 88–100, June 1994. 12
- [29] J. Lu, H. dong Chiang, and J. S. Thorp, "Partial eigenstructure assignment and its application to large scale systems," *IEEE transactions on Automatic Control*, vol. 36, pp. 340–347, March 1991. 12
- [30] P.-H. Huang and Y.-Y. Hsu, "Eigenstructure assignment in a longitudinal power system via excitation control," *Power Systems, IEEE Transactions on*, vol. 5, pp. 96–102, February 1990. 12, 13
- [31] J. Lu, H. Chiang, and J. Thorp, "Eigenstructure assignment by decentralized feedback control," *Automatic Control, IEEE Transactions on*, vol. 38, pp. 587–594, April 1993. 12, 13

- [32] P. M. Anderson and A. A. Fouad, *Power System Control and Stability*. IEEE Press, 1993. 17
- [33] G. Verghese, I. Perez-Arriaga, and F. Schweppe, “Selective modal analysis with applications to electric power systems, part i: Heuristic introduction, part ii: The dynamic stability problem,” *IEEE Transactions on Power Apparatus and Systems*, vol. PAS-101, pp. 3117–3134, Sep 1982. 21
- [34] F. Pagola, I.J.Pérez-Arriaga, and G. Verghese, “On sensitivities, residues and participations: applications to oscillatory stability analysis and control,” *IEEE Transactions on Power Systems*, vol. 4, pp. 278–285, Feb. 1989. 21, 22, 27, 33, 154
- [35] N. Martins and L. Lima, “Determination of suitable locations for power system stabilizers and static var compensators for damping electromechanical oscillations in large scale power systems,” *Power Systems, IEEE Transactions on*, vol. 5, pp. 1455–1469, Nov 1990. 27
- [36] D. Ostojic, “Identification of optimum site for power system stabiliser applications,” *Generation, Transmission and Distribution, IEE Proceedings C*, vol. 135, pp. 416–419, Sep 1988. 28
- [37] J. Nelder and R. Mead, “A simplex method for function minimization,” *Computer Journal*, vol. 7, p. 308313, 1965. 78
- [38] R. B. Lehoucq, D. C. Sorensen, and C. Yang, “ARPACK users’ guide: Solution of large-scale eigenvalue problems with implicitly restarted arnoldi methods.” The software and this guide are available at URL <http://www.caam.rice.edu/software/ARPACK/>, Oct. 1997. 80, 160
- [39] R. Jabr, B. Pal, and N. Martins, “A sequential conic programming approach for the coordinated and robust design of power system stabilizers,” *Power Systems, IEEE Transactions on*, vol. 25, pp. 1627–1637, Aug 2010. 86

- [40] F. Hughes, O. Anaya-Lara, N. Jenkins, and G. Strbac, “A power system stabilizer for dfig-based wind generation,” *Power Systems, IEEE Transactions on*, vol. 21, pp. 763–772, May 2006. 111, 113
- [41] E. Hau, *Wind Turbines: Fundamentals, Technologies, Application, Economics*. Springer, 2005. 112
- [42] *IMSL: Fortran Subroutines for Mathematical Applications, Math Library, Volumes 1 and 2*. Visual Numerics, Inc, 1997. 165

Appendix A

Linearized State Equations

Dynamics of each the devices in the power system can be described using a first order nonlinear differential equation of device state variables

$$\dot{x}_d = f_d(x_d, v_d, u_d). \quad (\text{A.1})$$

where

($\dot{}$) is derivative of () with respect to time.

x_d is the n_d -dimensional states vector of the dynamic device.

v_d is the $2k$ -dimensional column vector of real and imaginary parts of bus voltages upon which the device dynamics depend. For one port devices (e.g., generator without remote sensing) $k = 1$; and for two port devices (e.g., HVDC system) or for remote bus voltage sensing devices (e.g. generator controlling remote bus voltage) $k > 1$.

u_d is the m_d -dimensional column vector of reference inputs to the device (e.g. V_{ref} of an exciter or P_{ref} of governing system of a prime mover).

f_d is a set of n_d non-linear functions of x_d , v_d , and u_d .

Current injected by each device into the network is expressed using a set of nonlinear algebraic equations as

$$i_d = g_d(x_d, v_d) \quad (\text{A.2})$$

where

i_d is the $2p$ -dimensional column vector of real and imaginary parts of current injected by the device. For one port devices (e.g., generator) $p = 1$ and for two port devices (e.g., HVDC system) $p > 1$.

g_d is a set of $2p$ non-linear functions of x_d, v_d .

The transmission network can be expressed using node equations as:

$$i = Y_n v \quad (\text{A.3})$$

where

i is the $2n_b$ -dimensional column vector of real and imaginary parts of the current being injected by dynamic devices into the network through n_b number of nodes, and is the combination of i_d in (A.2)

v is the $2n_b$ -dimensional column vector of real and imaginary parts of n_b number of nodes, and is a combination of vectors v_d in (A.2).

Y_n is the node admittance matrix including nonlinear loads

For the system, the equilibrium points are those points where the system is at rest and all the variables are constant and unvarying with time. The system is said to be asymptotically stable if, when it is subjected to a small perturbation, it returns to its original equilibrium point. The asymptotically stable points are also referred to as Stable Equilibrium Points (SEPs). The SEPs by definition satisfy

$$f_d(x_{d0}, v_{d0}, u_{d0}) = 0 \quad (\text{A.4a})$$

$$g_d(x_{d0}, v_{d0}) = i_{d0} \quad (\text{A.4b})$$

$$i_0 = Y_n v_0 \quad (\text{A.4c})$$

where the subscript 0 denotes the numerically evaluated vector at the SEPs. To study small-signal stability, the nonlinear functions in (A.1) and (A.2) can be linearized using

Taylor series expansion about x_{d0} , i_0 , and v_0 , to yield

$$\Delta \dot{x}_d = A_d \Delta x_d + B_d \Delta v_d + F_d \Delta u_d \quad (\text{A.5a})$$

$$\Delta i_d = C_d \Delta x_d + D_d \Delta v_d \quad (\text{A.5b})$$

where Δ denotes a deviation of variable from its steady state value at the SEP and

$$A_d = \left. \frac{\partial f_d(x_d, v_d, u_d)}{\partial x_d} \right|_{x_{d0}, v_{d0}, u_{d0}} \quad (\text{A.6a})$$

$$B_d = \left. \frac{\partial f_d(x_d, v_d, u_d)}{\partial v_d} \right|_{x_{d0}, v_{d0}, u_{d0}} \quad (\text{A.6b})$$

$$F_d = \left. \frac{\partial f_d(x_d, v_d, u_d)}{\partial u_d} \right|_{x_{d0}, v_{d0}, u_{d0}} \quad (\text{A.6c})$$

$$C_d = \left. \frac{\partial g_d(x_d, v_d)}{\partial x_d} \right|_{x_{d0}, v_{d0}} \quad (\text{A.6d})$$

$$D_d = \left. \frac{\partial g_d(x_d, v_d)}{\partial v_d} \right|_{x_{d0}, v_{d0}} \quad (\text{A.6e})$$

Such linearized equations for all the dynamic devices may be combined as:

$$\Delta \dot{x} = A_D \Delta x + B_D \Delta v + F_D \Delta u \quad (\text{A.7a})$$

$$\Delta i = C_D \Delta x + D_D \Delta v \quad (\text{A.7b})$$

where

x is the n -dimensional column vector of the states of the complete system.

A_D is the $n \times n$ block diagonal real non-symmetric matrix of A_d .

B_D is the $n \times 2n_b$ matrix obtained using block matrix B_d such that vector v in (A.7a) is consistent with that in (A.3).

F_D is the $n \times m$ diagonal matrix obtained using block matrix F_d .

C_D is the $2n_b \times 2n$ block diagonal matrix of C_d .

D_D is the $2n_b \times 2n_b$ matrix obtained using block matrix D_d such that v in (A.7b) is consistent with that in (A.3).

The $A_{d(D)}$, $B_{d(D)}$, $C_{d(D)}$, and $D_{d(D)}$ matrices in the above equations are intermedi-

ate matrices of the linearized power system and should not be confused with those encountered in the standard form of linear equations in the control system.

The relation between the perturbed values of i and v using network equation (A.3) is given by

$$\Delta i = Y_n \Delta v \quad (\text{A.8})$$

Using (A.7b) and (A.8), Δv can be expressed in terms of Δx ; and substituting it in (A.7a) yields

$$\begin{aligned} \Delta \dot{x} &= (A_D + B_D (Y_n - D_D)^{-1} C_D) \Delta x + F_D \Delta u \\ &= A \Delta x + F_D \Delta u \end{aligned} \quad (\text{A.9})$$

where the plant matrix of the complete system, A , is defined by

$$A \triangleq A_D + B_D (Y_n - D_D)^{-1} C_D. \quad (\text{A.10})$$

For the sake of brevity, the symbol Δ in (A.9) may be dropped. Thus, we have obtained the linearized equation of the dynamics of the state variables of the power system in its standard form of control system

$$\dot{x} = A x + B u \quad (\text{A.11})$$

Appendix B

Change in eigenvalue due to dynamic output feedback controller

The proposed PSS design algorithm optimally assigns eigenstructure by solving a multi-objective nonlinear program. In this thesis, the multi-objective nonlinear problem is solved by combining multiple objectives into a single objective function and then minimizing the function using some suitable optimization routine. During the minimization process, each evaluation of the objective function requires the approximate new locations of open-loop eigenvalues due to the implementation of the dynamic compensator type output feedback controller. In this appendix, the mathematical expression for the approximate new location of an open-loop eigenvalue due to implementation of the output feedback controller is presented. The mathematical expression derived is based on the sensitivity of eigenvalue λ to some parameter q of controller that is presented in [34]. In the following, first the results from [34] are reviewed and then the main results are presented.

Let the \bar{n} -states, \bar{m} -inputs, and \bar{r} -outputs Linear Time Invariant (LTI) control system be defined as:

$$\begin{aligned}\dot{\bar{x}}(t) &= \bar{A}\bar{x}(t) + \bar{B}\bar{u}(t) \\ \bar{y}(t) &= \bar{C}\bar{x}(t)\end{aligned}\tag{B.1}$$

Let the dynamic output feedback control law described as

$$\begin{aligned}\dot{z}(t) &= D z(t) + E \bar{y}(t) \\ \bar{u}(t) &= F z(t) + G \bar{y}(t)\end{aligned}\tag{B.2}$$

be applied to the system (B.1), where $z(t) \in \mathbb{R}^a$. The dynamics of the closed-loop system are given by:

$$\begin{pmatrix} \dot{\bar{x}}(t) \\ \dot{z}(t) \end{pmatrix} = A_c \begin{pmatrix} \bar{x}(t) \\ z(t) \end{pmatrix}; \quad A_c \triangleq \begin{pmatrix} \bar{A} + \bar{B} G \bar{C} & \bar{B} F \\ E \bar{C} & D \end{pmatrix}.\tag{B.3}$$

The resultant closed-loop system will have $n = \bar{n} + a$ states. This is a simplified expression of the closed-loop dynamic output feedback control system described by (4.4)-(4.6). Let λ be a distinct eigenvalue of A_c ; and let $v, w \in \mathbb{C}^n$ be the associated right and left eigenvectors respectively. There will be such n eigenvalues and the following results apply to each of them. The eigenvalue and eigenvector hold the following relations.

$$A_c v = \lambda v\tag{B.4}$$

$$w^T A_c = \lambda w^T\tag{B.5}$$

$$w^T v = 1\tag{B.6}$$

$$\lambda = w^T A_c v\tag{B.7}$$

Let us denote the derivative with respect to some parameter q of the dynamic output feedback controller as $(\cdot)'$. The derivative of the eigenvalue with respect to q using (B.7) is given by:

$$\lambda' = w^T A'_c v.\tag{B.8}$$

Let us analyze the terms on the right hand side of the above equation. Using the definition of A_c in (B.3), its derivative with respect to q is given by:

$$A'_c = \begin{pmatrix} \bar{B} G' \bar{C} & \bar{B} F' \\ E' \bar{C} & D' \end{pmatrix}.\tag{B.9}$$

The right and left eigenvectors, v and w respectively, associated with the eigenvalue λ of the plant matrix A_c can be partitioned according to the dimension of the system and the dynamic compensator state vectors as:

$$v = \begin{pmatrix} v_1 \\ v_2 \end{pmatrix}; \quad w = \begin{pmatrix} w_1 \\ w_2 \end{pmatrix} \quad (\text{B.10})$$

where $v_1, w_1 \in \mathbb{C}^{\bar{n}}$, and $v_2, w_2 \in \mathbb{C}^a$. Using (B.3)-(B.5) the relations between partitioned vectors can be shown to be

$$v_2 = M(\lambda) E \bar{C} v_1 \quad (\text{B.11})$$

$$w_2^T = w_1^T \bar{B} F M(\lambda) \quad (\text{B.12})$$

where

$$M(\lambda) = (\lambda I_a - D)^{-1}. \quad (\text{B.13})$$

Therefore

$$v = \begin{pmatrix} I_{\bar{n}} \\ M(\lambda) E \bar{C} \end{pmatrix} v_1 \quad (\text{B.14})$$

$$w^T = w_1^T \begin{pmatrix} I_{\bar{n}} & \bar{B} F M(\lambda) \end{pmatrix} \quad (\text{B.15})$$

Substituting (B.14), (B.15), and (B.9) into (B.8) yield

$$\lambda' = w_1^T \begin{pmatrix} I_{\bar{n}} & \bar{B} F M(\lambda) \end{pmatrix} \begin{pmatrix} \bar{B} G' \bar{C} & \bar{B} F' \\ E' \bar{C} & D' \end{pmatrix} \begin{pmatrix} I_{\bar{n}} \\ M(\lambda) E \bar{C} \end{pmatrix} v_1. \quad (\text{B.16})$$

The transfer function of the controller is given by:

$$H(s) = F M(s) E + G \quad (\text{B.17})$$

where

$$M(s) = (s I_a - D)^{-1}. \quad (\text{B.18})$$

So, the derivative of controller transfer function (B.17) with respect to q is given by

$$H'(s) = F' M(s) E + F M(s) D' M(s) E + F M(s) E' + G'. \quad (\text{B.19})$$

Expanding (B.16) and by substituting s with λ in (B.17) gives

$$\lambda' = w_1^T \bar{B} H'(\lambda) \bar{C} v_1. \quad (\text{B.20})$$

Using the above equation, the incremental change in eigenvalue $\Delta\lambda$ due to change in the dynamic output feedback controller parameters is given by

$$\Delta\lambda = w_1^T \bar{B} \Delta H(\lambda) \bar{C} v_1 \quad (\text{B.21})$$

where $\Delta H(\lambda)$ using (B.19) is given by

$$\Delta H(\lambda) = \Delta F M(\lambda) E + F M(\lambda) \Delta D M(\lambda) E + F M(\lambda) \Delta E + \Delta G. \quad (\text{B.22})$$

In the above expression of $\Delta H(\lambda)$, the matrices D, E, F , and G are initial (unperturbed) values of the matrices and λ is an eigenvalue of the unperturbed plant matrix A_c in (B.3).

The approximate new location of an open-loop eigenvalue λ due to application of the dynamic compensator type output feedback controller (B.2) can be calculated using (B.21) and (B.22) as follows. Consider that firstly the dynamic output feedback controller with zero output gain is employed i.e. $F = 0$ and $G = 0$ in (2.20). The resulting closed-loop system using the definition of A_c in (B.3) is given by

$$A_c = \begin{pmatrix} \bar{A} & 0 \\ E \bar{C} & D \end{pmatrix}. \quad (\text{B.23})$$

Let λ be an eigenvalue of the open-loop system matrix \bar{A} and let v_1 and w_1 be the associated right and left eigenvectors. It can readily be shown that the λ is also an eigenvalue of A_c , and that v_1 and w_1 constitute the first \bar{n} entries of the associated right and left eigenvector v and w , respectively, as shown in (B.10). In order to implement the controller, the values of output gains F and G are changed from zero to their final values. The change in transfer function due to implementation of the gains using B.22 is

$$\Delta H(\lambda) = F M(\lambda) E + \Delta G \quad (\text{B.24})$$

and the approximate change in eigenvalue using (B.21) is

$$\Delta\lambda = w_1^T \bar{B} (F M(\lambda) E + \Delta G) \bar{C} v_1. \quad (\text{B.25})$$

Appendix C

Computational Methods for a Very Large Power System

Power system controller design using optimal eigenstructure assignment requires optimization of the objective function value that uses knowledge of eigenvalue and eigenvector of the control system, and requires many different mathematical operations on matrices during calculation of the eigenvalues, eigenvectors and objective function value. Design of PSSs using the proposed algorithm for the systems presented in this thesis was accomplished by developing a program in the Fortran language using commercially available software: Compaq Visual Fortran Ver. 6.0. The storage and computation can be performed using conventional methods for the matrices having dimension up to several hundred. For a large power system, the number of states (which equals the dimension of plant matrix and eigenvalues) may easily exceed 10,000. A plant matrix of such a dimension is well outside the range of the conventional methods used to find eigenvalues and eigenvectors. Special techniques are available in such cases to find a sub-set of eigenvalues of the complete system. This appendix describes one of such techniques, modified Arnoldi method, that is employed while developing the Fortran computer program to design a PSS for a very large power system.

C.1 Calculation of Eigenvalue and Eigenvector of Very Large Power System

C.1.1 The Arnoldi Factorization Method

Implicitly restarted Arnoldi method (IRAM) is an efficient algorithm for finding a subset of the eigenvalues and associated eigenvectors of a very large sparse matrix. The method and algorithm is described in [38]. In the following, the underlying concept of the algorithm is presented.

The Arnoldi factorization of a matrix is defined as follows.

If $A \in C^{n \times n}$, then a relation of the form

$$AV_k = V_k H_k + f_k e_k^T \tag{C.1}$$

where $V_k \in C^{n \times k}$ has orthonormal columns, $V_k^T f_k = 0$, and $H_k \in C^{k \times k}$ is upper Hessenberg with non-negative subdiagonal elements is called a k -step Arnoldi factorization of A . If λ is an eigenvalue of H_k and v is the associated right eigenvector, then $H_k v = \lambda v$, and the vector $x = V_k v$ will yield

$$\begin{aligned} \|Ax - x\lambda\| &= \|AV_k v - V_k v \lambda\| \\ &= \|(AV_k - V_k H_k)v\| \\ &= \|f_k e_k^T v\| \\ &= \|f_k\| |e_k^T v| \end{aligned} \tag{C.2}$$

From the above, it can be observed that if $\|f_k\| = 0$, then λ is the exact eigenvalue of original matrix A , and the associated right eigenvector can be computed using $V_k v$. This forms the basis of the Arnoldi method and the algorithm drives $\|f_k\|$ to zero iteratively by continually modifying V_k . In the implicitly restarted Arnoldi algorithm, the vectors V_k are reevaluated implicitly after a certain number of iterations to preserve the orthogonality of V_k and to accelerate convergence.

C.1.2 The ARPACK Software

The IRAM has been implemented in the ARPACK software package, which is a collection of subroutines to calculate a certain number of eigenvalues based on certain criteria for a large system. This software is used in the SSAT tool of the commercially available DSA Power Tool program. Therefore, the same program was considered for a small-signal analysis of large power system during the research so that the analysis results can be validated and yield consistent results.

The following describes two important features of the software:

1. A reverse communication interface:

With reverse communication, the control is returned to the calling program whenever interaction with the matrix A is required. The required operation on the matrix is indicated by the reverse communication parameter. This is a very convenient feature for power system applications where, as will be seen, the matrix vector product cannot be obtained in a straight forward manner and requires lengthy computation.

A sample Fortran code that demonstrates usage of reverse communication is shown below:

```
DO
  CALL ZNAUPD ( IDO, 'I', N, WHICH, NEV, TOL, RESID, NCV, &
              V, LDV, IPARAM, IPNTR, WORKD, WORKL, LWORKL, &
              RWORK, IERR ),
  IF((IDO.EQ.-1).OR.(IDO.EQ.1)) THEN
    CALL OPV( N, WORKD(IPNTR(1)), WORKD(IPNTR(2)), IPATH, FNAME)
  ELSE
    EXIT
  ENDF
END DO
```

The `ZNAUPD` is a top level subroutine supplied with the software. The code performs the action based on parameter `IDO` set by `ZNAUPD`.

The subroutine `OPV` is a user defined subroutine, which multiples the matrix (of which eigenvalue to be found) with a vector stored in `WORKD(IPNTR(1))` (supplied by `ZNAUPD`) and stores resultant vector at `WORKD(IPNTR(2))`, which is used by subroutine `ZNAUPD` during next iteration.

Upon successful convergence of the `ZNAUPD`, the results are post-processed using the subroutine `ZNEUPD` to get eigenvalues of the original problem and the corresponding eigenvectors.

2. Calculations of limited eigenvalue, based on a criterion, and associated eigenvector:

The program returns a certain number of eigenvalues that satisfy a criterion (e.g. largest absolute value, largest real part, largest algebraic value) along with the associated right eigenvectors. The desired number of eigenvalues and the criterion is selected in prior by the user. If the left eigenvector is desired, then the operation be performed on A^T whenever the operation on the matrix is requested by the program, realizing that finding the left eigenvector is a dual problem of finding the right eigenvector.

C.1.3 The Shift and Invert Transformation

As mentioned earlier, the ARPACK software has the ability to calculate the eigenvalues that satisfy user criteria (e.g. largest absolute value, largest real part, largest algebraic value). However, the software is the most efficient in finding eigenvalues with the largest absolute value. In conjunction with selecting the criteria of the largest absolute value, the shift invert transformation on matrix A , whose eigenvalues are to be found, can be applied to achieve convergence to a desired neighborhood of the spectrum.

If λ and w are the eigenvalue and associated eigenvector of matrix A and $\sigma \neq \lambda$,

then

$$(A - \sigma I_n)^{-1} w = \frac{1}{\lambda - \sigma} w = \beta w. \quad (\text{C.3})$$

The largest magnitude eigenvalues of transformed matrix $(A - \sigma I_n)^{-1}$ corresponds to the eigenvalues of the original matrix A that are nearest to shift σ in absolute value. Once the largest eigenvalues of the transformed matrix are found, the eigenvalues of the original matrix can easily be computed as

$$\lambda = \sigma + 1/\beta. \quad (\text{C.4})$$

Computation of the eigenvalues of matrix A around shift σ using ARPACK software requires computation of vector $u = (A - \sigma I_n)^{-1} v$ when `ZNAUPD` requests operation on the matrix through parameter `IDO` during reverse communication. The technique for computing u for a large power system is described in following section.

C.1.4 Computing $u = (A - \sigma I_n)^{-1} v$

For a given vector v , the method to compute

$$u = (A - \sigma I_n)^{-1} v \quad (\text{C.5})$$

specifically for the power system plant matrix A , described in [6], is presented in following.

As shown in (A.10), the plant matrix of a power system is given by

$$A \triangleq A_D + B_D (Y_n - D_D)^{-1} C_D. \quad (\text{C.6})$$

where A_D, B_D, C_D , and D_D are block diagonal matrices and Y_n is the node admittance matrix. It is impossible to explicitly evaluate plant matrix A using the above equation because it involves inversion of a large sparse matrix. Therefore, the resultant vector u in (C.5) is evaluated indirectly as shown in the following.

Upon substituting definition of A from (C.6) in to (C.5) and rearranging

$$(A_D - \sigma I_n)u + B_D (Y_n - D_D)^{-1} C_D u = v \quad (\text{C.7a})$$

$$u + (A_D - \sigma I_n)^{-1} B_D (Y_n - D_D)^{-1} C_D u = (A_D - \sigma I_n)^{-1} v \quad (\text{C.7b})$$

$$C_D u + C_D (A_D - \sigma I_n)^{-1} B_D (Y_n - D_D)^{-1} C_D u = C_D (A_D - \sigma I_n)^{-1} v \quad (\text{C.7c})$$

By defining a new vector q as

$$q = (Y_n - D_D)^{-1} C_D u \quad (\text{C.8})$$

and rearranging the above equation yield

$$C_D u = (Y_n - D_D) q. \quad (\text{C.9})$$

Substituting (C.8) and (C.9) in (C.7c) and rearranging yields

$$(Y_n - D_D + C_D (A_D - \sigma I_n)^{-1} B_D) q = C_D (A_D - \sigma I_n)^{-1} v. \quad (\text{C.10})$$

Thus, solution of u in (C.5) can be accomplished in two steps: (1) solve (C.10) for q and (2) solve (C.9) for u . As can be seen by examination of the equations, the problem of finding vectors q and u is equivalent to, after a few operations on the matrices and the vectors, finding a solution of x for a set of linear equations $Ax = b$. The solution to the set of linear equations can be obtained using the sparse matrix factorization method. Note the evaluation of $A_e = (A_D - \sigma I_n)^{-1}$ is not difficult to achieve because A_D is a block diagonal of matrices having dimensions in the order of a few tens, and, therefore, the A_e can be obtained by inverting each of these matrices individually using the conventional small matrix inversion technique. The subroutines used to evaluate matrix-matrix multiplications, and to obtain the solution of a set of linear equations are described in following sections.

C.2 Multiplication of Large Sparse Matrices

The SMMP package available in the *aicm* library, which is freely available at www.netlib.org, was implemented for matrix-matrix multiplication. The multiplication is performed

in two steps. First, the nonzero structure of the resulting matrix is determined symbolically using subroutine `SYMBMM`. Once the nonzero structure for the resultant matrix is known, the numerical matrix-matrix multiplication is computed using the subroutine `NUMBMM`.

The subroutines support the old Yale sparse format for the matrices. The matrix, M , in old Yale sparse matrix format is stored using two integer vectors, $IA(N + 1)$ and $JA(NZ)$, and one real or complex vector $A(NZ)$, where N is dimension of matrix and NZ is number of non-zero elements of M . The column index of non-zero elements of row I are stored in $JA(IA(I))$ through $JA(IA(I + 1) - 1)$. For element $A(J)$, the column index is $JA(J)$.

C.3 Solution to a Sparse System of Linear Equations

The subroutines available in the IMSL Fortran 90 MP Library distributed with Compaq Visual Fortran software, were implemented in the program to solve the system of linear equations

$$Ax = b \tag{C.11}$$

where A is large and sparse. The solution to linear equations is obtained in two steps. As a first step, the LU factorization of coefficient matrix A is obtained using `DLFTZG` subroutine. Then in second step, the system of linear equations is solved using the LU factorization of the coefficient matrix obtained in first step [42].

Appendix D

Dynamic Device Data

D.1 2-Area 4-Generator Sample System of Chapter 3

Generator 1 - 4 Data (GENROU)

$$T'_{d0} = 8.0, T''_{d0} = 0.03, T'_{q0} = 0.4, T''_{q0} = 0.05, H = 6.5, D = 1.0, X_d = 1.8, \\ X_q = 1.7, X'_d = 0.3, X'_q = 0.55, X''_d = X''_q = 0.25, X_l = 0.1,$$

Generator MVA base = 900 MVA

Exciter 1 - 4 Data (AC4A)

$$T_r = 0.01, T_c = 1.0, T_b = 2.0, K_a = 200.0, T_a = 0.01$$

D.2 2-Area 4-Generator Sample System of Chapter 6

Generator 1 Data (GENROU)

$$T'_{d0} = 8.0, T''_{d0} = 0.0, T'_{q0} = 0.4, T''_{q0} = 0.0, H = 6.5, D = 10.0, X_d = 1.8, \\ X_q = 1.7, X'_d = 0.3, X'_q = 0.3, X''_d = X''_q = 0, X_l = 0.0,$$

Generator MVA base = 900 MVA

Generator 2 Data (GENROU)

$$T'_{d0} = 8.0, T''_{d0} = 0.0, T'_{q0} = 0.4, T''_{q0} = 0.0, H = 6.5, D = 1.0, X_d = 1.8, \\ X_q = 1.7, X'_d = 0.3, X'_q = 0.3, X''_d = X''_q = 0, X_l = 0.0, \\ \text{Generator MVA base} = 900 \text{ MVA}$$

Generator 3 Data (GENROU)

$$T'_{d0} = 8.0, T''_{d0} = 0.0, T'_{q0} = 0.4, T''_{q0} = 0.0, H = 6.5, D = 6.5, X_d = 1.8, \\ X_q = 1.7, X'_d = 0.3, X'_q = 0.3, X''_d = X''_q = 0, X_l = 0.0, \\ \text{Generator MVA base} = 900 \text{ MVA}$$

Generator 4 Data (GENROU)

$$T'_{d0} = 8.0, T''_{d0} = 0.0, T'_{q0} = 0.4, T''_{q0} = 0.0, H = 6.5, D = 1.2, X_d = 1.8, \\ X_q = 1.7, X'_d = 0.3, X'_q = 0.3, X''_d = X''_q = 0, X_l = 0.0, \\ \text{Generator MVA base} = 900 \text{ MVA}$$

Exciter 1 - 4 Data (AC4A)

$$T_r = 0.01, T_c = 1.0, T_b = 10, K_a = 100.0, T_a = 0.01$$

D.3 Kelsey Generating System Data

Generator Data (GENSAL)

$$T'_{d0} = 3.6, T''_{d0} = 0.05, T''_{q0} = 0.0, H = 4.1, D = 0, X_d = 0.915, X_q = 0.5411, \\ X'_d = 0.244, X''_d = 0.1624, X_l = 0.133, R_a = 0.0002, \\ \text{Generator MVA base} = 262.5 \text{ MVA}$$

Exciter Data (IEEET1)

$$T_r = 0, K_a = 12.0, T_a = 0.2, V_{rmax} = 1.0, V_{rmin} = -1, K_e = 0, T_e = 0.4, \\ K_f = 0.133, T_f = 1.0, E_1 = 2.3659, S_E(E_1) = 0.13, E_2 = 3.1546, S_E(E_2) = 0.37$$

Governor Data(IEESGO)

$$T_1 = 0.44, T_2 = 0.671, T_3 = 74.4, T_4 = 0.0, T_5 = 0.63, T_6 = 0.0, K_1 = 24.4, \\ K_2 = 3.0, K_3 = 0.0, P_{max} = 0.92, P_{min} = 0.0$$

Appendix E

Nelder-Mead Simplex Algorithm

The Nelder-Mead Simplex method is employed in this thesis to find the minimum of the multi-objective function. The simplex method is an efficient iterative algorithm for unconstrained nonlinear optimization. The minimization achieved using the simplex algorithm is not guaranteed to be globally minimum, but it is able to crawl out of some local minima to find better minima. It requires only function evaluations and does not use derivatives. A simplex is a geometric figure in n -dimensional space specified by $n + 1$ linearly independent vertices (e.g., a triangle for $n = 2$ and a tetrahedron for $n = 3$).

The simplex size is continuously changed and mostly diminished, so that finally it is small enough to contain the minimum with the desired accuracy. The operations of changing the simplex optimally at a given iteration that determine a new simplex for the next iteration are either reflection, expansion, contraction, or shrinking. The overall effect is for the simplex to crawl around the parameter space, creeping down valleys and shrinking to get to the very bottom of narrow valleys. The Nelder-Mead simplex minimization algorithm may be explained using pseudo code.

Simplex Pseudo Code

1. Select coefficients of *reflection*(ρ), *expansion*(χ), *contraction*(γ), and *shrinkage*(σ).

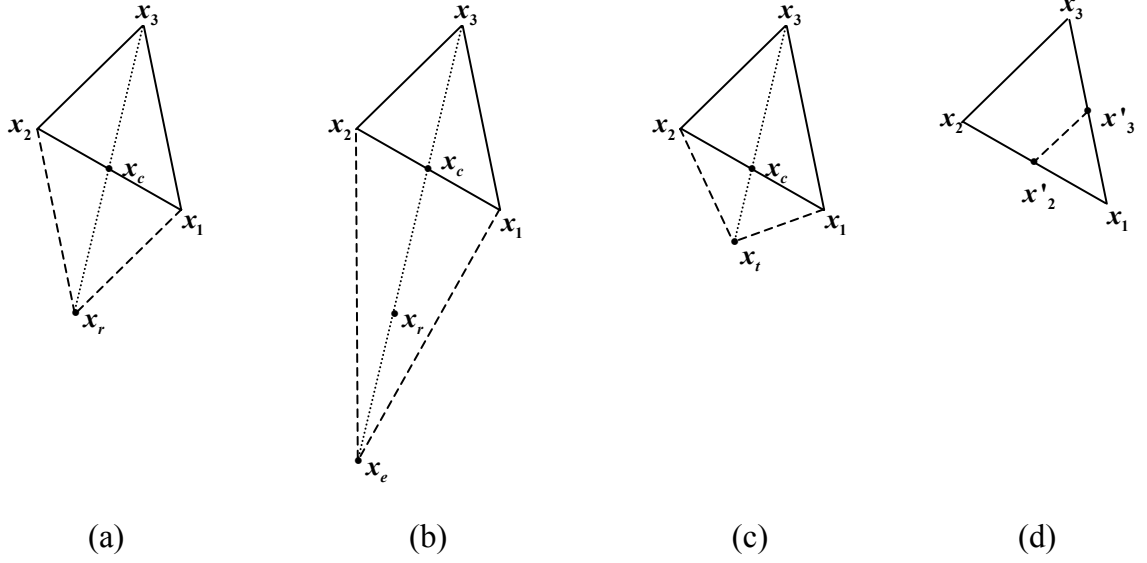


Figure E.1: New simplex after (a) *reflection* step (b) *expansion* step (c) *contraction* step; and (d) *shrinking*. The simplex at the beginning of iteration is shown with a solid line and the new simplex at the end of one iteration is shown with a dashed line.

Typical choices of these coefficient are

$$\rho = 1, \chi = 2, \gamma = \frac{1}{2}, \text{ and } \sigma = \frac{1}{2}. \quad (\text{E.1})$$

2. Create a simplex defined by $n + 1$ vertices; and calculate the function values at these vertices.
3. Order $n + 1$ vertices such that $f_1 \leq f_2, \leq \dots \leq f_{n+1}$ where f_i denotes $f(x_i)$.
4. Calculate the centroid of first n best points $x_c = \sum_{i=1}^n x_i/n$; and the reflection point x_r using

$$x_r = x_c + \rho(x_c - x_{n+1}). \quad (\text{E.2})$$

Evaluate $f_r = f(x_r)$. If $f_1 < f_r < f_n$, then replace x_{n+1} with x_r and go to step 8 before proceeding to the next iteration.

5. If $f_r < f_1$ calculate expansion point x_e from

$$x_e = x_c + \chi(x_r - x_c) \quad (\text{E.3})$$

and evaluate $f_e = f(x_e)$. If $f_e < f_r$, then replace x_{n+1} with x_e , otherwise with x_r . Go to step 8 before proceeding to the next iteration.

6. If $f_n \leq f_r < f_{n+1}$, calculate the contraction point from

$$x_t = x_c + \gamma(x_r - x_c) \tag{E.4}$$

and evaluate $f_t = f(x_t)$. If $f_t < f_r$, replace x_{n+1} with x_t and go to step 8. Otherwise go to the next step to shrink the simplex.

7. A point at least better than x_n is not found; therefore, shrink the simplex. Calculate n new points from

$$x'_i = x_1 + \sigma(x_i - x_1), \quad i = 2, \dots, n + 1. \tag{E.5}$$

Replace x_2, \dots, x_{n+1} with x'_2, \dots, x'_{n+1}

8. If the termination criteria is not met, then go to step 3.